NTNU

Norwegian University of
Science and Technology

Effect of Cadmium on the marine diatoms Seminavis robusta and Phaeodactylum tricornutum: A comparative study

Anitha Madasamy

Srinivasan Babu

Environmental Toxicology and Chemistry

Submission date: June 2016

Supervisor: Åse Krøkje, IBI

Co-supervisor: Atle Bones, IBI

Per Winge, IBI

Norwegian University of Science and Technology

Department of Biology

NTNU – Trondheim
Norwegian University of
Science and Technology

Effect of Cadmium on the marine diatoms *Seminavis robusta* and *Phaeodactylum tricornutum*: A comparative study

Anitha Madasamy Srinivasan Babu

Trondheim, June 2016

Supervisor: Åse Krøkje

Co-supervisors: Atle Bones

Per Winge

Norwegian University of Science and Technology

Department of Biology

Acknowledgement:

This thesis for the Master degree program was carried out at the Department of Biology in the Norwegian University of Science and Technology (NTNU).

I extend my heartfelt thanks to associate professor Åse Krøkje, professor Atle M Bones and associate professor Per Winge, my supervisors for the Master thesis. Their trust in my ability and the constant support helped me to keep pushing ahead. My humble thanks to Tore Brembu who helped me in choosing the appropriate experimental parameters with a special mention to primer designing. Special thanks to Torfinn Sparstad for his assistance with qPCR. I am very much grateful to Marianne Nymark for her friendly guidance throughout the experiment. I would like to thank Olav Vadstein from the Department of Biotechnology for the permission to access the flow cytometer. My sincere thanks to Amit Sharma and Charlotte Volpe for their support in the laboratory work.

I am very much indebted to my four-year-old daughter, Krisha Kamaraj for her invaluable support and love.

"Once you have a target, follow it until you hit it. You must behave like a heat-seeking missile. Whatever you start you should finish!"– Master Choa Kok Sui

Abstract:

Background: Heavy metals cause a harmful effect on marine ecosystems because of their toxicity, persistence and bioaccumulation properties. Cadmium (Cd) is speculated to be a unique heavy metal due to its diverse toxic effects. It is released into the environment through point sources and also capable of long range transports. An extensive laboratory study was carried out in order to explore the toxic effects of cadmium on diatoms. Diatoms were chosen as the study organisms because of their vital role as primary producers in the marine ecosystem.

Experiment: Two marine benthic diatom species *Seminavis robusta* and *Phaeodactylum tricornutum* were separately cultured in aquil medium and exposed to seven different concentrations of cadmium (Cd^{2+}) (0.01, 0.05, 0.25, 1.25, 6.25, 31.25, 156.25 mg/l) for approximately 4 days (day and night cycles). The toxic effects were analyzed in three different biological levels. Growth rate (at population level), chlorophyll fluorescence and cell granularity (at cell physiology level) and gene expression changes (at molecular transcription level) were analyzed.

Results and conclusion: In *Seminavis robusta,* cadmium at low level concentrations is suggested to induce the expression of CA1 gene that might have resulted in the increase of growth rate. In *Phaeodactylum tricornutum*, the overall growth rate did not seem to be suppressed by cadmium. Genes responsible for the cellular uptake of cadmium, VIT1 and ZIP-T1 were induced in *P. tricornutum,* while *S. robusta* did not show an indication of uptake of cadmium through these genes. NTF2L gene was shown to be significantly ($p=0.001$) upregulated at very high levels of cadmium in *S. robusta*. A similar trend was observed in *P. tricornutum* ($p=0.01$). The role of NTF2L in cadmium efflux in diatoms is presented for the first time in this study. The genes used to monitor oxidative stress, CAT1, SOD1, GSR2 were not significantly activated in any of the two species on exposure to cadmium under the given experimental conditions. The results of this study do not support the hypothesis that *S. robusta* due to its expanded gene inventory, shows a better tolerance to heavy metal stress.

Keywords: diatom, cadmium, *Seminavis*, *Phaeodactylum*, growth, chlorophyll, granularity, gene, qPCR

Table of contents

List of figures:

List of tables:

Abbreviations:

APX	Ascorbate-peroxidase
µ	Growth rate
AGC1	Aggrecan1
CA1	Carbonic anhydrase1
CAT1	Catalase1
Cd	Cadmium
Chl	Chlorophyll
ChlF	Chlorophyll fluorescence
Cq	Quantification cycle
Ct	Threshold cycle
Cu	Copper
CYCB1	Cyclin B1
CYP	Cytochrome P450
DLST	Dihydrolipoamide S-succinyltransferase
Fm	Maximum chlorophyll fluorescence
Fo	Minimal chlorophyll fluorescence
FSC	Forward scattered
Fv	Variable chlorophyll fluorescence
G2	Gap2
G3P	Glyceraldehyde 3 phosphate
GR	Glutathione reductase
GSH	Glutathione
GSR2	Glutathione-disulphide reductase2
H4A	Histone H4A
Hg	Mercury
HMA2	Heavy Metal ATPase2
M	Mitosis
mRNA	Messenger ribo-nucleic acid
MT	Metallothionein
NTF2L	Nuclear Transporter Factor 2-Like
PAM	Pulse amplitude modulation
PC	Phytochelatin
PCS	Phytochelatin synthase
PCS1	Phyto Chelatin Synthase1
PPX	Pyrogallol-peroxidase
PS	Photosystem
Qy	Quantum yield
RC	Reaction center
RIN	RNA integrity number
ROS	Reactive oxygen species
RPS5	Ribosomal Protein S5
Se	Selenium

SOD1	Superoxide dismutase1
SOW	Synthetic ocean water
SSC	Side scattered
Tm	Melting temperature
VIT1	Vacuolar Ion Transporter1
VPS35	Vacuolar Protein Sorting35
ZIP-T1	Zinc regulated transporter, Iron regulated transporter like Protein Transporter1
Zn	Zinc

1. INTRODUCTION

History has proved that oceans are not a safe disposal unit for pollutants. Even at very low levels, many chemical contaminants including sewage and industrial effluents, petroleum products, organochlorine compounds and heavy metals have adverse effects on marine environment. Wastes generated due to human activities including habitat destruction contaminate the marine and coastal environment with toxic substances (Torres et al., 2008).

Amongst the major pollutants, heavy metals pose a notable threat to human health, living organisms and ecosystems due to their toxicity, persistence and bioaccumulation characteristics. Heavy metals are also capable of long range atmospheric transport. It has been well documented that much of the heavy metal deposition in Southern Norway originates from the heavy industrialized part of Europe (Steinnes, 1987). Reduction in the species diversity and their abundance are a direct effect of accumulation of heavy metals in living organisms and in marine food chains. Eventually, this can lead to destruction of marine ecosystems besides causing an economic loss because marine resources support food, industry and recreation sectors (Naser, 2013).

Heavy metals are natural elements that have high atomic weight and a density higher than 5 g/cm^3. Metals are naturally released into soils by physical and chemical weathering processes. Heavy metals are capable of entering a water supply through industrial and commercial waste and even from acid rain that contaminates streams, lakes, rivers and groundwater. Volcanic eruptions also contribute by releasing metals into the atmosphere, surface waters and soils (Chapman and Wang, 2000). Human activities increase the concentration of heavy metals in the environment. Heavy metals are one of the major groups of environmental contaminants as a result of rapid increase in their industrial, domestic, agricultural, medical and technological applications (Tchounwou et al., 2012). The release of heavy metals in biologically available forms may damage the natural ecosystems.

1.1. Cadmium

Cadmium (Cd) is a group IIB element in the periodic table with an atomic number 48. It tends to show similarities with other group IIB elements especially zinc (Zn) and mercury (Hg). Cd (II) (Cd^{2+}) is more stable with a valence two and found to occur in most aquatic systems in this state (Hasan et al., 2009). Because of its diverse toxic effects, Cd is considered to be unique among the other heavy metals. In human beings, Cd is associated with nephrotoxicity, chronic

pulmonary disease, skeletal effects, cardiovascular effects, neurotoxicity and carcinogenicity (Tokar et al., 2013). The sources of Cd are agricultural, mining and industrial activities, and automobile exhaust (Das et al., 1998). Cd is primarily found in batteries, electroplating, stabilizers, and in pigments. It is used as the negative electrode in the Cd-Ni batteries. Electroplated Cd provides excellent protection against corrosion and is extensively used for automotive and aircraft applications. Cd is used as one of the main components to create pigments for paint. It is also used as stabilizers for the plastic industry and as a barrier to control nuclear fission. Worldwide the Cd production in 2014 was around 22,000 metric tons. It has to be noted that the actual figure would be much higher since the data from United States was withheld in the report (Tolcin, 2015).

Cd is a pollutant of concern because of its high toxicity and great tendency to dissolve in water that increases the bioavailability in aquatic ecosystems. It is generally considered to have no described biological function (Das et al., 1998). But there is evidence of biological role played by Cd in the marine diatom *Thalassirosira weissflogii* under low Zn conditions which is a typical characteristic in the marine environment (Lane and Morel, 2000).

The ability of cadmium to be both beneficial and deleterious has resulted in the evolution of multiple and complex mechanisms at the cellular level of the organism. They regulate the availability and location of the cadmium inside the cell (Ballatori et al., 2012). Cd has varied effects on living cells involving different pathways and to different degrees. Two major events take place when exposing cells to Cd, first is to select the heavy metals that are essential for growth and excluding those which are not essential, the second is to maintain the essential metals at optimum concentrations (Perales-Vela et al., 2006).

1.2. Diatoms

Diatoms are a group of microscopic photosynthetic eukaryotic phytoplankton. They are found throughout marine and freshwater environments. Diatoms belong to the division Bacillariophycea and comprises an estimated 10,000 - 100,000 species in 250 genera (Kroth, 2007). The name is derived from the Greek word *diatmos*, which means ‘cut in half’, referring to their unique two-part cell walls made of silica. The external wall of diatoms is composed of amorphous silica [$(SiO_2)n(H_2O)$] known as the frustule and consists of two halves which fits together like a Petri dish with lid. Diatoms are classified based on the symmetry of the frustules. Centric diatoms are radially symmetrical and tend to be planktonic. Whereas, pennate diatoms are bilaterally symmetrical and are often benthic (Falciatore and Bowler, 2002).

Diatoms are ecologically important because they form the basis of the food web in the oceans (Chepurnov et al., 2008). They contribute to approximately one quarter of the global primary production and 40% of marine organic carbon production (Siaut et al., 2007). Diatoms play a crucial role in biogeochemical cycles of elements such as carbon, silicon, nitrogen and iron (Bowler et al., 2010). Diatoms can generate energy by breaking down fat like animals and can also produce metabolic intermediates from the breakdown similar to plants (Armbrust, 2009). Diatoms play a significant role in the industrial fields including the biofuel production, nanotechnology and pharmaceutics (Huysman et al., 2014). Properties such as the highly ornamented and organised silica cell wall and the capability to produce various lipids and pigments have facilitated this widespread application in the industrial fields.

In spite of the abundance of diatoms in the oceans and their biogeochemical and ecological significance, molecular mechanisms underlying diatoms' ecological success are greatly unexplored (Depauw et al., 2012).

The biological effects of Cd on marine organisms are studied in diatoms because of the significant role played by them in the environment and the diatoms are highly sensitive facilitating the detection of potential toxic effects (Torres et al., 2000). However, practically it is difficult to identify one diatom species that is of universal ecological importance. In modern experimental biology, 'model-systems' approach is used in order to overcome this difficulty (Chepurnov et al., 2008). The species of diatoms that were used for this study are discussed below.

1.2.1. *Seminavis robusta*

Seminavis robusta was introduced as a candidate model species by Chepurnov et al. (2008) due to its heterothallic mating system. Sexual crosses could possibly be made in this species for forward genetics. *Seminavis robusta (fig 1.1)* is a pennate diatom that is convenient to monitor in the laboratory because of its large size (up to 80 µm long) and benthic life style. There is an upward trend in the number of research studies on this emerging model species that eventually lead to the adoption of *Seminavis robusta* as one of the model species in this study.

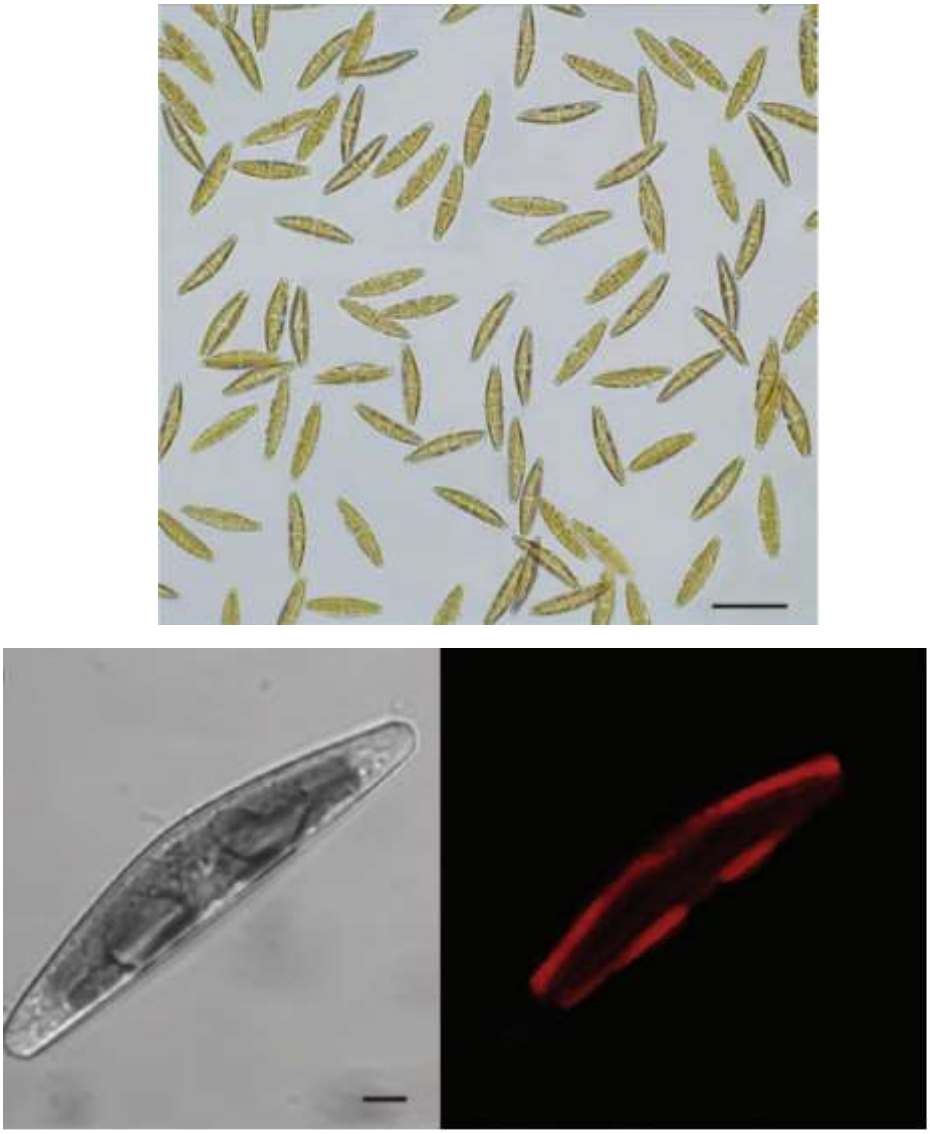

Figure 1.1. Illustration of *Seminavis robusta*. (Top) light microscopy image. Scale bar= 50 µm (Bottom) Confocal laser scanning microscopy of a *S. robusta* cell (Left) transmission light (Right) autofluorescence of the chloroplasts in red. Scale bar = 5 µm. (Adapted from Huysman et al. (2014)).

1.2.2. *Phaeodactylum tricornutum*

Phaeodactylum tricornutum (fig 1.2) is a well-known model species for pennate diatoms (Brembu et al., 2011). This species is suggested to be found worldwide and is frequently used in toxicity assays (Torres et al., 2000). Earlier studies have suggested that *P. tricornutum* is highly tolerant to Cd, and a high concentration of Cd affected a large set of protein encoding genes that are responsible for metal transport, energy production, cell signaling and detoxification processes (Masmoudi et al., 2013). However, other uncharacterized pathways were expected to be involved in responding to Cd exposure (Brembu et al., 2011).

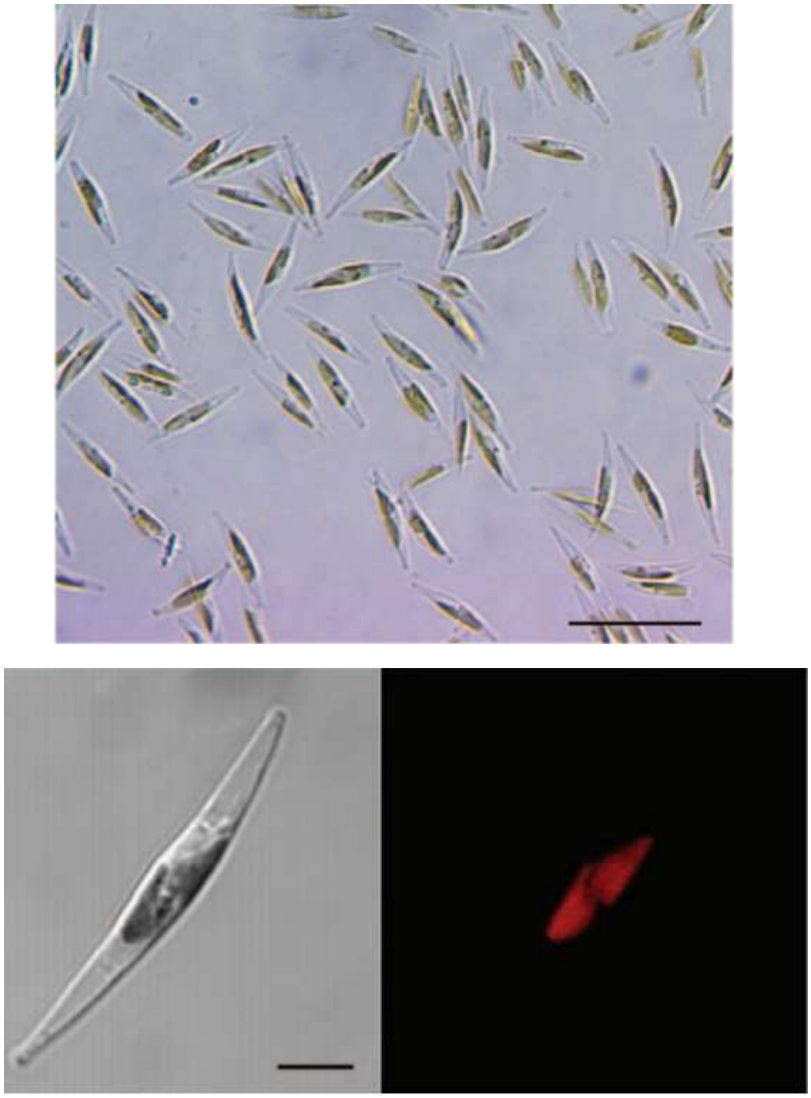

Figure 1.2. Illustration of *Phaeodactylum tricornutum*. (Top) light microscopy image. Scale bar = 50 µm (Bottom) Confocal laser scanning microscopy of a *P. tricornutum* cell (Left) transmission light (Right) autofluorescence of the chloroplasts in red. Scale bar = 5 µm. (Adapted from Huysman et al. (2014)).

1.3. Mechanisms of toxicity and tolerance

The principal mechanism of the toxic effects of Cd on algae is suggested to be the damage to enzymes. Cd exhibits specific forms of molecular mimicry that disrupts enzyme function. The essential metal in the enzyme is displaced by the Cd ion, which may block the ability to fulfil the biological activity. In this way, many metalloenzymes can be inhibited resulting in the inhibition of respiratory rate, cellular and growth processes (Torres et al., 2000).

Cd is capable of getting incorporated into chlorophyll resulting in the collapse of the photosynthesis process by preventing the usage of photosynthetic active light. Photosynthesis is the process of conversion of sun's radiant energy into biochemical energy (Mattoo et al., 1989). A crucial event during photosynthesis involve an integral membrane-protein complex

called reaction center (RC) which is the principal component of the photochemical conversion of light into chemical energy (Allen and Williams, 1998). It creates a charge separation across the thylakoid membrane after the incident of light. RC couples to secondary electron donors and acceptors, thus allowing the transfer of electrons and protons to other parts of the photosynthetic apparatus, which finally gets converted into chemically rich compounds such as ATP and NADP. Organisms such as algae, plants and cyanobacteria have two photochemical RCs embedded to the thylakoid membrane of the chloroplasts; photosystem 1 (PS1) and photosystem 2 (PS2). Their function is to move electrons against the redox potential gradient using the energy acquired through an excited chlorophyll. Electrons from water is being extracted by PS2 and passed on to PS1 through an electron transport chain. The electrons are then carried on to the low potential acceptors such as $NADP^+$ (Mattoo et al., 1989).

Metallic stress also results in ultrastructural changes such as partial mitochondrial degeneration, cytoplasmic vacuolization, membranous debris accumulation and formation of autophagosome. This indicates the cytotoxic effect by Cd and the alterations made by the cell to immobilize the toxic metal ions (Jamers et al., 2009).

Cd causes oxidative stress either by inducing the synthesis of reactive oxygen species (ROS) that in turn produces serious damage to macromolecules (Masmoudi et al., 2013) or by decreasing the concentrations of enzymatic and non-enzymatic antioxidants (Hasan et al., 2009). Cd is not a redox-active metal and thus will not take part in Haber-Weiss reaction (Clemens, 2006). However, symptoms of oxidative stress such as lipid peroxidation occur because of glutathione (GSH) depletion. This happens due to the binding of Cd^{2+} to GSH and the formation of GSH-derived phytochelatins (PCs).

Hydroxyl radicals (•OH) are very reactive and are capable of oxidizing biological macromolecules that lead to cellular damages such as DNA alterations, protein oxidation and lipid peroxidation. ROS is a general term for oxygen radicals such as superoxide ($O2•^-$) and hydroxyl radicals, and nonradical oxidizing agents like hydrogen peroxide (H_2O_2) (Bayr, 2005). ROS are generally formed as a natural byproduct of oxygen metabolism and has a crucial role in cell signaling and maintenance of homeostasis. Natural defense mechanisms involve both enzymatic and non-enzymatic antioxidant systems that scavenge the ROS. Non-enzymatic antioxidants include glutathione, phenolics and ascorbate, enzymatic defense include superoxide dismutase (SOD), glutathione reductase (GR), catalase (CAT) and a group

of peroxidases such as pyrogallol- and ascorbate-peroxidase (PPX and APX) (Morelli and Scarano, 2004).

Cytochrome P450 (CYP) proteins have diverse cellular functions such as serving an important role in the production of pigments, growth regulation and detoxification. They contain a heme cofactor. CYP enzymes convert the endogenous and exogenous compound into a more water soluble compound. Cd is suggested to reduce the production of CYP proteins because of increased heme degradation that is due to induction of heme oxygenase. This pathway is supposed to take place when GSH is limited and heme oxygenase is expected to supply the cells with antioxidants. Reduction in CYP protein levels would affect the potential of the organism to biotransform endogenous compounds and other xenobiotics (Andresen and Kupper, 2013).

Metals such as Cd act in at least four different ways to affect the expression of eukaryotic genes; (i) as an environmental signal eliciting a signal transduction response that alters the cellular gene transcription, (ii) as a cofactor mediating signaling protein function in transducing the environmental information to the genome, (iii) as modifier in altering messenger ribo-nucleic acid (mRNA) activity or stability, and (iv) as a cofactor for the activity of proteins (Ballatori et al., 2012).

In general, elements with similar physical and chemical properties interact antagonistically in the biological system. Part of the Cd toxicity is due to its interference in Zn-dependent processes. Cd and Zn tend to compete for the same transport and storage sites in the cell displacing the other in utilizing the reactive enzymes and receptor binding sites. On the other hand, selenium (Se) may act synergistically to Cd, while, copper (Cu) toxicity is inhibited by Cd (Das et al., 1998).

Cd is a strong inhibitor of ATPase activity probably because of the association of Cd^{2+} with proteic free radicals, mostly the –SH groups. This has a huge impact on the detoxification systems such as metallothionein (MT) (cysteine rich protein) synthesis and efflux pumps that consume energy (Torres et al., 2000).

Microalgae have developed the ability to produce peptides that can bind to heavy metals. The peptides are classified as group II and group III. The former is gene-coded, whereas, the latter is enzyme-synthesized (post-translational response). The short-chained peptides referred as group III peptides are called PCs or class III MT. Their amino acid structure is $(\gamma\text{-Glu-Cys})_n$,where n ranges from 2 to 11 depending on the species. Metal ions are bound with these

molecules by thiolate coordination (Torres et al., 1997). The PC pathway involves two steps i) metal-activated synthesis of peptides and the ii) transport of metal-PC complexes into the vacuole (Clemens, 2006). Cd^{2+} is the most potent activator of class III MT. MTIII are synthesized by the enzyme, phytochelatin synthase (PCS). However, under natural conditions, GSH is the substrate for MTIII synthesis and primarily involved in binding heavy metals. Besides facilitating an adequate control on the cytoplasmic concentration of Cd^{2+}, MTIII in its oxidized form is suggested to scavenge ROS (Perales-Vela et al., 2006).

The detoxification mechanism could also include the production of ferritin which is an iron-storage molecule that offers protection against oxidative stress (Armbrust, 2009).

Discovering a heavy metal resistant strain can help in bioremediation where diatoms could be used as living 'vacuum cleaners' to trap excess metal concentrations, but first the toxic effect on the next trophic level predator has to be thoroughly analyzed. Torres et al., (2014) demonstrated that *Phaeodactylum tricornutum* has a very good potential for bioremediation of Cd^{2+} ions in saline habitats (Torres et al., 2014). On the other hand, sensitive species can be strongly affected by Cd^{2+}. Species that do not adapt or detoxify either decline in abundance or disappear. Understanding ecological responses to environmental changes and interaction of the chemical with the species will help to define crucial chemical and molecular processes that help to maintain biodiversity and ecosystem functionality (Ianora et al., 2011). Studying diatoms in a controlled laboratory environment is suggested to be the first step in predicting the responses due to environmental changes.

1.4. Designing the research question

It has always been a daunting task to generalize the risks associated with heavy metals because of the following reasons (Chapman and Wang, 2000):

(i) Heavy metals occur naturally and the levels can increase to very high concentrations due to non-anthropogenic sources. As a result, organisms can and do adapt to a range of metal concentrations.
(ii) Metals can play an essential role in mediating the biotic health.
(iii) Adverse biological effects can only occur if metals are bioavailable.
(iv) The possibility of toxicity and bioavailability are generally determined by the external environmental conditions, for example pH and ligands.

Adverse effects may not be observed in the diatoms because of detoxification and adaptation. Adaptation is genetic in origin and it extends beyond the lifespan of the individual and takes

place without significant metabolic cost. Due to the fact that metals exist since the origin of the planet Earth, organisms are more or less adapted to the background levels of metals (Chapman and Wang, 2000).

1.5. Objective

The objective of this thesis was to compare the toxic effects of Cd in two marine diatoms *Seminavis robusta* and *Phaeodactylum tricornutum*. Different endpoints were observed at different biological organization levels. The endpoints were analyzed in order to have a deep understanding on the toxic effects and mechanisms of the potentially toxic compound.

It was hypothesized that *Seminavis robusta* possibly has a better tolerance mechanism than *Phaeodactylum tricornutum* because of an extensive secondary metabolism that is indicated by their expanded CYP gene family (Strøm Midthun, 2012). Also, because of their benthic lifestyle and tendency to stick on surfaces, the chances of encountering toxins from other living organisms in addition to environmental toxicants are high. Hence, it was speculated that *Seminavis robusta* has a well-developed defense system.

1.6. Working principle of the analytical techniques

In this section, the principle behind the analytical techniques used in this thesis are very briefly stated.

1.6.1 Flow cytometry

Flow cytometry is a technology that measures and analyzes multiple physical characteristics of cells through a beam of light as the cells flow in a fluid stream (Biosciences, 2000). The tendency of the cell to scatter the incident light and its fluorescence emission are recorded. After which, the physical characteristics are determined using the optical-to-electronic coupling system.

Light scatter: The extent to which the cell scatters the laser light that falls on it depends upon the cell's size and its internal complexity. Other factors include cell membrane, nucleus, granular material inside the cell, cell shape and surface topography. Forward-scattered light (FSC) is proportional to cell-surface area or size, whereas, side-scattered light (SSC) varies proportionally to the cell granularity or internal complexity *(fig 1.3).*

Fluorescence: A fluorescent compound absorbs light energy over a range of wavelength that is specific for the compound. This results in the excitation of electrons in the fluorescent

compound that re-emits the energy absorbed as photons of light. The term fluorescence refers to this transmission of light.

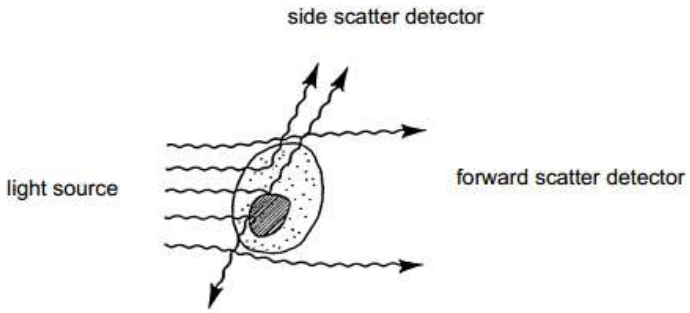

Figure 1.3. Light getting scattered after hitting the cell. (Adapted from the learning guide to flow cytometry (Biosciences, 2000)).

A holistic view on the principles of a flow cytometer is represented in *fig 1.4*.

A flow cytometer is comprised of three main systems: 1) fluidics (to transport the particles in a stream), 2) optics (lasers to illuminate the particles, optical filters to channel the light signals into the detectors) and 3) electronic system to convert the light signals into digital signals that can be processed by the computer.

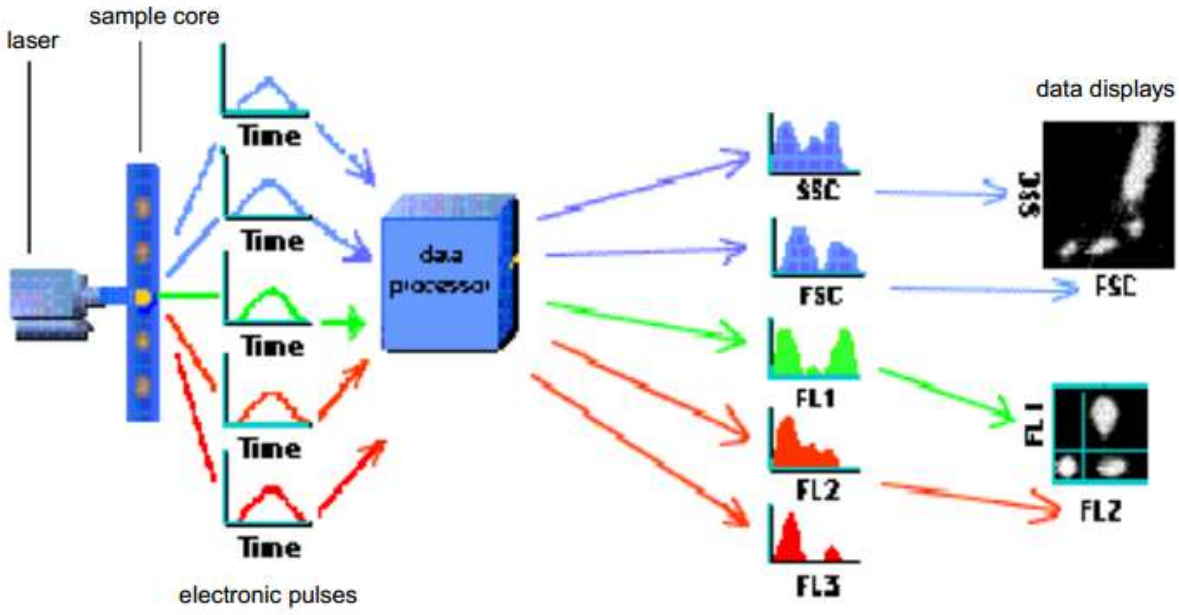

Figure 1.4. Laser beam passes through the sample core and depending on the requirements, the optical signals are collected using the appropriate filters and the data is represented as graph. (Adapted from the learning guide to flow cytometry (Biosciences, 2000)).

1.6.2 Chlorophyll fluorescence

A Photosynthetic process takes place under actinic irradiation, supply of water and CO_2 molecules. Molecules such as chlorophyll (Chl) and carotenoids absorb the incident photons and transfer the excitation energy to RCs of PS2 and PS1. Other competitive pathways for the utilization of photons include thermal dissipation (de-excitation in the form of heat), and chlorophyll fluorescence (ChlF) (radiative de-excitation of Chl molecules) (Rohacek and Bartak, 1999). Chlorophyll is a green color pigment and it absorbs all the non-green light such as the blue (~425-450 nm), the red and yellow (600-700 nm).

A toxic impact on photosynthesis at the molecular level is associated with low electron transport through PS2 or/and structural injury to PS2 and light-harvesting complexes (Guan et al., 2015).

Thus the principle behind ChlF analysis is relatively simple. Light energy absorbed by Chl a and c molecules in the diatom cells undergoes one of the three fates: driving photosynthesis (photochemistry), energy getting dissipated as heat or re-emitted as light- ChlF *(fig 1.5)*. The efficiency of one pathway results in the decrease of the other two possibilities. By measuring the yield of ChlF, information about photochemistry changes can be obtained.

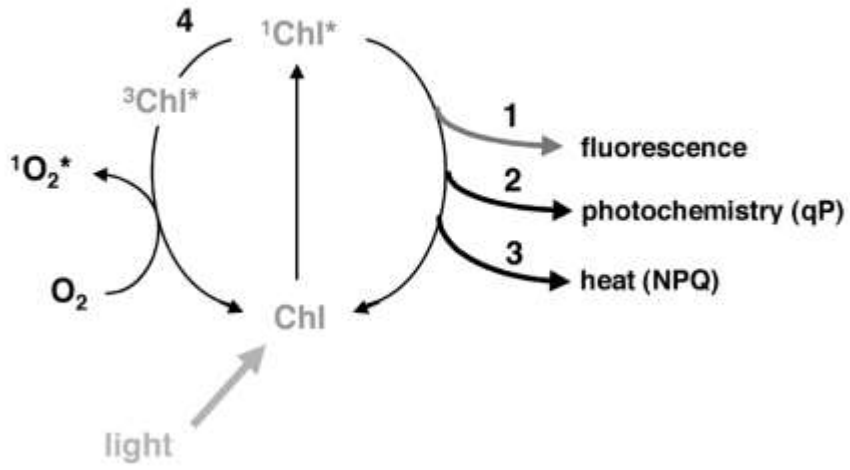

Figure 1.5. Possible fates of excited Chl. From the excited Chl* state, Chl relaxes to the ground state by emitting light as fluorescence or dissipating heat or fueling photosynthetic reactions. The last two mechanisms reduce the amount of fluorescence. (Adapted from Muller et al. (2001)).

Chl *a* fluorescence signal can be recorded with highest precision and expected to be very sensitive to photochemistry changes. Pulse amplitude modulated (PAM) fluorometers is inclusive of specific filters to isolate the effect of actinic light that drives photosynthesis from

the low-intensity probing light that measures fluorescence intensity. A high intensity short duration flash of light closes all the PS2 RCs. Under this condition, the fluorescence would be the maximum, Fm. This would be compared with the fluorescence value in the absence of photosynthetic light with functional RCs open. This value would be the minimum fluorescence value, Fo. Fluorescence by itself has no meaning and hence a well-defined reference method is applied for a proper interpretation of the data (Kalaji et al., 2014).

Quantum yield (Qy) is measured using the chlorophyll flourometer. The calculation behind the output (Rohacek and Bartak, 1999) is shown below:

$Qy = (F_v/F_m)$ A normalized ratio obtained by dividing variable fluorescence by maximum fluorescence. Where,

$F_v = (F_m-F_o)$ Maximum variable ChlF

F_o = Minimal ChlF measured with open RCs

F_m = Maximum ChlF measured with closed RCs

1.6.3 Real time- quantitative polymerase chain reaction (RT- qPCR)

Polymerase chain reaction (PCR) is used to estimate the initial quantity of specific template nucleic acid. It is a method to amplify the DNA sequences starting with a very tiny amount of DNA. By using the pre-existing DNA as the template, several copies are made using the enzyme DNA polymerase. The product obtained could be used for a variety of analyses including sequencing and cloning (Clark and Pazderbuj, 2013). The advantages of using PCR include sensitivity, reproducibility, dynamic range and throughput.

The components of PCR, in general include a DNA template (original DNA molecule), primers (single-stranded DNA segments that matches the sequence of interest), DNA polymerase (Taq polymerase from *Thermus aquaticus*), a supply of nucleotides and a PCR machine. A schematic representation of PCR mechanism is represented in *fig 1.6*.

In the traditional PCR methods, the end product after the last cycle is analyzed by running electrophoresis gels. This method gives no information about the initial concentration of the DNA used. This is overcome by using real time (RT) PCR, which measures the DNA concentration at the exponential phase of amplification.

In qPCR, the fluorescent signal through SYBR Green I dye, that intercalates between the double stranded DNA, is recorded. The cycle number at which the fluorescent signal of the

reaction crosses the threshold is referred as threshold cycle (Ct) or quantification cycle (Cq). It is obtained from the amplification curve (*fig 1.7*). Threshold is the level of the signal that reflects a statistically significant increase over the baseline signal. The threshold cycle number, Ct is used to calculate the initial DNA copy number. Ct is inversely related to the amount of the starting DNA template.

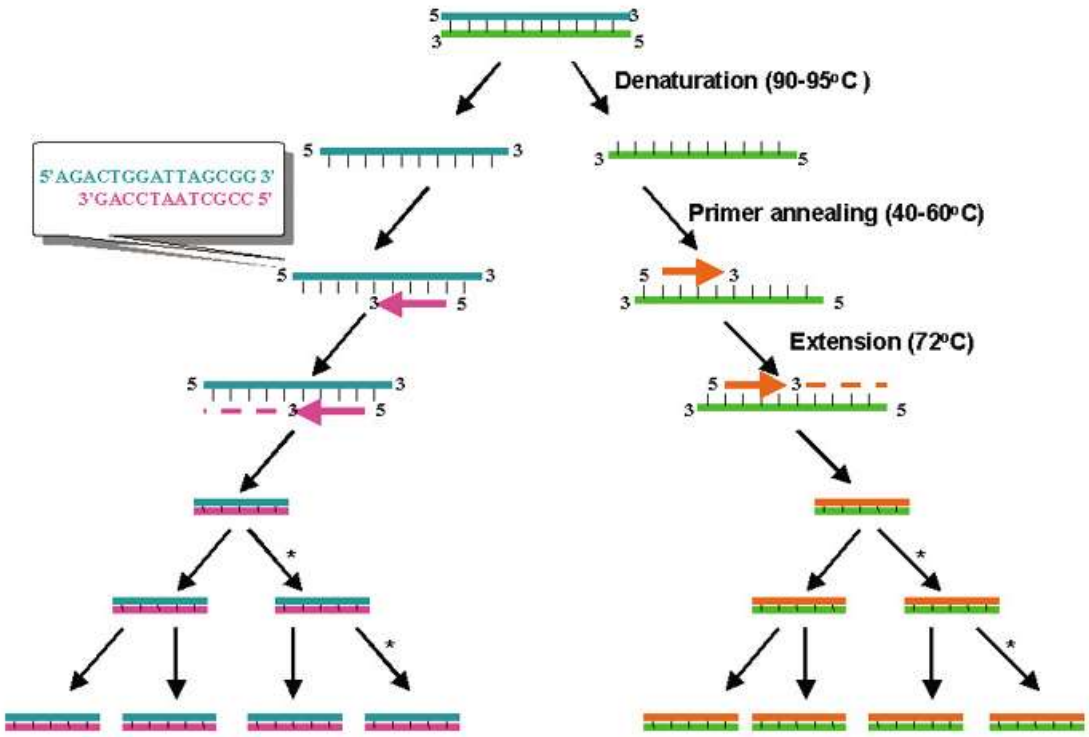

Figure 1.6. Each cycle of the PCR starts with heat denaturation of the double stranded DNA into single strands followed by the annealing of single stranded primers to the sequence of interest. As the final step, the annealed primer is extended using DNA polymerase and nucleotide triphosphates. The next cycle begins after the extension step. Amplified target sequence is obtained after repeated cycles. (Adapted from Kim and Gelder (2006)).

Amplification through SYBR Green I assay does not mean that the fluorescence signal was derived from the target gene. In order to check the reaction specificity, a dissociation analysis is performed using melting curves (*refer A.8 in appendix* for illustration). It charts the change in fluorescence observed when the double stranded DNA melts into single stranded DNA. A sudden decrease in fluorescence is detected when melting temperature (Tm) is reached due to the dissociation of DNA strand and subsequent release of the dye. When the change in fluorescence divided by change the temperature is plotted against temperature, a peak is obtained. Ideally only one peak should be observed. This indicates that the reaction was highly specific.

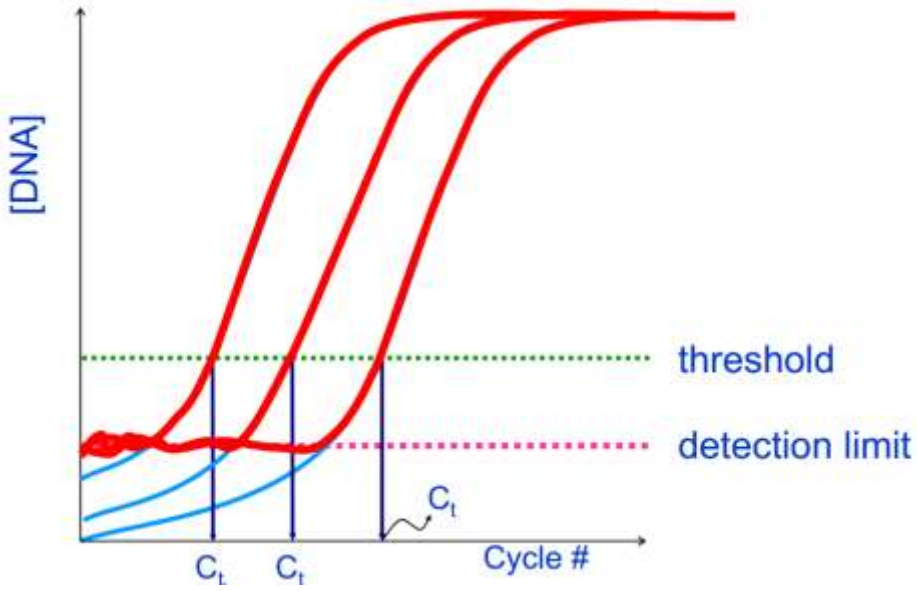

Figure 1.7. Ct is the PCR cycle number at which the intensity of the fluorescence signal, indicated by DNA intercalating SYBR Green I, crosses the threshold value of fluorescence in the exponential phase. (Adapted from (Cutler)).

2. MATERIALS AND METHODS

The experimental methodology of this study is described in this section. Background theory on the experimental techniques is briefly described in chapter 1.5. Recipes of the solutions and their preparation procedures are enclosed in the appendix.

2.1. Experimental design

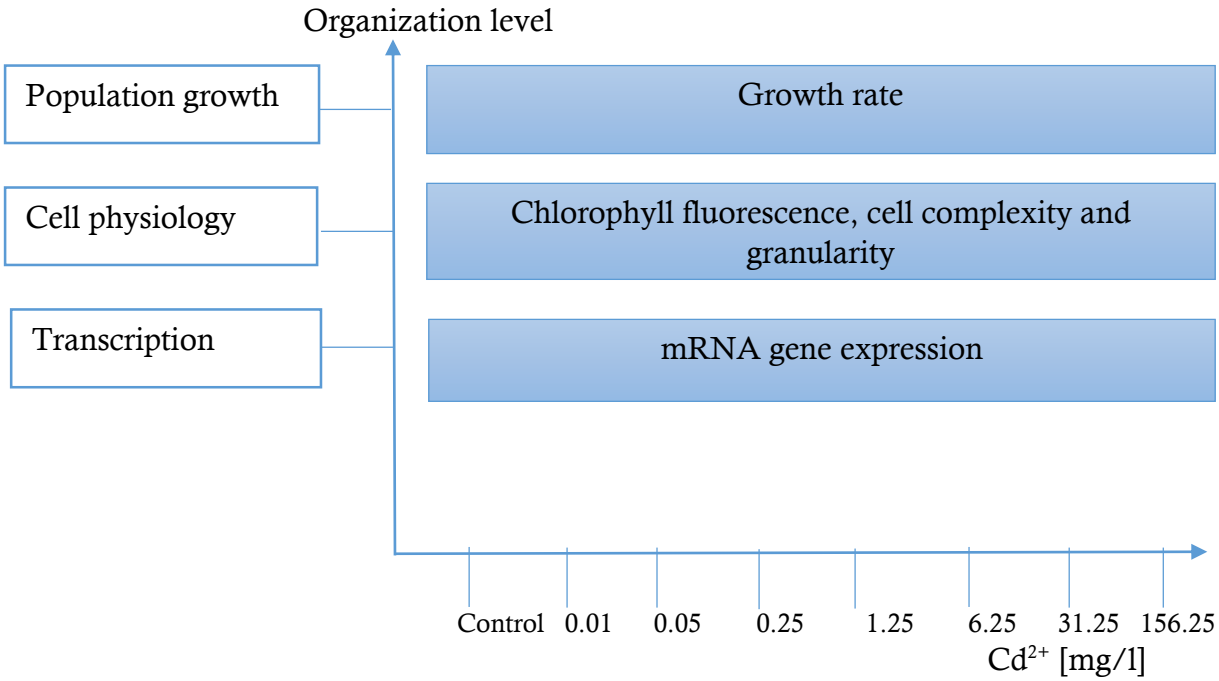

Figure 2.1. Outline of experimental set up of the thesis. Diatoms were exposed to seven different concentrations of cadmium for a period of three days *(Seminavis robusta)* and five days *(Phaeodactylum tricornutum)*. Different endpoints at three different biological levels were observed and analyzed.

2.2. Diatom growth observation

In order to understand the growth pattern of the diatoms in batch culture, a preliminary observation was carried out during summer 2015 using f/2 medium (Guillard and Ryther, 1962) as the growth medium.

Cultures of *Seminavis robusta* D6 were prepared from cryopreserved cultures obtained from the PAE culture collection of diatoms from Ghent University, Belgium.

Phaeodactylum tricornutum Bohlin clone CCMP2561 obtained from the culture collection of 'Provasoli-Guillard National Center for culture of marine phytoplankton, Bigelow laboratory for ocean sciences, USA' was used in this study.

2.3. Diatom cultivation

Choosing the appropriate growth medium for the study is a crucial factor considering the metal utilization and toxicity in algae, because, the biological availability and the toxicity of metals are strongly dependent on the properties of the growth medium. Control of trace metal speciation is extremely necessary for Cd - diatom interaction research (Morel and Rueter, 1979). In order to achieve this, aquil medium was utilized to culture the diatoms. The medium was prepared according to Price et al. (1989) (*refer A.1 in the appendix*). The glassware used in the medium preparation were acid washed to avoid trace metal contaminants into the medium (*refer A.2 in the appendix*).

Aquil medium is a synthetic ocean water (SOW) enriched with macro- and micronutrients. The primary objective of the design of aquil medium was to know the trace metal speciation in the medium as precisely as possible. This medium has been also considered to be suitable for toxicity of metals such as copper, zinc, nickel, cobalt, mercury, lead and cadmium that remain primarily in the cationic form in the aquatic systems. Additional advantage of using the aquil medium was that it makes precipitation of various solids thermodynamically unfavorable since it has sufficiently low concentrations of major nutrients and trace metals. Most importantly, this tends to closely imitate the natural conditions in ocean water. The origin of aquil could be easily traced to the standard recipes: vitamins are similar to the f/2 medium and the nutrients and trace metals are approximately 50-fold dilution of the medium f (Morel and Rueter, 1979).

Exactly 5 ml of the diatom culture cells that had acclimatized to the experimental conditions for more than 2 weeks was added to 50 ml of aquil medium in a 75cm^2 sterile cell culture flask. The pH of the medium was 7.9. Diatom cells were grown at an irradiance of approximately 150 µmol photons m^{-2} s^{-1} under a 16:8 light cycle at 22 ± 1^oC in light photoperiod and at 18 ± 1^oC in dark photoperiod.

Sterility was monitored by inoculating the diatom culture into peptone enriched f/2 medium in the dark. Peptone nourishes bacteria if present in the culture. Dark conditions permit the selective growth of bacteria and not that of the diatoms. The test was carried out by adding 0.5 ml of culture to tubes containing 5 ml of f/2 added 1 mg/ml peptone. The tube was wrapped in an aluminum foil and stored under dark conditions for a period of 7 days. The presence of bacteria was checked by monitoring the turbidity of the solution. The culture used in this study was slightly turbid and not completely axenic.

2.4. Exposure to contaminants

A wide range of concentrations were chosen for exposure, starting from 0.01 mg/l of Cd^{2+} up to 156.25 mg/l of Cd^{2+} with five time concentration increase after each dose level (*ref A.3 in the appendix*). The different exposure groups were control, 0.01 mg/l, 0.05 mg/l, 0.25 mg/l, 1.25 mg/l, 6.25 mg/l, 31.25 mg/l, and 156.25 mg/l of Cd^{2+} in the growth medium.

Cross contamination was monitored on a daily basis, and homogenous mixtures were used in the study. In order to ensure uniform exposure to the diatoms, the flasks were frequently shaken in the culture room.

Both the species of diatoms, *S. robusta* and *P. tricornutum* were cultured under the same conditions (media, illumination, temperature). In order to avoid cross contamination, two different laboratories were employed for the analysis.

2.5. Diatom cell counting

The first set of experiments focused on observing the effect of Cd on the growth rate and the chlorophyll fluorescence of diatoms. Two independent experiments were carried out in order to ensure reproducibility and accuracy, in flask 1 and flask 2.

Cell concentration (number of diatom cells per ml) helps in studying the rate of cell division and in harvesting the diatoms for RNA, DNA, and protein analyses. Inhibition of growth that could be inferred by the reduction in the number of diatom cells with increasing Cd concentrations has always been perceived as a good indicator of Cd toxicity (Torres et al., 2000).

The cells were counted every day after the inoculation at the same time and plotted on a graph. Both *S. robusta* and *P. tricornutum* cells were counted using a flow cytometer.

S. robusta cells adhere to the bottom and hence scraped using a 25cm sterile scraper to make a homogenous suspension. *P. tricornutum* flasks were gently shaken before sampling. Homogenous sample aliquots of few ml of the cell suspension were used for counting. Counting was performed using NovoCyte flow cytometer 2000.

The filter parameters used was BL4 alias PerCP. With the help of gating, noise from debris, doublets and microorganisms were avoided from getting included in the cell count. The absolute count of cells was noted directly from the computer. Rinsing was done after each sample to avoid contamination. The samples were vortexed before loading and analyzed one at a time. This ensures accuracy of data by eliminating error due to the benthic nature of diatoms which settle at the bottom. An illustration of the calculation of absolute cell count using flow cytometry and the data obtained are presented in the appendix (*refer A.7, A.10 in the appendix*).

2.6. Chlorophyll fluorescence

Chl Fluorometer (Aquapen-C AP-C 100) was used for measuring ChlF. Approximately 1.5ml of the sample aliquot was used for the measurement of Qy. The reading was noted after 1 minute of loading the sample. Qy value for *S. robusta* and *P. tricornutum* were directly read from the display.

2.7. Diatom harvesting

Diatoms cells were exposed to three different concentrations of Cd^{2+} (0.01 mg/l, 0.05 mg/l and 1.25 mg/l) and harvested by centrifugation at two time intervals (after 48 hours and 72 hours). This was done in order to observe changes in gene expression by quantifying mRNA during the exponential phase of growth. About 50 ml of the aliquot was taken and transferred into a 50 ml falcon tube. After centrifugation at 4500 Xg for 15 minutes at room temperature, pellets were obtained. The supernatant was discarded and the pellet was resuspended and transferred into a 2 ml tube. This was centrifuged again at 4300 Xg for 1 minute at room temperature. After removing the supernatant, the pellet was frozen in liquid nitrogen and stored at -80^{o}C.

2.8. Gene expression analysis

In order to observe the toxic effects of Cd on the regulation of genes, qRT- PCR was performed. Toxic effects due to Cd exposure may not be evident at the population level, but still there might exist remarkable effects at the molecular level of the organism. Gene expression studies may serve as early warning indicators in risk assessment of potential toxicants.

2.8.1. RNA isolation

Frozen samples of diatom cells mounted on a pre-cooled adapter set were homogenized using a Tissue Lyser (Qiagen) for 2 minutes at 25 Hertz. RNA isolation was performed using Spectrum™, Plant total RNA kit (Sigma Aldrich). Eluted total RNA was quantified using a Nanodrop ND-100 Spectrophotometer (Nanodrop technologies). All the values for A260/A280 were above 2. Besides this, RNA integrity was checked on a 2100 Bioanalyzer (Agilent) using the assay class: plant RNA nano. The RNA integrity number (RIN) were above 7.90 (*S. robusta*) and above 6.70 (*P. tricornutum*). Thus, RNA obtained was of high quality.

2.8.2. cDNA synthesis

From the mRNA, complementary DNA (cDNA) was synthesized using the QuantiTect Reverse Transcription Kit (Qiagen). This was performed in order to convert the RNA obtained into double-stranded cDNA for further PCR analysis.

2.8.3. qPCR

cDNA obtained was diluted in the ratio of 1:10 with autoclaved milliQ water. Exactly 5 µl of the diluted cDNA was added along with 15 µl of the corresponding Master Mix (*refer A.4 in the appendix*) in a 96-well PCR plate. The PCR plates were run on Light Cycle 96 instrument (Roche). Program details of the PCR runs are shown in the table below (*Table 2.1*).

Table 2.1. RT-qPCR program

Step	Temperature [^{o}C]	Duration [seconds]	Number of cycles
PreIncubation	95	600	1
Amplification	95	10	45
	55	10	
	72	10	
Melting	95	5	1
	65	60	
	97	1	
Cooling	37	30	1

The details of all primers used for nine different target genes are enclosed in the appendix (*refer A.5*).

Quantification cycle (Cq) for each well in the 96-well plate was taken from the output of the Light Cycler 96. These values were the input for analysis using qbase+. The mean PCR efficiency of each gene required by qbase+ was calculated using LinReqPCR software. The slope of the amplification curve in its exponential phase gives the PCR efficiency of each sample. Only samples with PCR efficiencies above 1.8 were used for this study.

The gene expression ratio was analyzed automatically based on reference genes. geNorm is a unique feature embedded in qbase+ that helps in the selection of suitable reference genes. Each gene belonging to the set of candidate reference genes is allotted a specific value and those with the lowest values are suggested to be used for gene expression analysis. For *S. robusta*, the reference genes used were, aggrecan 1 (AGC1), histone H4A (H4A), vacuolar protein sorting 35 (VPS35). The reference genes used in *P. tricornutum* were ribosomal protein s5 (RPS5) and dihydrolipoamide s-succinyltransferase (DLST).

The advantage of qbase+ is the range of statistical analysis available. The data was automatically detected to be normally distributed and the system suggested One-way ANOVA for data analysis.

2.9. Data handling

Data analysis in this thesis was performed using Excel 2013. Software programs used include NovoExpress (1.2.1), NanoDrop 1000 (3.7.1), Agilent 2100 Expert (B.02.08.SI648 (SR2)), LightCycler 96 (1.1), LinReqPCR (2014.5), qbase+ (2.6.1 (201403031710). A one-way ANOVA was performed to analyze the PCR results.

3. RESULTS

An overview of the results observed while exposing two different species of diatoms (*S. robusta* and *P. tricornutum*) to three different concentrations of Cd (0.01, 0.05, 1.25 mg/l Cd^{2+}) during the exponential phase (48 hours) can be found in *fig 3.1* and *3.2*.

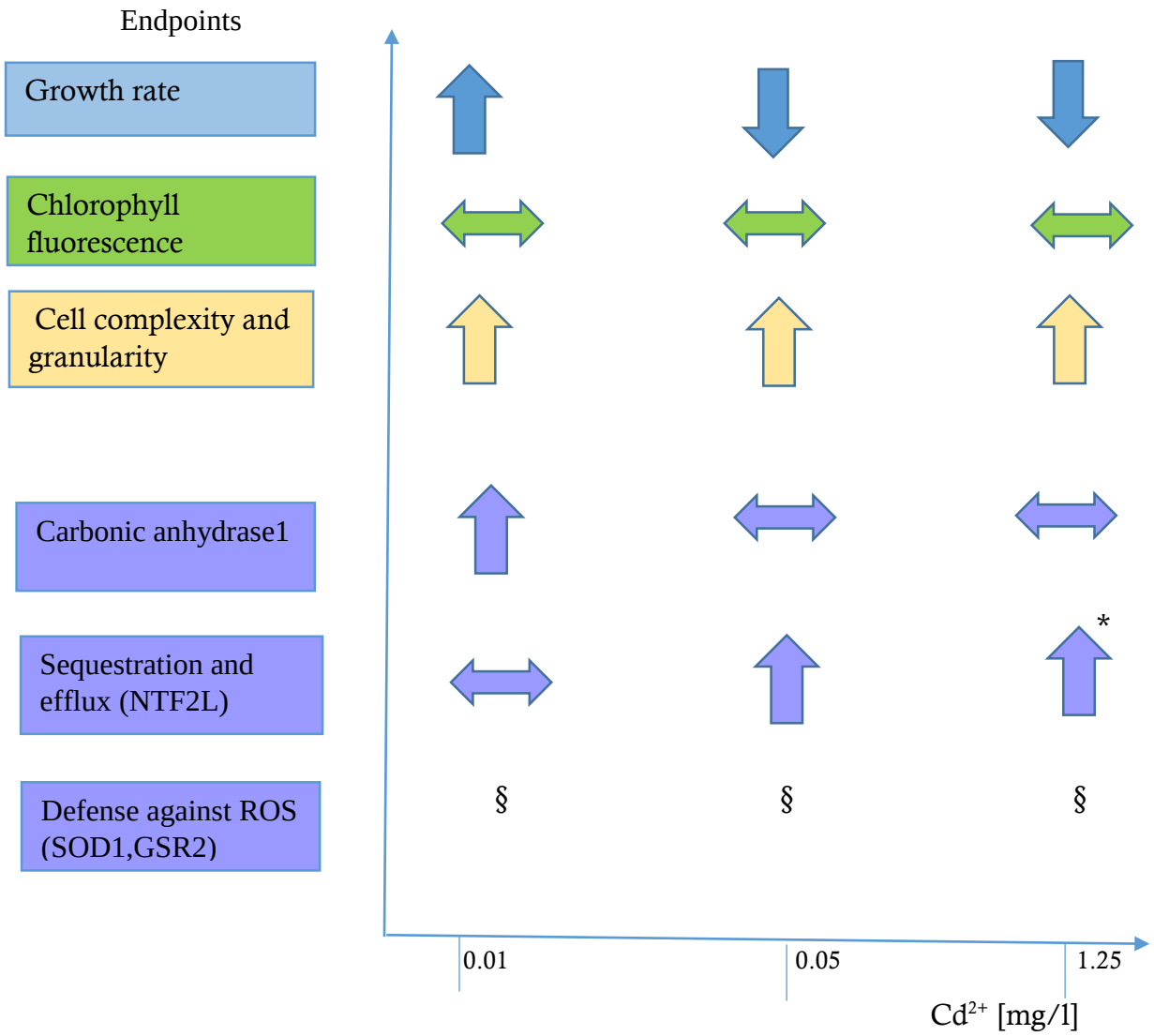

Figure 3.1. An overview of the results: *S. robusta* exposed to three concentration levels of Cd^{2+} for 48 hours.

⇧ Increase in response ⇩ Decrease in response ⇔ No significant change in response

§ - Excess background noise * Significant data

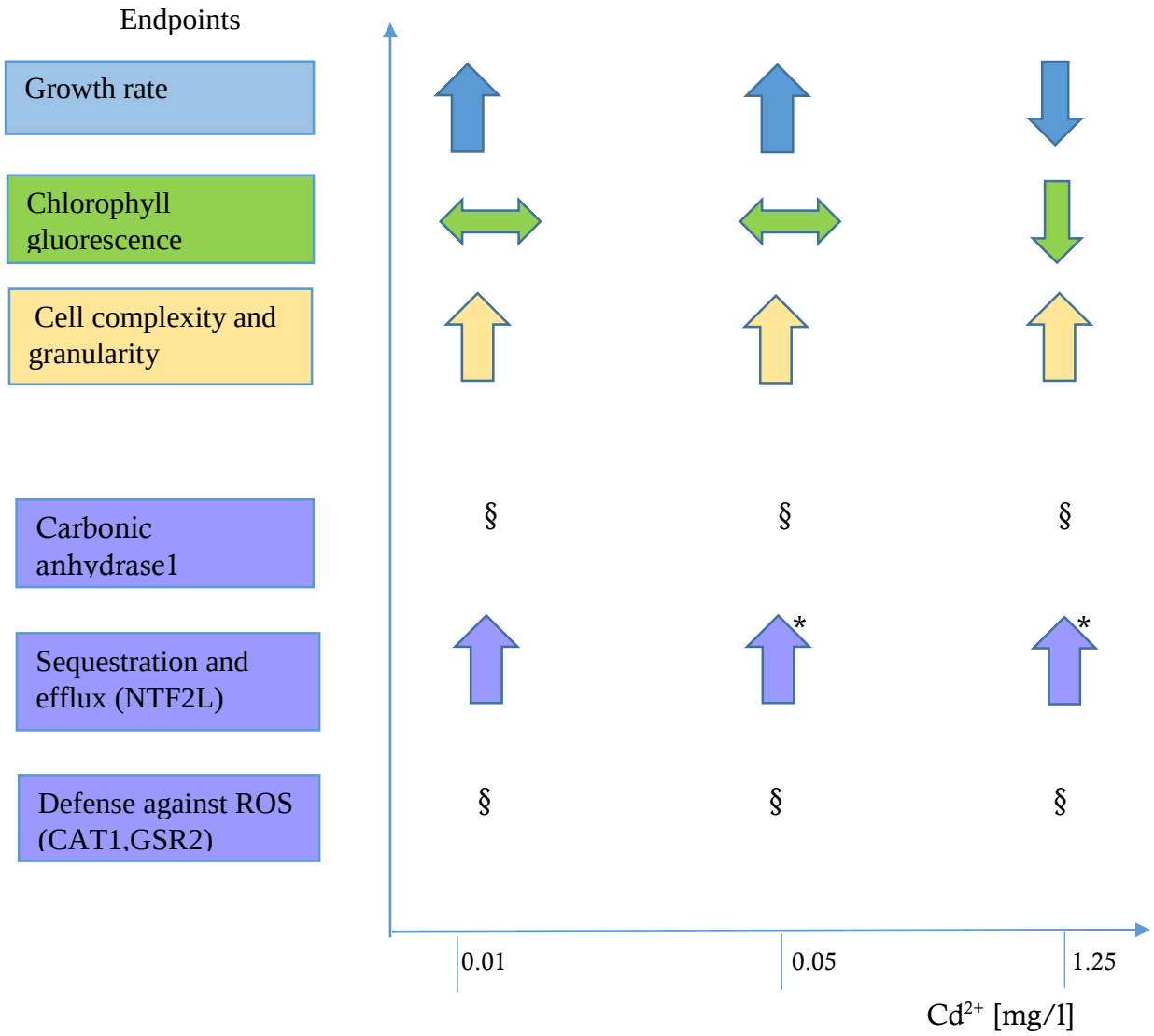

Figure 3.2. An overview of the results: *P. tricornutum* exposed to three concentration levels of Cd^{2+} for 48 hours.

⇧ Increase in response ⇩ Decrease in response ⇔ No significant change in response

§ - Excess background noise * Significant data

3.1. Effect on Growth

The population growth was studied using the number of living cells as the parameter to check the impact of Cd on diatom growth. The cell number was counted based on a proxy measurement of chlorophyll concentration which tends to be linearly correlated to the cell number. The cell numbers were recorded until the stationary phase of growth *(fig 3.3 and fig 3.4)*. In *S. robusta* and *P. tricornutum*, results indicate that low Cd^{2+} concentration exposure groups showed an increase in the cell count that varies from 10 to 50 percent increase when compared to the control during the exponential phase of growth.

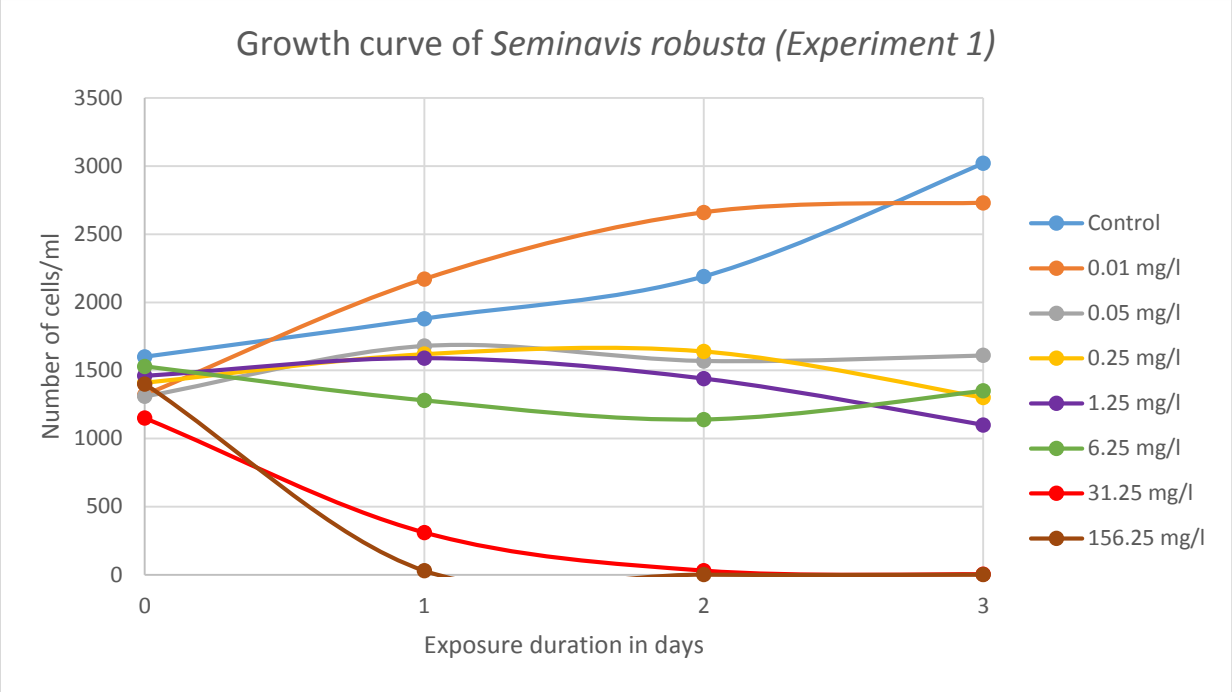

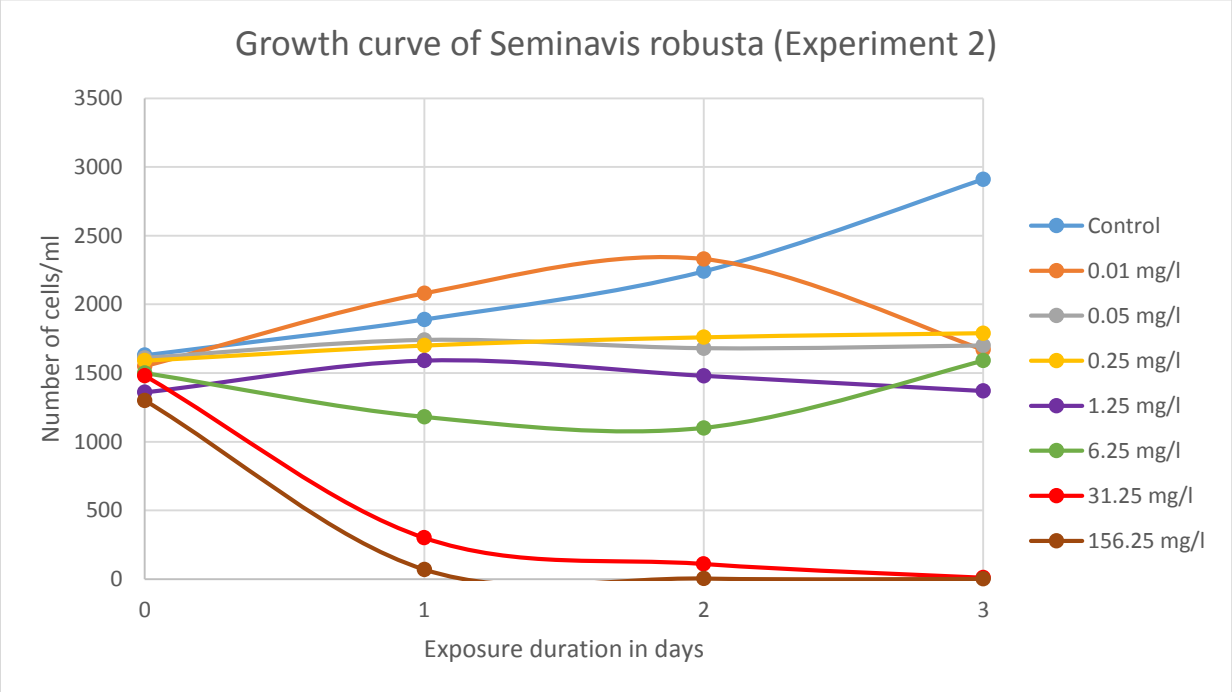

Figure 3.3. Population growth rate of *Seminavis robusta* analyzed using flow cytometer for seven different Cd^{2+} exposure groups during a period of three days through two independent experiments. Different colors represent the different exposure groups used in the experiment. Values are represented as the cell count.

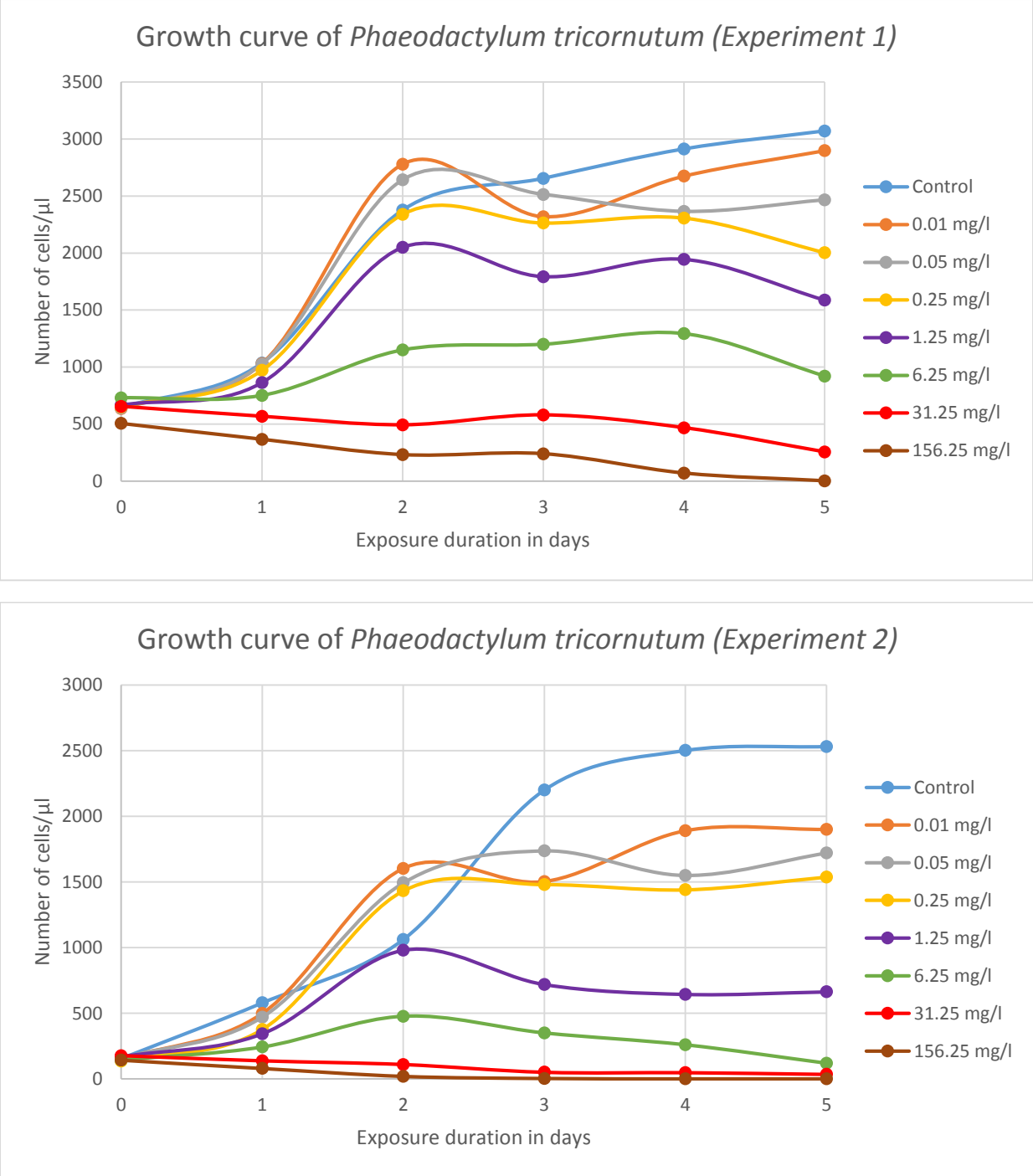

Figure 3.4. Population growth rate of *Phaeodactylum tricornutum* analyzed using flow cytometer for seven different Cd^{2+} exposure groups during a period of five days through two independent experiments. Different colors represent the different exposure groups used in the experiment. Values are represented as the cell count.

Growth rate (µ) during the exponential phase was calculated based on the rate of increase in the number of cells proportional to the initial cell count at the unit of time *(table 3.1 and table 3.2).* The data is expressed as percentage of control (Andersen, 2005) (*refer A.6 in the appendix for calculation illustration*). For *S. robusta*, it was inferred that except the first and third

exposure group (0.01 and 0.25 mg/l Cd^{2+}), live cell count did not increase and the value of μ was close to 0.

Table.3.1. Growth rate (μ) through two independent experiments calculated during the exponential phase of *Seminavis robusta* exposed to seven different concentrations of Cd^{2+} (expressed as percentage of control).

Group exposed	**Growth rate (μ) in *Seminavis robusta***							
	Control	**0.01 mg/l**	**0.05 mg/l**	**0.25 mg/l**	**1.25 mg/l**	**6.25 mg/l**	**31.25 mg/l**	**156.25 mg/l**
Expt 1	100	133	~0	8	~0	~0	~0	~0
Expt 2	100	67	~0	20	~0	~0	~0	~0

Expt-Experiment

Table.3.2. Growth rate (μ) through two independent experiments calculated during the exponential phase of *Phaeodactylum tricornutum* exposed to seven different concentrations of Cd^{2+} (expressed as percentage of control).

	Growth rate (μ) in *Phaeodactylum tricornutum*							
Group exposed	**Control**	**0.01 mg/l**	**0.05 mg/l**	**0.25 mg/l**	**1.25 mg/l**	**6.25 mg/l**	**31.25 mg/l**	**156.25 mg/l**
Expt 1	100	92	81	83	78	52	3	~0
Expt 2	100	91	82	92	43	5	~0	~0

Expt-Experiment

For *P. tricornutum*, approximately 50% reduction in growth rate was observed in the first experiment at 6.25 mg/l of Cd^{2+} in the medium and at 1.25 mg/l of Cd^{2+} in the second experiment.

3.2. Effect on Chlorophyll

Toxic effect on the photosynthesis process was indirectly measured using the Qy value. Lower value of Qy when compared with control indicates less functional RCs and it is an indication of stress *(table 3.3 and table 3.4)*.

S. robusta values show that there was a notable reduction in the Qy value at 31.25 mg/l of Cd^{2+} after 24 hours of exposure. The other exposure groups did not show a notable change. However, almost no fluorescence was observed at 156.25 mg/l of Cd^{2+}.

P. tricornutum values show that there was a reduction in the 1.25 mg/l Cd^{2+} exposure group after 24 hours. The other exposure groups did not show a notable change. It has to be noticed that even at very high concentrations (156.25 mg/l) of Cd^{2+}, *P. tricornutum* showed fluorescence activity and continued to survive.

The decrease in Qy could also be because of higher number of cells rather than decrease in fluorescence value of the culture. Due to confounding effect of the cell density, data after 72 hours exposure is not considered.

Table.3.3. Quantum yield (Qy) through two independent experiments recorded in *Seminavis robusta* culture after exposure to seven different concentrations of Cd^{2+} for three days.

	Qy in *Seminavis robusta* (Experiment 1)							
Day	**Control**	**0.01 mg/l**	**0.05 mg/l**	**0.25 mg/l**	**1.25 mg/l**	**6.25 mg/l**	**31.25 mg/l**	**156.25 mg/l**
1	0.58	0.64	0.58	0.61	0.61	0.58	0.3	-
2	0.67	0.64	0.62	0.65	0.66	0.6	-	-
3	0.4	0.46	0.48	0.38	0.38	0.43	-	-
	Qy in *Seminavis robusta* (Experiment 2)							
Day	**Control**	**0.01 mg/l**	**0.05 mg/l**	**0.25 mg/l**	**1.25 mg/l**	**6.25 mg/l**	**31.25 mg/l**	**156.25 mg/l**
1	0.62	0.62	0.63	0.62	0.6	0.6	0.44	-
2	0.7	0.68	0.67	0.69	0.68	0.58	-	-
3	0.57	0.61	0.6	0.58	0.49	0.59	-	-

Table.3.4. Quantum yield (Qy) through two independent experiments recorded in *Phaeodactylum tricornutum* culture after exposure to seven different concentrations of Cd^{2+} for five days.

	Qy in *Phaeodactylum tricornutum* (Experiment 1)							
Day	**Control**	**0.01 mg/l**	**0.05 mg/l**	**0.25 mg/l**	**1.25 mg/l**	**6.25 mg/l**	**31.25 mg/l**	**156.25 mg/l**
1	0.64	0.64	0.64	0.65	0.59	0.54	0.48	0.28
2	0.68	0.69	0.69	0.69	0.68	0.65	0.61	0.27
3	0.48	0.51	0.51	0.52	0.55	0.49	0.49	0.26
4	0.38	0.41	0.41	0.44	0.45	0.42	0.42	0.28
5	0.35	0.4	0.41	0.43	0.46	0.39	0.39	-
	Qy in *Phaeodactylum tricornutum* (Experiment 2)							
Day	**Control**	**0.01 mg/l**	**0.05 mg/l**	**0.25 mg/l**	**1.25 mg/l**	**6.25 mg/l**	**31.25 mg/l**	**156.25 mg/l**
1	0.71	0.72	0.71	0.7	0.68	0.64	0.58	0.27
2	0.68	0.68	0.69	0.69	0.68	0.64	0.51	0.17
3	0.57	0.61	0.61	0.62	0.52	0.48	0.45	-
4	0.45	0.46	0.49	0.51	0.44	0.37	0.4	-
5	0.37	0.41	0.44	0.46	0.41	0.42	0.4	-

- Almost no fluorescence observed

3.3. Effect on cell complexity and granularity

Metals that enter the algal cell are most frequently trapped in the intercellular sites. Suggestively they are precipitated in the polyphosphate granule. The other cellular compartment that plays a vital role in metals sequestration is the vacuole (Prasad, 2001). In general, the side scatter pulse area data (SSC-A) from flow cytometry is analyzed to reflect the "granularity" of the cells. Cells that contain a more complex internal structure tend to scatter light in all directions that was recorded by the side scatter detectors (Chioccioli et al., 2014). An increased Y-axis value of a plot with FSC-A against SSC-A was an indication of increase in granularity. An increase in X-axis value was due to result in the size increase. The flow cytometry data was analyzed and granularity was determined.

For *S. robusta*, the flow cytometric analysis indicated an increasing trend in granularity and complexity of cells with an increase in exposure duration. A similar trend as was described for *S. robusta* was observed for *P. tricornutum*.

However, there was a decrease in the cell granularity and complexity with increase in Cd^{2+} concentration in the growth medium in *P. tricornutum*. *S. robusta* did not show a huge difference in cell granularity and complexity with increasing Cd^{2+} concentration in the medium.

3.4. Effect on mRNA gene expression

The regulation of various genes due to Cd^{2+} exposure was studied using mRNA templates using RT-qPCR. Nine different genes were analyzed as target genes (*refer A.5 in appendix*). Cq values of all the genes analyzed are enclosed in the appendix (*refer A.9*). Three independent experiments were conducted and the data presented is the average of the triplicates. The column "ratio" represents the fold change between the experimental group and the control group (*Table 3.5 and 3.6*). The control group holds a value 1. If the ratio of the experimental group is greater than 1, the gene is up-regulated. If the ratio of the gene is less than 1, then it is downregulated. An additional method to analyze the data is by plotting a bar chart for the gene expressions in various Cd^{2+} exposure groups. The 95% confidence intervals are represented as standard deviation.

Seminavis robusta: There were insignificant changes in the expression of the target genes related to growth. The highest upregulation of carbonic anhydrase 1 (CA1) was recorded for the 0.01 mg/l Cd^{2+} group after 48 hours of exposure (*fig.3.5).* No remarkable effect was observed with cyclin b 1 (CYCB1) on the three different exposure groups (*fig. 3.6*).

There was a significant level (p=0.001) of approximately 10 fold induction in the expression of nuclear transporter factor 2- like (NTF2L) gene (*fig.3.7).* Also, the expression of heavy metal ATPase 2 (HMA2) clearly increased with increasing concentration of Cd^{2+} although not significantly (*fig. 3.8*).

CA1

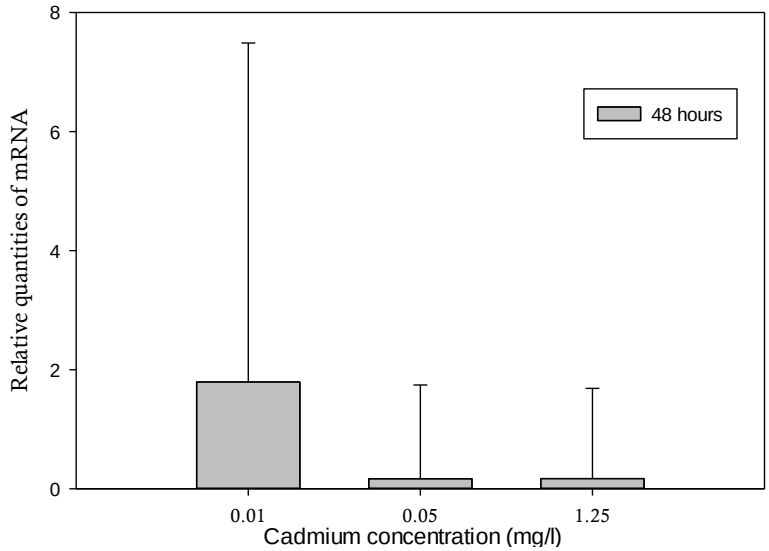

Figure 3.5. Bar chart of CA1 expression in *S. robusta*. X axis shows the experimental conditions, and the gene expression ratio is given on Y axis (mean±SD, n=3, p=0.3). The control sample is set to 0.

CYCB1

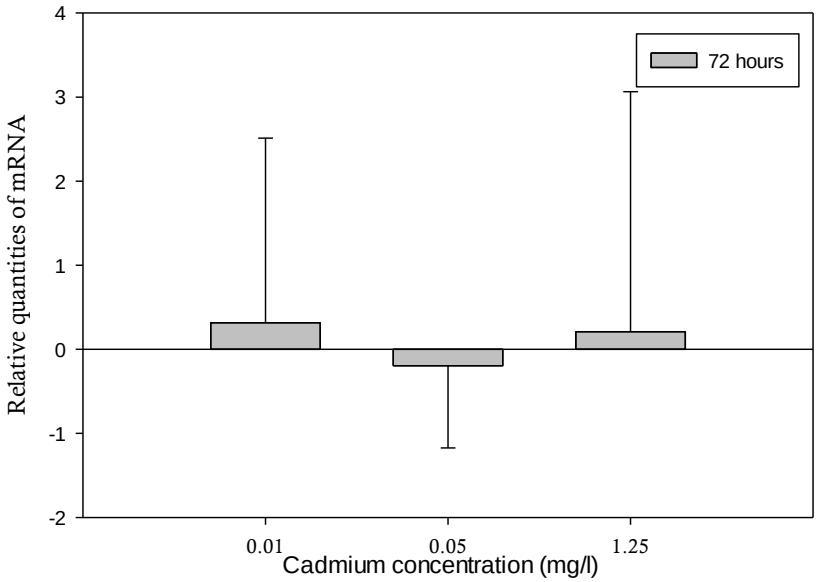

Figure 3.6. Bar chart of CYCB1 expression in *S. robusta*. X axis shows the experimental conditions, and the gene expression ratio is given on Y axis (mean±SD, n=3, p=0.9). The control sample is set to 0.

NTF2L

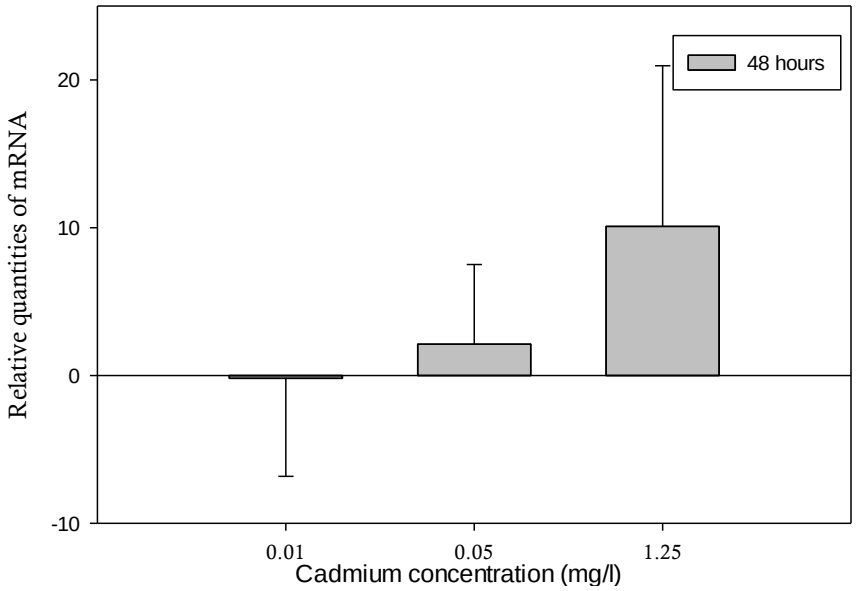

Figure 3.7. Bar chart of NTF2L expression in *S. robusta*. X axis shows the experimental conditions, and the gene expression ratio is given on Y axis (mean±SD, n=3, p=0.001). The control sample is set to 0.

HMA2

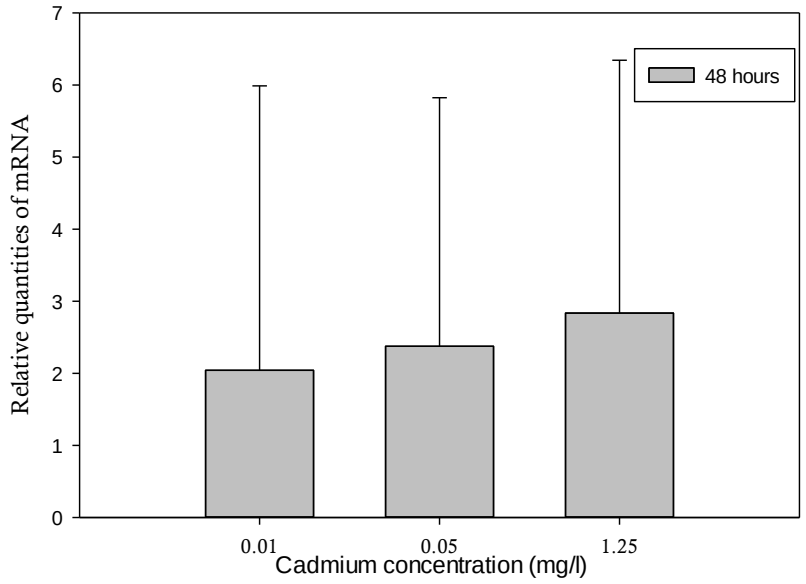

Figure.3.8. Bar chart of HMA2 expression in *S. robusta*. X axis shows the experimental conditions, and the gene expression ratio is given on Y axis (mean±SD, n=3, p=0.6). The control sample is set to 0.

An insignificant increase in the expression of superoxide dismutase 1 (SOD1) was recorded at 1.25 mg/l exposure group (*fig.3.9*).

SOD1

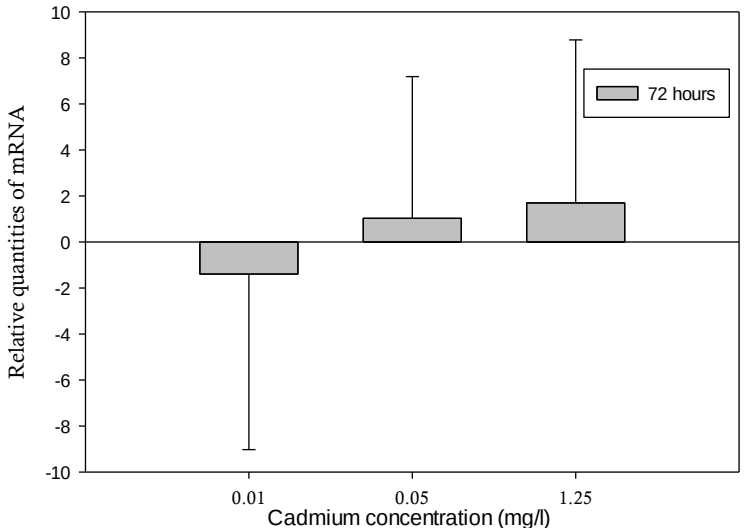

Figure.3.9. Bar chart of SOD1 expression in *S. robusta*. X axis shows the experimental conditions, and the gene expression ratio is given on Y axis (mean±SD, n=3, p=0.9). The control sample is set to 0.

Table.3.5. Genes showing transcriptional response in *S. robusta* in three different concentrations of Cd^{2+} (0.01, 0.05, 1.25 mg/l) after 48 and 72 hours of exposure.

ci- confidence interval

Gene	Exposure groups	Mean gene expression	95% value ci low	95% value ci high
CA1 (p=0.32)	48hrs_0	1.000E+000	3.434E-001	2.912E+000
	48hrs_0.01	3.466E+000	2.173E-001	5.528E+001
	48hrs_0.05	1.124E+000	3.078E-001	4.103E+000
	48hrs_1.25	1.125E+000	3.173E-001	3.986E+000
CYCB1 (p=0.85)	48hrs_0	1.000E+000	1.395E-001	7.171E+000
	48hrs_0.01	9.576E-001	1.497E-002	6.125E+001
	48hrs_0.05	5.052E-001	8.204E-002	3.111E+000
	48hrs_1.25	8.446E-001	1.699E-001	4.199E+000
NTF2L (p=0.001)	**48hrs_0**	**1.000E+000**	**2.233E-005**	**4.478E+004**
	48hrs_0.01	**8.740E-001**	**7.624E-003**	**1.002E+002**
	48hrs_0.05	**4.332E+000**	**4.026E-001**	**4.661E+001**
	48hrs_1.25	**1.096E+003**	**4.055E+002**	**2.963E+003**
HMA2 (p=0.6)	48hrs_0	1.000E+000	5.953E-004	1.680E+003
	48hrs_0.01	4.113E+000	8.645E-001	1.956E+001
	48hrs_0.05	5.185E+000	1.668E+000	1.612E+001
	48hrs_1.25	7.134E+000	2.747E+000	1.853E+001

PCS1 (p=0.44)	48hrs_0	1.000E+000	7.819E-001	1.279E+000
	48hrs_0.01	1.918E+000	3.340E-001	1.102E+001
	48hrs_0.05	9.107E-001	1.832E-001	4.526E+000
	48hrs_1.25	9.693E-001	5.012E-001	1.875E+000
ZIP-T1 (p=0.32)	48hrs_0	1.000E+000	4.136E-001	2.418E+000
	48hrs_0.01	4.410E-001	2.163E-001	8.988E-001
	48hrs_0.05	2.944E-001	1.498E-002	5.784E+000
	48hrs_1.25	1.033E+000	1.576E-001	6.768E+000
VIT1 (p=0.32)	48hrs_0	1.000E+000	6.771E-002	1.477E+001
	48hrs_0.01	5.064E-001	4.003E-001	6.407E-001
	48hrs_0.05	1.301E+000	7.195E-001	2.354E+000
	48hrs_1.25	2.007E+000	1.014E+000	3.971E+000
SOD1 (p=0.32)	48hrs_0	1.000E+000	2.114E-002	4.729E+001
	48hrs_0.01	8.937E+000	3.768E-001	2.120E+002
	48hrs_0.05	1.020E+000	7.895E-001	1.318E+000
	48hrs_1.25	1.871E+000	7.039E-002	4.971E+001
GSR2 (p=0.85)	48hrs_0	1.000E+000	5.852E-002	1.709E+001
	48hrs_0.01	2.047E+000	2.972E-002	1.410E+002
	48hrs_0.05	1.548E+000	4.300E-001	5.570E+000
	48hrs_1.25	1.080E+000	1.332E-001	8.762E+000
CA1 (p=0.91)	72hrs_0	1.000E+000	2.254E-001	4.436E+000
	72hrs_0.01	1.304E+000	1.925E-001	8.830E+000
	72hrs_0.05	1.999E+000	2.117E-001	1.887E+001
	72hrs_1.25	1.507E+000	9.520E-001	2.386E+000
CYCB1 (p=0.94)	72hrs_0	1.000E+000	7.429E-002	1.346E+001
	72hrs_0.01	1.244E+000	1.058E+000	1.461E+000
	72hrs_0.05	8.730E-001	2.683E-001	2.841E+000
	72hrs_1.25	1.156E+000	1.590E-001	8.398E+000
HMA2 (p=0.91)	72hrs_0	1.000E+000	2.002E-001	4.994E+000
	72hrs_0.01	1.103E+000	1.274E-003	9.545E+002
	72hrs_0.05	5.531E-001	3.587E-001	8.528E-001
	72hrs_1.25	9.462E-001	2.668E-001	3.356E+000
PCS1 (p=0.91)	72hrs_0	1.000E+000	8.127E-001	1.230E+000
	72hrs_0.01	8.880E-001	3.172E-001	2.486E+000
	72hrs_0.05	8.078E-001	6.209E-001	1.051E+000
	72hrs_1.25	1.234E+000	2.103E-001	7.243E+000

ZIP-T1 (p=0.91)	72hrs_0	1.000E+000	9.310E-002	1.074E+001
	72hrs_0.01	2.426E+000	6.485E-002	9.072E+001
	72hrs_0.05	6.321E-001	9.042E-002	4.419E+000
	72hrs_1.25	1.830E+000	2.008E-001	1.668E+001
VIT1 (p=0.66)	72hrs_0	1.000E+000	2.558E-001	3.910E+000
	72hrs_0.01	7.114E-001	1.209E-001	4.187E+000
	72hrs_0.05	5.268E-001	8.752E-002	3.172E+000
	72hrs_1.25	1.954E+000	1.061E+000	3.600E+000
SOD1 (p=0.91)	72hrs_0	1.000E+000	1.081E-001	9.248E+000
	72hrs_0.01	3.816E-001	7.294E-004	1.996E+002
	72hrs_0.05	2.041E+000	5.660E-002	7.359E+001
	72hrs_1.25	3.247E+000	7.571E-002	1.393E+002
GSR2 (p=0.94)	72hrs_0	1.000E+000	1.176E-001	8.505E+000
	72hrs_0.01	1.155E+000	8.418E-003	1.586E+002
	72hrs_0.05	6.768E-001	5.692E-002	8.047E+000
	72hrs_1.25	1.043E+000	2.452E-001	4.439E+000

For the genes represented in the bar charts, further analysis was performed on the Cq data. Scatter plots were made in order to check the presence of outliers that might have reduced the significance of data. In CA1 (*fig 3.10)*, CYCB1 (*fig 3.11)* and HMA2 (*fig 3.12)*, outliers were present in the dataset. Whereas, in SOD1 (*fig 3.13)*, no huge deviation was found.

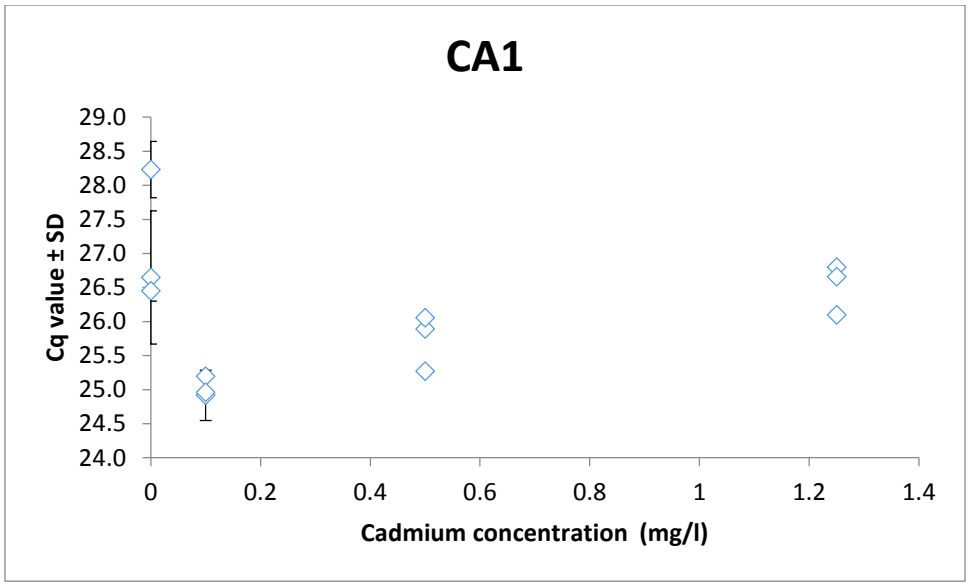

Figure.3.10. Scatter plot of CA1 expression in *S. robusta* after 48 hours of Cd^{2+} exposure. X axis shows Cd concentration, and the Cq value is given on Y axis (mean±SD, n=3).

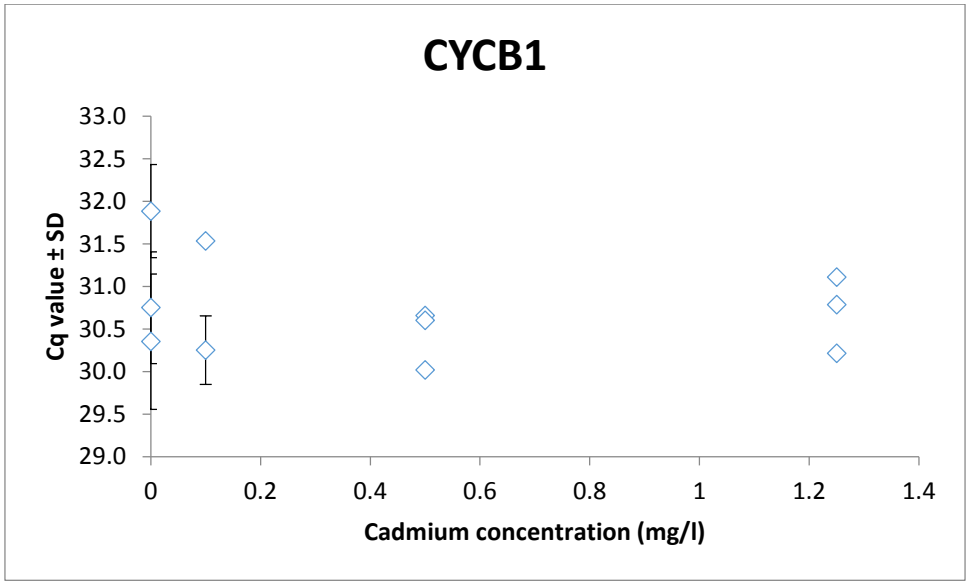

Figure.3.11. Scatter plot of CYCB1 expression in *S. robusta* after 72 hours Cd^{2+} exposure. X axis shows Cd concentration, and Cq value is given on Y axis (mean±SD, n=3 (2 for 0.01 mg/l)).

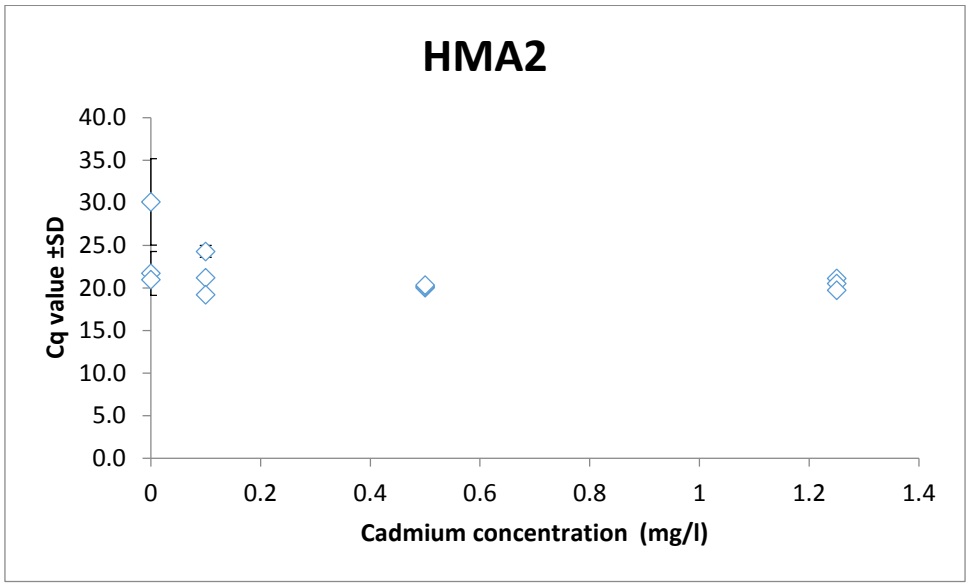

Figure.3.12. Scatter plot of HMA2 expression in *S. robusta* after 48 hours Cd^{2+} exposure. X axis shows Cd concentration, and Cq value is given on Y axis (mean±SD, n=3).

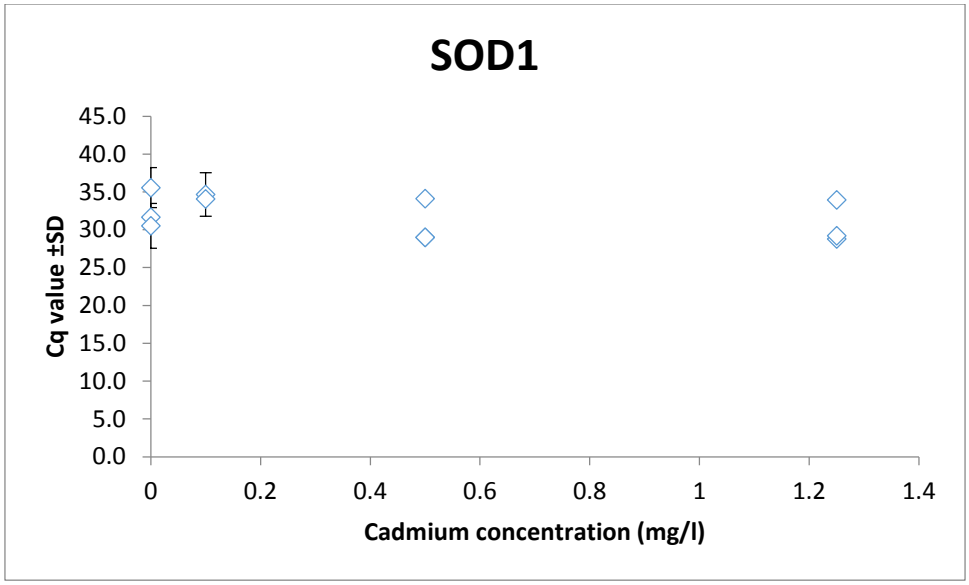

Figure.3.13. Scatter plot of SOD1 expression in *S. robusta* after 72 hours Cd^{2+} exposure. X axis shows Cd concentration, and Cq value is given on Y axis (mean±SD, n=3).

Phaeodactylum tricornutum:

There was a significant dose dependent response in the NTF2L gene expression when *P. tricornutum* was exposed to Cd^{2+} for 48 hours (*fig.3.14*). The gene expression significantly increased with increase in concentration (p=0.01).

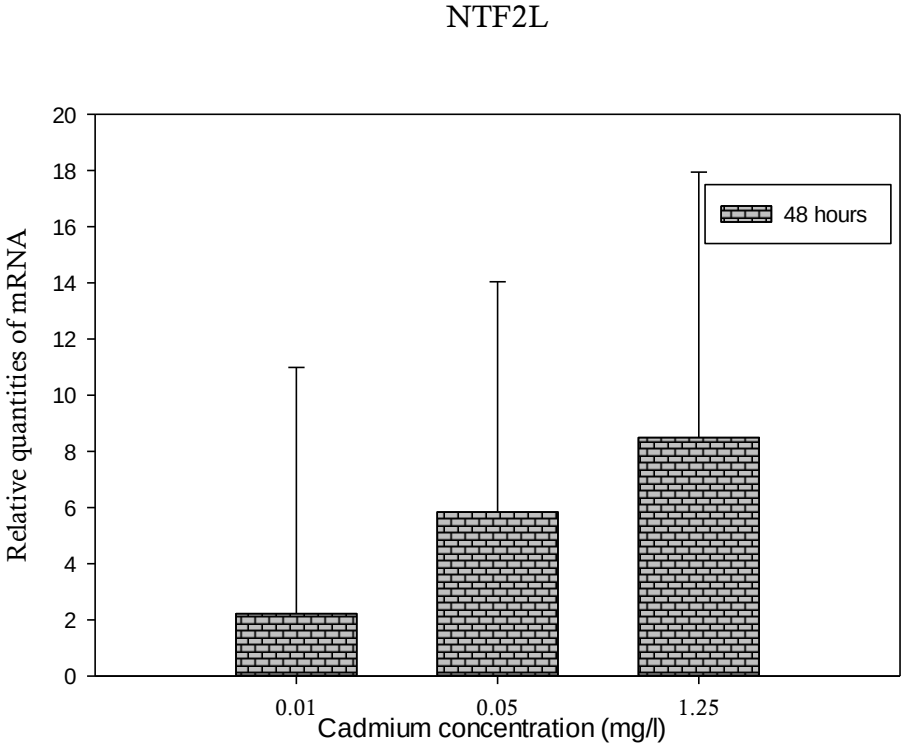

Figure 3.14. Bar chart of NTF2L expression in *P. tricornutum* after 48 hours Cd^{2+} exposure. X axis shows the experimental conditions, and the gene expression ratio is given on Y axis (mean±SD, n=3). The control sample is set to 0.

Cd mediated changes in the expression of vacuolar ion transporter 1 (VIT1) (*fig.3.16)*, zinc regulated and iron regulated transporter like protein transporter 1 (ZIP-T1) (*fig.3.15)* and phytochelatin synthase 1 (PCS1) (*fig.3.17)* genes were also studied. Though changes in the gene expression were not significant, a dose dependent increase in the response to Cd^{2+} was observed (except VIT1). ZIP-T1 was expressed 28 times higher when compared with the control and VIT1, 11 times when compared with the control.

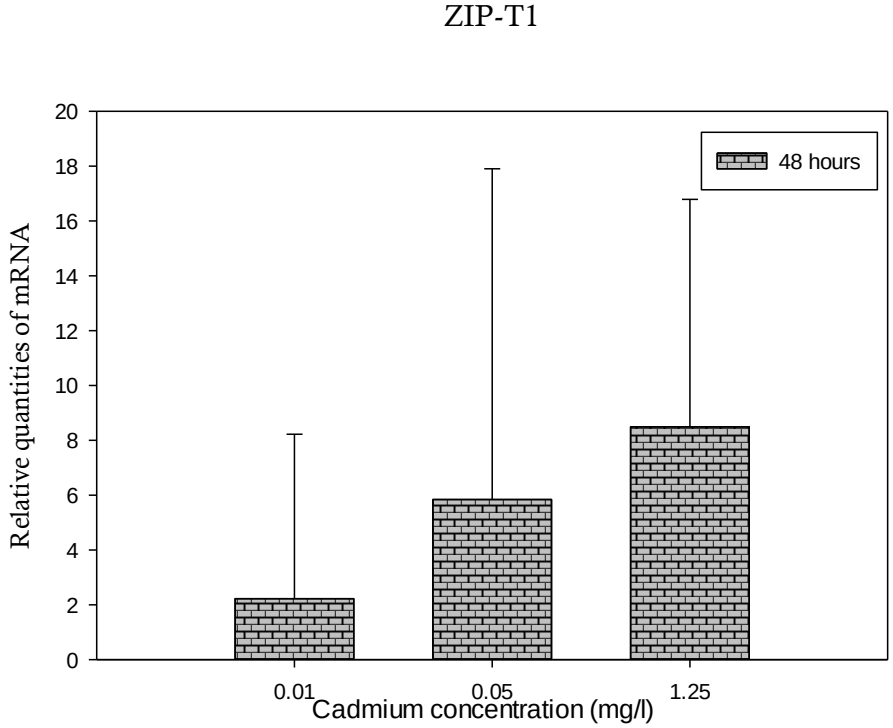

Figure 3.15. Bar chart of ZIP-T1 expression in *P. tricornutum* after 48 hours Cd^{2+} exposure. X axis shows the experimental conditions, and the gene expression ratio is represented on Y axis (mean±SD, n=3, p=0.8). The control sample is set to 0.

VIT1

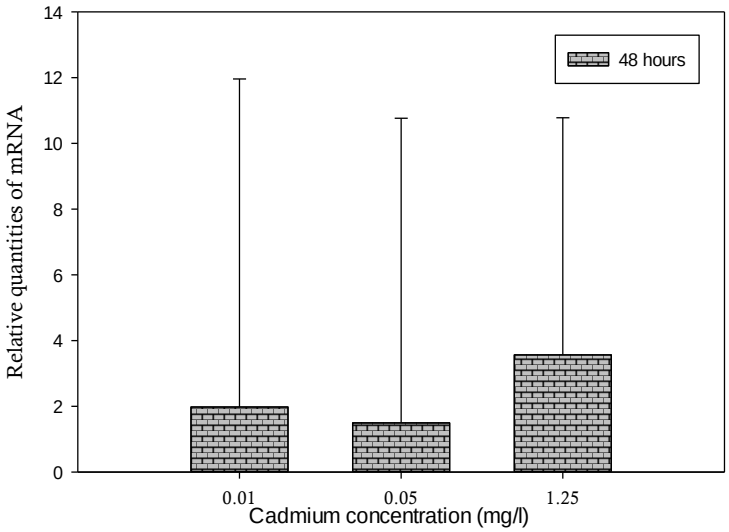

Figure 3.16. Bar chart of VIT1 expression in *P. tricornutum* after 48 hours Cd^{2+} exposure. X axis shows the experimental conditions, and the gene expression ratio is represented on Y axis (mean±SD, n=3, p=0.9). The control sample is set to 0.

PCS1

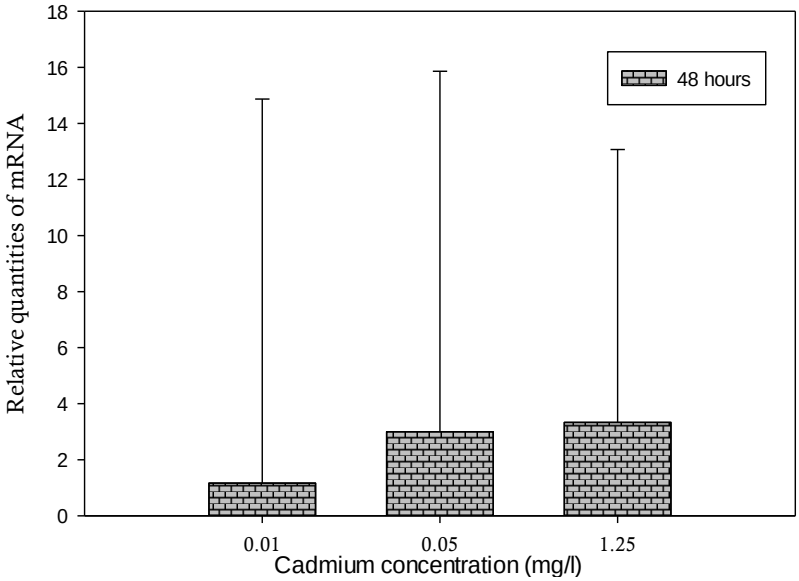

Figure 3.17. Bar chart of PCS1 expression in *P. tricornutum* after 48 hours Cd^{2+} exposure. X axis shows the experimental conditions, and the gene expression ratio is represented on Y axis (mean±SD, n=3, p=0.9). The control sample is set to 0.

Table.3.6.. Genes showing transcriptional response in *P. tricornutum* three different concentrations of Cd^{2+} (0.01, 0.05, 1.25 mg/l) after 48 and 72 hours of exposure.

ci- Confidence Interval

Gene	Exposure groups	Mean gene expression	95% value ci low	95% value ci high
CA1 (p=0.99)	48hrs_0	1.000E+000	4.202E-005	2.380E+004
	48hrs_0.01	5.395E+000	4.045E-004	7.195E+004
	48hrs_0.05	5.232E+000	7.353E-006	3.723E+006
	48hrs_1.25	2.203E+001	4.499E-002	1.079E+004
NTF2L (p=0.01)	**48hrs_0**	**1.000E+000**	**4.030E-002**	**2.481E+001**
	48hrs_0.01	**4.650E+000**	**4.883E-002**	**4.429E+002**
	48hrs_0.05	**5.718E+001**	**9.288E+000**	**3.520E+002**
	48hrs_1.25	**3.596E+002**	**1.217E+002**	**1.062E+003**
ZIP-T1 (p=0.83)	48hrs_0	1.000E+000	2.801E-002	3.571E+001
	48hrs_0.01	3.030E+000	1.367E-001	6.712E+001
	48hrs_0.05	6.092E+000	8.634E-003	4.298E+003
	48hrs_1.25	2.889E+001	2.424E+000	3.443E+002
VIT1 (p=0.99)	48hrs_0	1.000E+000	6.569E-002	1.522E+001
	48hrs_0.01	3.941E+000	1.527E-002	1.017E+003
	48hrs_0.05	2.819E+000	1.279E-002	6.214E+002
	48hrs_1.25	1.180E+001	8.629E-001	1.612E+002
PCS1 (p=0.99)	48hrs_0	1.000E+000	6.449E-003	1.551E+002
	48hrs_0.01	2.238E+000	3.746E-004	1.337E+004
	48hrs_0.05	7.979E+000	8.510E-003	7.481E+003
	48hrs_1.25	1.006E+001	1.168E-001	8.664E+002
CYCB1 (p=0.99)	48hrs_0	1.000E+000	1.530E-001	6.538E+000
	48hrs_0.01	1.068E+000	2.612E-002	4.363E+001
	48hrs_0.05	9.378E-001	1.341E-002	6.556E+001
	48hrs_1.25	9.001E-001	2.573E-002	3.149E+001
HMA2 (p=0.99)	48hrs_0	1.000E+000	8.952E-002	1.117E+001
	48hrs_0.01	1.525E+000	1.714E-003	1.356E+003
	48hrs_0.05	2.253E+000	8.752E-003	5.801E+002
	48hrs_1.25	2.310E+000	2.382E-002	2.241E+002

GSR2 (p=0.99)	48hrs_0	1.000E+000	1.068E-001	9.367E+000
	48hrs_0.01	1.357E+000	6.196E-003	2.972E+002
	48hrs_0.05	2.548E+000	1.067E-002	6.084E+002
	48hrs_1.25	3.248E+000	3.546E-002	2.975E+002
CAT1 (p=0.99)	48hrs_0	1.000E+000	6.031E-001	1.658E+000
	48hrs_0.01	1.088E+000	2.553E-001	4.639E+000
	48hrs_0.05	1.206E+000	6.073E-001	2.396E+000
	48hrs_1.25	1.442E+000	3.367E-001	6.178E+000
NTF2L (p=0.99)	72hrs_0	1.000E+000	8.653E-002	1.156E+001
	72hrs_0.05	9.840E+000	5.436E-002	1.781E+003
	72hrs_1.25	1.407E+001	1.062E+000	1.864E+002
ZIP-T1 (p=0.99)	72hrs_0	1.000E+000	1.461E-001	6.846E+000
	72hrs_0.05	1.601E+000	3.115E-002	8.233E+001
	72hrs_1.25	5.619E-001	8.323E-003	3.794E+001
VIT1 (p=0.99)	72hrs_0	1.000E+000	1.084E-002	9.224E+001
	72hrs_0.05	1.176E+000	5.799E-002	2.384E+001
	72hrs_1.25	2.527E+000	1.204E-001	5.304E+001
PCS1 (p=0.99)	72hrs_0	1.000E+000	5.257E-003	1.902E+002
	72hrs_0.05	1.308E+000	5.866E-002	2.917E+001
	72hrs_1.25	3.817E-001	1.690E-004	8.620E+002
CA1 (p=0.99)	72hrs_0	1.000E+000	9.801E-004	1.020E+003
	72hrs_0.05	4.016E-001	1.560E-005	1.034E+004
	72hrs_1.25	7.589E-001	1.693E-003	3.403E+002
CYCB1 (p=0.99)	72hrs_0	1.000E+000	3.633E-002	2.753E+001
	72hrs_0.05	1.009E+000	4.349E-002	2.341E+001
	72hrs_1.25	7.907E-001	3.545E-002	1.764E+001
HMA2 (p=0.99)	72hrs_0	1.000E+000	3.342E-003	2.992E+002
	72hrs_0.05	2.481E+000	3.344E-002	1.840E+002
	72hrs_1.25	1.427E+000	3.442E-002	5.915E+001
CAT1 (p=0.99)	72hrs_0	1.000E+000	6.712E-001	1.490E+000
	72hrs_0.05	1.103E+000	6.869E-001	1.770E+000
	72hrs_1.25	5.999E-001	1.144E-001	3.147E+000

GSR2 (p=0.99)	72hrs_0	1.000E+000	1.883E-002	5.310E+001
	72hrs_0.05	1.060E+000	1.580E-002	7.107E+001
	72hrs_1.25	8.933E-001	6.690E-003	1.193E+002

For the genes represented in bar charts, further analysis was performed on the Cq data. Scatter plots were made in order to check the presence of outliers that might have reduced the significance of data. In PCS1 (*fig. 3.20)*, data points were more scattered in the 0.01 mg/l exposure group. Whereas, in the ZIPT1 *(fig. 3.18)* and VIT1 (*fig. 3.19)*, no major outlier was found in the dataset.

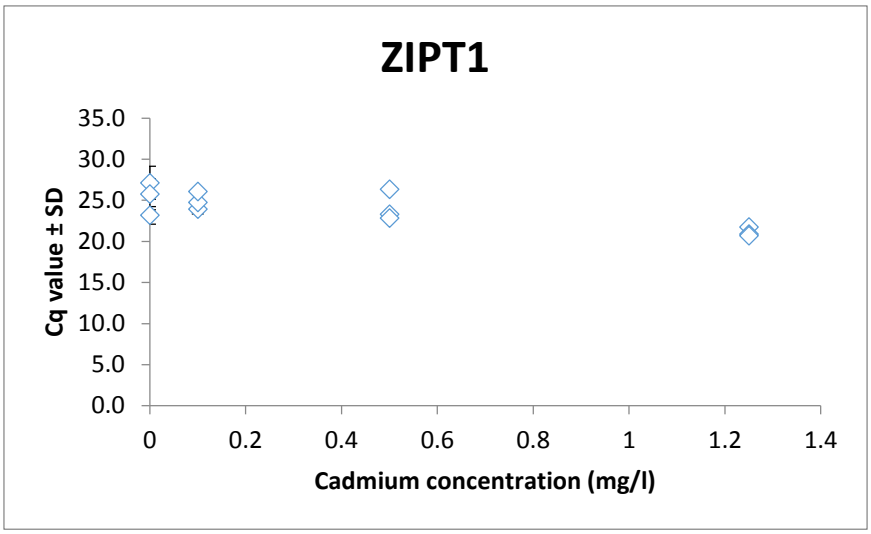

Figure.3.18. Scatter plot of ZIPT1 expression in *P. tricornutum* after 48 hours Cd^{2+} exposure. X axis shows Cd concentration, and Cq value is given on Y axis (mean±SD, n=3).

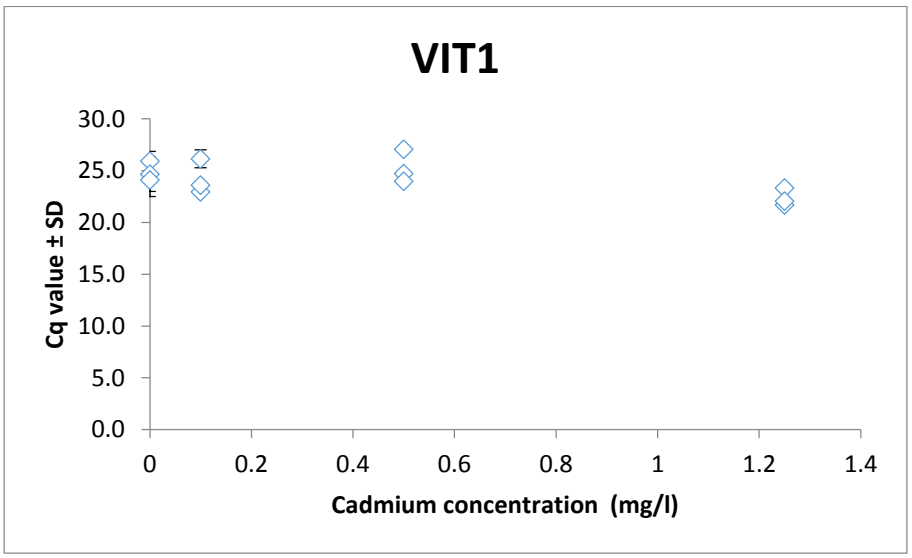

Figure.3.19. Scatter plot of VIT1 expression in *P .tricornutum* after 48 hours Cd^{2+} exposure. X axis shows Cd concentration, and Cq value is given on Y axis (mean±SD, n=3).

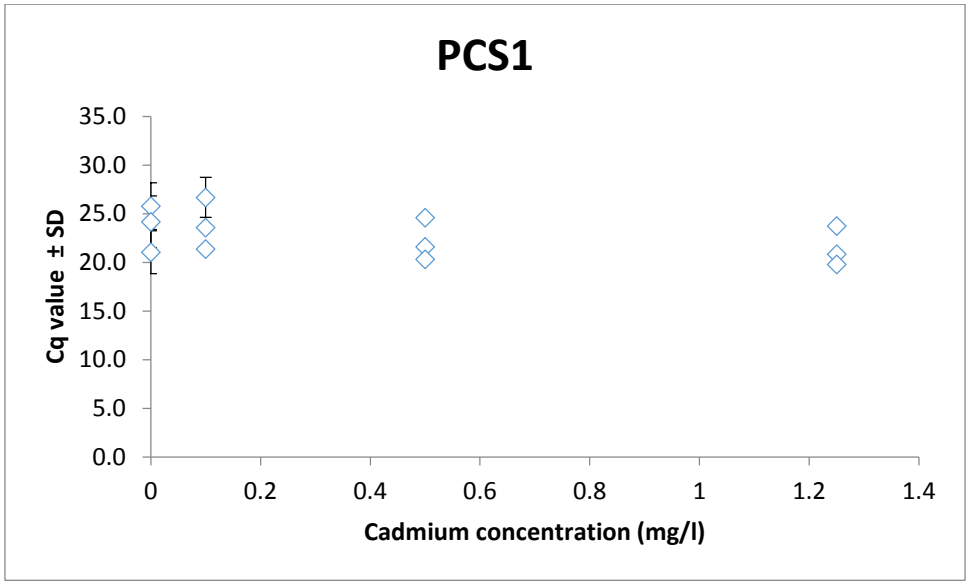

Figure.3.20. Scatter plot of PCS1 expression in *P. tricornutum* after 48 hours Cd^{2+} exposure. X axis shows Cd concentration, and Cq value is given on Y axis (mean±SD, n=3).

4. DISCUSSION

Variations in the population growth rate, cell physiology and gene regulation on exposure to Cd were observed on diatoms in this study.

The data obtained is analyzed in three different aspects: The mechanistic insights (i), the dose specific toxicity (ii), and the toxic effects of Cd in comparison with Zn, Cu and Hg (iii).

4.1. Mechanistic outlook

The pathways discussed in this section are listed below:

- Interaction of Cd in the growth process (survival parameter)
- Sequestration and efflux of Cd upon entry into the cell (tolerance)
- Antioxidant enzymes against oxidative stress generated by Cd (detoxification)

4.1.1. Survival parameter

At very low exposure concentrations, growth curves show that Cd resulted in increase in the growth rate of *S. robusta* (0.01mg/l) and *P. tricornutum* (0.01 and 0.05 mg/l) under the given experimental conditions.

Carbonic anhydrase is a Zn dependent enzyme which helps several species of microalgae in carbon sequestration (in the CO_2 form) that enters the Calvin cycle. Studies have shown that the increase in growth rate was strongly correlated to an increase in CA activity (Lane and Morel, 2000). As shown in the figure *(fig 4.1)*, glyceraldehyde-3-phosphate (G3P) produced after Calvin cycle, could possibly be utilized for the growth of algae.

At the transcript level, in *S. robusta* an insignificant upregulation of CA1 was noticed after 48 hours. Cd might have displaced Zn in the intracellular enzyme CA or function as the metal center in Cd-specific CA1 or liberate the Zn from other metal proteins that could possibly upregulate the CA1 activity.

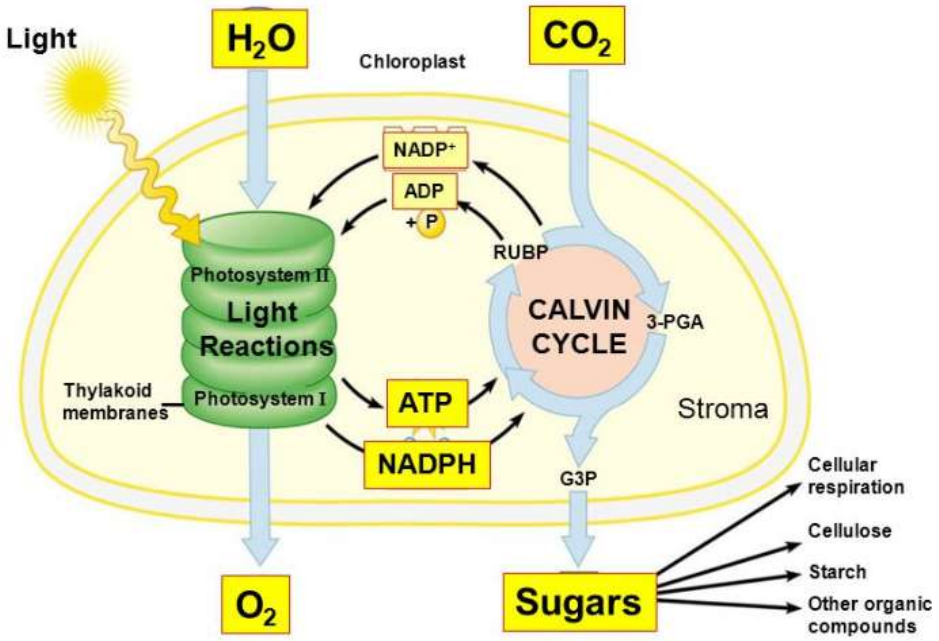

Figure 4.1. A simplified overview of photosynthesis. (Adapted from Campbell and Reece (2005)). Glyceraldehyde-3-phosphate (*G3P*) produced in the cell through Calvin cycle is synthesized using carbon dioxide.

It is interesting to note that, in *S. robusta* particularly at 0.05 mg/l Cd^{2+} exposure group, the growth rate (μ) dipped to 0. This is supported by the downregulation of CYCB1 gene in the qPCR data.

CYCB1 is a late-phase cell cycle gene (G2 to M transition phase) that ensures normal progression of growth. Our data does not suggest that Cd affects cell division through CYCB1.

However, we cannot draw a strong conclusion since the qPCR data was not significant.

4.1.2. Tolerance

Cd is suggested to be taken up by plants and algae (Clemens, 2006). Regulation of genes that are responsible for Cd uptake and translocation is dealt with in this section.

An indication of elevated Cd concentration in the cells, is through the synthesis of PCs (Clemens, 2006). PCs bind to heavy metal-ions before vacuolar sequestration (Vivares et al., 2005). No other environmental factor except metal stress can cause PC accumulation. The presence of excess Cd ions in the cell results in the synthesis of PCs and this in turn indicates the uptake of Cd from the growth medium.

In *S. robusta*, our experiment demonstrated a very small increase in the level of phytochelatin synthase 1 (PCS1) only in the highest dosage group (1.25 mg/l Cd^{2+}) after 72 hours of exposure.

In *P. tricornutum*, there was excessive background noise and we were therefore not able to get any useful information on the gene regulation. According to Brembu et al. (2011), PCS activity is generally post-transcriptional and transcription of PCS was not induced by Cd exposure in their study on *P. tricornutum*.

Heavy metal transporting P-type ATPase utilize energy through ATP hydrolysis and translocates cations across the membranes (Qiu et al., 2012). Heavy metal ATPase 2 (HMA2) from this family is responsible for Zn translocation to main homeostasis (Hussain et al., 2004). It was inferred that Cd is capable of using this pathway due to its chemical similarities with Zn.

In *S. robusta*, the expression of HMA2 increased with increasing concentration of Cd in the growth medium. The lack of significant data does not support the credibility of the results.

Brembu et al. (2011) demonstrated upregulation of HMA2 in *P. tricornutum* at very high concentrations of Cd after 24 hours exposure. Also, it was predicted that HMA2 is responsible for the removal of Cd by pumping the ions outside the cell. Whereas, vacuolar ion transporter 1 (VIT1) and zrt and irt like protein transporter 1 (ZIP-T1) are responsible for the intake of Cd^{2+} into the vacuole and the cell respectively (*fig 4.2*).

Our study recorded an upregulation of VIT1 and ZIP-T1 at higher concentrations though not significantly.

Thus, according to the results of the present study, it is suggested that in order to counterbalance the Cd influx, efflux mechanism got upregulated in *P. tricornutum*.

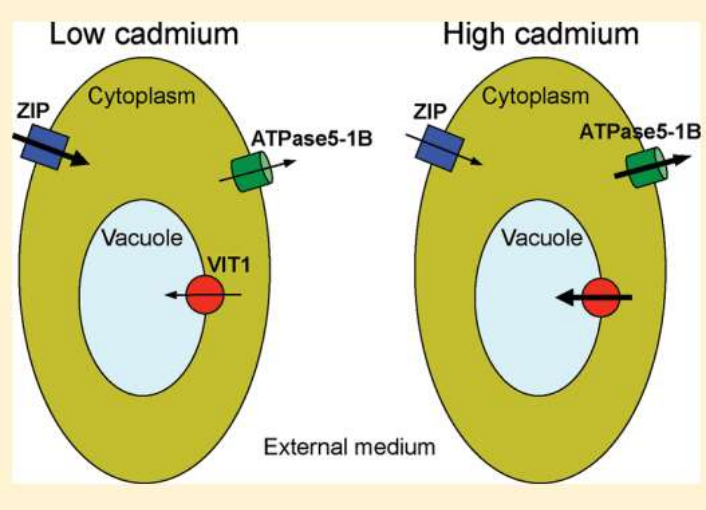

Figure 4.2. Presentation of the results obtained on exposing *P. tricornutum* to Cd for 24 hours. Adapted from Brembu et al. (2011).

The regulation of nuclear transporter factor 2-like (NTF2L) was observed for the first time in the present study. NTF2L helps in the transport of proteins between the nucleus and the cytoplasm. Even though there has not been much studies on this gene in diatoms, a study on yeast by Toone et al. (1998) showed that nuclear transporter factor genes help in the exclusion of fusion proteins. On the other hand, in mammalian proximal tubule cells, activation of nuclear factors are suggested to protect the cells against Cd toxicity (Thévenod et al., 2000).

One possible explanation could be that proteins which trap Cd are exported out of the nucleus that is inferred by a significant upregulation of NTF2L at very high concentrations of Cd in *S. robusta*. A similar trend was noticed also in *P. tricornutum*. Notably, at high concentration (1.25 mg/l Cd^{2+}), the expression of NTF2L in *S. robusta* was approximately 1000 times higher on comparison with the control, whereas, 400 times higher than the control in *P. tricornutum*.

Even though at molecular level, genes that help in the efflux of Cd (HMA2, NTF2L) are upregulated with increasing Cd concentration, cell granularity inferred by flow cytometry was higher on comparison with control at all concentrations. This hints that the efflux mechanism does not suggestively overcome the sequestration pathways of Cd. A possible explanation could be the inhibitory effect of Cd on ATPase activity as explained in Chapter 1.3.

From the results, the rate of uptake of Cd is suggested to be comparatively at a higher rate in *P. tricornutum* than the uptake rate in *S. robusta*. A possible explanation could be the absence of silica on the cell wall of *P. tricornutum* (Johansen, 1991).

Cd uptake has been shown to decrease in plants when supplied with silicon (Sahebi et al., 2015). It is possible that the silicon supplied is capable of covalently binding with Cd thus reducing its toxicity both at intracellular and extracellular levels (Sahebi et al., 2015). Silicon sequesters heavy metals in the vacuoles inside the cell and limits the penetration of heavy metals at the extracellular level.

4.1.3. Detoxification

Oxidative stress in *S. robusta* was studied by observing superoxide dismutase 1 (SOD1) and glutathione-disulphide reductase 2 (GSR2). In *P. tricornutum*, the target gene was catalase 1 (CAT1) and GSR2.

No significant data was obtained for genes related to oxidative stress in this study, except a slight increase of SOD1 in *S. robusta* at high Cd concentration. Brembu et al., (2011) did not

notice a significant change in oxidative stress related genes after 24 hours of Cd exposure in *P. tricornutum*.

Since Cd is not a redox active metal the mechanism of oxidative dress is not clearly established. A study performed on human cancerous cells showed that Cd might either act on the respiratory enzymes on mitochondria, down-regulate the antioxidant enzymes or release heavy metals like Cu from intracellular depots that might release in oxidative stress (Henkler et al., 2010).

4.2. Concentration gradient observation

The toxic effects of Cd were studied in three different exposure groups. The lowest concentration represents approximately 40 times the highest environmental relevant concentration (0.01 mg/l) (Torres et al., 1997). The next level concentration represents a point source (0.05) (Torres et al., 2000) and the highest concentration represents very heavily polluted areas (1.25 mg/l) (WorldHealthOrganization, 2011).

It was noticed both in *S. robusta* and *P. tricornutum* that exposure to very low concentrations of Cd resulted in an increase of growth rate. Possible explanations for the cellular uptake of Cd could be due to nutrient deficiency in the growth medium or interference with Zn associated enzymes. Stress related genes were not activated neither in *S. robusta* nor in *P. tricornutum*. By the upregulation of sequestration genes it is inferred that, Cd is possibly transported into the cell using the pathways for Zn uptake.

At the next level of Cd exposure (0.05 mg/l) the growth rate seems to be affected in *S. robusta*. This concentration represents a possible point source environment, though the concentration range can vary depending on the type of point source releasing Cd. The growth rate of *P. tricornutum* did not seem to be affected significantly.

At very high Cd concentrations, the growth was suppressed as expected. Also, the tolerance pathways to trap and translocate Cd were upregulated at the given experimental conditions.

At 6.25 mg/l Cd^{2+} concentration in *S. robusta*, an interesting trend in growth was recorded. The cells managed to grow after 48 hours of exposure. However, since the concentration is ecologically not relevant, not much attention was paid to it. But such high concentrations were included in the study in order to cover a wide range of Cd concentration in studying toxicity on emerging model species.

4.3. Chemical specific effects

The toxic effects of Cd are compared with Zn, Hg and Cu.

Hg has been shown to cause genotoxic effects in the marine diatom *Chaetoceros tenuissimus.* Hg exposed cultures showed a decrease in DNA integrity (Sarker et al., 2016). Diatoms were suggested to be effectively used for biomonitoring of environmental pollution if the extent of DNA damage in diatoms can be correlated to the damage in other aquatic species.

The present study did not investigate any genotoxic effect. However, while extracting the mRNA, a particular exposure group in *P. tricornutum* (0.01 mg/l Cd^{2+} after 72 hours of exposure) showed very poor RIN values. Even though the capacity of Cd to affect the stability of mRNA had been mentioned in Chapter 1.3, such an effect would have resulted in cell death which was not recorded in this study. Loss of mRNA integrity could have been caused randomly, also there is lack of evidence to support the observation.

Exposure to Zn as suggested by Nguyen-Deroche Tle et al. (2012), increased in growth rate. Zn resulted in the increase in growth rate through mitosis for a short period of time before it reduced the cell density. This is due to the fact that even though Zn plays a major role in mitosis, the growth of algae is primarily dependent on photosynthesis (Nguyen-Deroche Tle et al., 2012).

On exposing *P. tricornutum* to Cu, CAT was the major enzyme for scavenging H_20_2. glutathione and its derivatives were suggested to be the first line of defense against ROS generated by Cu. At least three antioxidant enzymes were shown to be involved eventually in combating oxidative stress induced by Cu (Morelli and Scarano, 2004). The current study varied drastically on this pathway probably because Cd does not follow Haber-Weiss reaction. On the other hand, a study by Wei et al. (2014) indicated that even though cell division and photosynthesis process were inhibited, cell biomass kept increasing on exposing *P. tricornutum* to Cu. A similar tolerant nature of *P. tricornutum* was shown towards Cd exposure in the present study.

A study by Smith et al. (2014) showed that *P. tricornutum* produced more PCs on exposure to Cu, when compared with another species of diatom *Ceratoneis closterium*. Also the chain length of PC produced was comparatively longer in *P. tricornutum.*

4.4. Limitations of the study

The data obtained in this study showed extensive background noise providing high variability between the samples. A possible reason could be the reference genes used in the interpretation of qPCR data. Since Cd has a wide range of toxic effects, identifying a good reference marker was challenging. The reference genes used in this study were not the best based on the geNorm result and better genes could have been used.

The noise could have resulted from the small sample size (3). If the sample size was increased, the noise might have been reduced. Also, the noise was particularly higher in the experimental group that was analyzed after 72 hours of Cd exposure. This might hint the possibility of some secondary effects in the diatoms of Cd exposure that prevent the significance of gene expression data.

Skillset in handling the algae culture, for example, closing the flask's lid, scrapping the *S. robusta* cells, arranging the culture flaks under light etc. seemed to play a crucial role. Also, the aquil medium has numerous ingredients and weighing errors are possible.

Further research on the PCR products might have provided a more clear picture of the results obtained.

5. CONCLUSION

According to this study, it is probable that *S. robusta* is capable of utilizing lower concentration of cadmium for growth using carbon-concentration mechanism. It is suggested that efflux mechanism is upregulated through nuclear transporters, and signs of Cd stress are shown only at very high concentration. The significant role played by NTF2L gene in Cd transportation is presented for the first time in the present study.

As expected, this study shows that cadmium is uptaken by *P. tricornutum* without significant toxic effect on the growth rate after 48 hours of exposure. The efflux mechanism in the removal of the cellular Cd does not seem to compensate the rate of sequestration.

Cytotoxic effects such as increase in cell granularity and cell complexity has been well documented in both the species. The cellular uptake of Cd is suggested to be comparatively at a faster rate in *P. tricornutum* than *S. robusta* from the qPCR and flow cytometry data.

Antioxidant enzymes systems that defend the cell against oxidative stress were not induced under the given experimental conditions in neither *S. robusta* nor *P. tricornutum*.

On a comparative basis, *S. robusta* does not seem to be more tolerant to Cd than *P. tricornutum*. At the given experimental conditions, *S. robusta* tend to be more sensitive to Cd than *P. tricornutum*.

More studies are required on the NTF2L gene to compare the efflux mechanisms of the two marine diatoms.

6. FUTURE PERSPECTIVES

Information on Cd uptake kinetics can be a valuable information that could be concentrated on in the future studies. Biochemical parameters like intracellular Cd concentration, Cd adsorbed on the cell surfaces and decrease of Cd in the medium help in validating the sequestration and efflux mechanisms. Measurement of silica can also help in understanding the mechanism behind silica mediated Cd tolerance.

In order to test the hypothesis that *S. robusta* has a better metabolic capacity due to an extensive gene family, a study on the differences in metabolite pool due to Cd exposure at metabolome level can be a good endpoint in the future.

It would be really interesting to know about the protein that binds to NTF2L gene. What could be its function under Cd stress and why does it have to be transported outside the nucleus in the cell? Or does Cd bind to NTF2L for clearance and the additional gene may or may not play a role in Cd tolerance?

Even though the present study had a small sample size (n=3) in the experimental design, it does show a clear indication of pathways to be explored in *S. robusta* in the future studies.

REFERENCES

ALLEN, J. & WILLIAMS, J. 1998. Photosynthetic reaction centers. *FEBS letters,* 438**,** 5-9.

ANDERSEN, R. A. 2005. *Algal culturing techniques*, Academic press, 271-272.

ANDRESEN, E. & KUPPER, H. 2013. Cadmium toxicity in plants. *Metal Ions in Life Sciences,* 11**,** 395-413.

ARMBRUST, E. V. 2009. The life of diatoms in the world's oceans. *Nature,* 459**,** 185-192.

BALLATORI, N., CHERIAN, M. G., DAWSON, D., DELNOMDEDIEU, M., DRUET, P., FISHER, B., GOERING, P., GOYER, R., HIMENO, S. & IMURA, N. 2012. *Toxicology of metals: biochemical aspects*, Springer Science & Business Media, 467.

BAYR, H. 2005. Reactive oxygen species. *Critical Care Medicine,* 33**,** S498-S501.

BIOSCIENCES, B. 2000. Introduction to Flow Cytometry: A learning guide. *Manual Part,* 1.

BOWLER, C., VARDI, A. & ALLEN, A. E. 2010. Oceanographic and biogeochemical insights from diatom genomes. *Annual Review of Marine Science,* 2**,** 333-365.

BREMBU, T., JORSTAD, M., WINGE, P., VALLE, K. C. & BONES, A. M. 2011. Genome-wide profiling of responses to cadmium in the diatom Phaeodactylum tricornutum. *Environtal Science & Technology,* 45**,** 7640-7647.

CAMPBELL, N. A. & REECE, J. B. 2005. Biology. Pearson/Benjamin Cummings Publishing, San Francisco, California.

CHAPMAN, P. M. & WANG, F. 2000. Issues in Ecological Risk Assessment of Inorganic Metals and Metalloids. *Human and Ecological Risk Assessment: An International Journal,* 6**,** 965-988.

CHEPURNOV, V. A., MANN, D. G., VON DASSOW, P., VANORMELINGEN, P., GILLARD, J., INZE, D., SABBE, K. & VYVERMAN, W. 2008. In search of new tractable diatoms for experimental biology. *Bioessays,* 30**,** 692-702.

CHIOCCIOLI, M., HANKAMER, B. & ROSS, I. L. 2014. Flow cytometry pulse width data enables rapid and sensitive estimation of biomass dry weight in the microalgae Chlamydomonas reinhardtii and Chlorella vulgaris. *PLoS One,* 9**,** e97269.

CLARK, D. P. & PAZDERBUJ, N. J. 2013. Molecular Biology. Second ed.: AP cell press, 928.

CLEMENS, S. 2006. Toxic metal accumulation, responses to exposure and mechanisms of tolerance in plants. *Biochimie,* 88**,** 1707-19.

CUTLER, C. A Brief Introduction to Quantitative PCR and Applications. [Accessed April 2016].

DAS, P., SAMANTARAY, S. & ROUT, G. R. 1998. Studies on Cadmium toxicity in plants: A review. *Environmental Pollution,* 98**,** 29-36.

DEPAUW, F. A., ROGATO, A., RIBERA D'ALCALA, M. & FALCIATORE, A. 2012. Exploring the molecular basis of responses to light in marine diatoms. *Journal of Experimental Botany,* 63**,** 1575-91.

FALCIATORE, A. & BOWLER, C. 2002. Revealing the molecular secrets of marine diatoms. *Annual Review of Plant Biology,* 53**,** 109-130.

GUAN, X. K., SONG, L., WANG, T. C., TURNER, N. C. & LI, F. M. 2015. Effect of Drought on the Gas Exchange, Chlorophyll Fluorescence and Yield of Six Different-Era Spring Wheat Cultivars. *Journal of Agronomy and Crop Science,* 201**,** 253-266.

GUILLARD, R. R. & RYTHER, J. H. 1962. STUDIES OF MARINE PLANKTONIC DIATOMS: I. CYCLOTELLA NANA HUSTEDT, AND DETONULA CONFERVACEA (CLEVE) GRAN. *Canadian journal of microbiology,* 8**,** 229-239.

HASAN, S. A., FARIDUDDIN, Q., ALI, B., HAYAT, S. & AHMAD, A. 2009. Cadmium: Toxicity and Tolerance in plants. *Journal of Environmental Biology,* 30**,** 165-174.

HENKLER, F., BRINKMANN, J. & LUCH, A. 2010. The role of oxidative stress in carcinogenesis induced by metals and xenobiotics. *Cancers (Basel),* 2**,** 376-96.

HUSSAIN, D., HAYDON, M. J., WANG, Y., WONG, E., SHERSON, S. M., YOUNG, J., CAMAKARIS, J., HARPER, J. F. & COBBETT, C. S. 2004. P-type ATPase heavy metal transporters with roles in essential zinc homeostasis in Arabidopsis. *Plant Cell,* 16**,** 1327-39.

HUYSMAN, M. J., VYVERMAN, W. & DE VEYLDER, L. 2014. Molecular regulation of the diatom cell cycle. *Journal of Experimental Botany,* 65**,** 2573-84.

IANORA, A., BENTLEY, M. G., CALDWELL, G. S., CASOTTI, R., CEMBELLA, A. D., ENGSTROM-OST, J., HALSBAND, C., SONNENSCHEIN, E., LEGRAND, C., LLEWELLYN, C. A., PALDAVICIENE, A., PILKAITYTE, R., POHNERT, G., RAZINKOVAS, A., ROMANO, G., TILLMANN, U. & VAICIUTE, D. 2011. The relevance of marine chemical ecology to plankton and ecosystem function: an emerging field. *Marine Drugs,* 9**,** 1625-48.

JAMERS, A., LENJOU, M., DERAEDT, P., BOCKSTAELE, D. V., BLUST, R. & COEN, W. D. 2009. Flow cytometric analysis of the cadmium-exposed green algaChlamydomonas reinhardtii(Chlorophyceae). *European Journal of Phycology,* 44**,** 541-550.

JOHANSEN, J. R. 1991. Morphological variability and cell wall composition of Phaeodactylum tricornutum (Bacillariophyceae). *The Great Basin Naturalist***,** 310-315.

KALAJI, H. M., SCHANSKER, G., LADLE, R. J., GOLTSEV, V., BOSA, K., ALLAKHVERDIEV, S. I., BRESTIC, M., BUSSOTTI, F., CALATAYUD, A., DABROWSKI, P., ELSHEERY, N. I., FERRONI, L., GUIDI, L., HOGEWONING, S. W., JAJOO, A., MISRA, A. N., NEBAUER, S. G., PANCALDI, S., PENELLA, C., POLI, D., POLLASTRINI, M., ROMANOWSKA-DUDA, Z. B., RUTKOWSKA, B., SERODIO, J., SURESH, K., SZULC, W., TAMBUSSI, E., YANNICCARI, M. & ZIVCAK, M. 2014. Frequently asked questions about in vivo chlorophyll fluorescence: practical issues. *Photosynthesis Research,* 122**,** 121-58.

KIM, E. & GELDER, R. N. V. 2006. Duane's Ophthalmology on CD-ROM. *In:* TASMAN, W. S. & JAEGER, E. A. (eds.) *Molecular Diagnostics of Ocular Infectious Disease: Polymerase Chain Reaction Diagnostics of Ophthalmic Disease.* Philadelphia, United States: Lippincott Williams and Wilkins.

KROTH, P. 2007. Genetic transformation; a tool to study protein targeting in diatoms, chap. 17. *Methods in molecular biology, 2nd edn., Totowa, NJ, USA: Humana Press*.

LANE, T. W. & MOREL, F. M. M. 2000. A biological function for cadmium in marine diatoms. *Proceedings of the National Academy of Sciences,* 97**,** 4627-4631.

MASMOUDI, S., NGUYEN-DEROCHE, N., CARUSO, A., AYADI, H., MORANT-MANCEAU, A., TREMBLIN, G. & SCHOEFS, B. 2013. Cadmium, copper, sodium and zinc effects on diatoms: from heaven to hell-A review. *Cryptogamie, Algologie,* 34**,** 185-225.

MATTOO, A. K., MARDER, J. B. & EDELMAN, M. 1989. Dynamics of the photosystem II reaction center. *Cell,* 56**,** 241-246.

MOREL, F. M. M. & RUETER, J. G. 1979. Aquil: a chemically defined phytoplankton culture medium for trace metal studies. *Journal of Phycology,* 15**,** 135-141.

MORELLI, E. & SCARANO, G. 2004. Copper-induced changes of non-protein thiols and antioxidant enzymes in the marine microalga Phaeodactylum tricornutum. *Plant Science,* 167**,** 289-296.

MULLER, P., LI X & NIYOGI, K. N. 2001. Nonphotochemical quenching. A response to excess light energy. *Plant Physiology,* 125**,** 1558-1566.

NASER, H. A. 2013. Assessment and management of heavy metal pollution in the marine environment of the Arabian Gulf: a review. *Marine Pollution Bulletin,* 72**,** 6-13.

NGUYEN-DEROCHE TLE, N., CARUSO, A., LE, T. T., BUI, T. V., SCHOEFS, B., TREMBLIN, G. & MORANT-MANCEAU, A. 2012. Zinc affects differently growth, photosynthesis, antioxidant enzyme activities and phytochelatin synthase expression of four marine diatoms. *ScientificWorldJournal,* 2012**,** 982957.

PERALES-VELA, H. V., PEÑA-CASTRO, J. M. & CAÑIZARES-VILLANUEVA, R. O. 2006. Heavy metal detoxification in eukaryotic microalgae. *Chemosphere,* 64**,** 1-10.

PRASAD, M. N. V. 2001. *Metals in the environment: analysis by biodiversity*, CRC Press.

PRICE, N. M., HARRISON, G., I, HERING, J. G., HUDSON, R. J., NIREL, P. M. V., PALENIK, B. & MOREL, F. M. M. 1989. Preparation and chemistry of the artificial algal culture medium aquil. *Biological oceanography,* 6**,** 443-461.

QIU, R.-L., TANG, Y.-T., ZENG, X.-W., THANGAVEL, P., TANG, L., GAN, Y.-Y., YING, R.-R. & WANG, S.-Z. 2012. Mechanisms of Cd Hyperaccumulation and Detoxification in Heavy Metal Hyperaccumulators: How Plants Cope with Cd. *Progress in Botany 73.* Springer.

ROHACEK, K. & BARTAK, M. 1999. Technique of the modulated cholorophyll fluorescence: basic concepts, useful parameters, and some applications. *Photosynthetica,* 37**,** 339-363.
SAHEBI, M., HANAFI, M. M., SITI NOR AKMAR, A., RAFII, M. Y., AZIZI, P., TENGOUA, F. F., NURUL MAYZAITUL AZWA, J. & SHABANIMOFRAD, M. 2015. Importance of silicon and mechanisms of biosilica formation in plants. *Biomed Research International,* 2015**,** 396010.
SARKER, S., DESAI, S. R., VERLECAR, X. N., SAHA SARKER, M. & SARKAR, A. 2016. Mercury-induced genotoxicity in marine diatom (Chaetoceros tenuissimus). *Environmental Science and Pollution Research,* 23**,** 2770-7.
SIAUT, M., HEIJDE, M., MANGOGNA, M., MONTSANT, A., COESEL, S., ALLEN, A., MANFREDONIA, A., FALCIATORE, A. & BOWLER, C. 2007. Molecular toolbox for studying diatom biology in Phaeodactylum tricornutum. *Gene,* 406**,** 23-35.
STEINNES, E. 1987. Impact of long-range atmospheric transport of heavy metals to the terrestrial environment in Norway. John Wiley & Sons Ltd: New York, NY, USA.
STRØM MIDTHUN, E. 2012. *Characterization of the Cytochrome p450 Family in the unique Diatom Seminavis robusta.* Master thesis.
TCHOUNWOU, P. B., YEDJOU, C. G., PATLOLLA, A. K. & SUTTON, D. J. 2012. Heavy metal toxicity and the environment. *Experientia Supplementum,* 101**,** 133-64.
THÉVENOD, F., FRIEDMANN, J. M., KATSEN, A. D. & HAUSER, I. A. 2000. Up-regulation of multidrug resistance P-glycoprotein via nuclear factor-κB activation protects kidney proximal tubule cells from cadmium-and reactive oxygen species-induced apoptosis. *Journal of Biological Chemistry,* 275**,** 1887-1896.
TOKAR, E., BOYD, W., FREEDMAN, J. & WAALKES, M. 2013. *Casarett and Doull's toxicology: the basic science of poisons [Editor: Klaassen, Curtis D]*, McGraw-Hill New York (NY).
TOLCIN, A. C. 2015. *U.S. Geological Survey; Mineral Commodity Summaries* [Online]. Available: http://minerals.usgs.gov/minerals/pubs/mcs/ [Accessed June 2016].
TOONE, W. M., KUGE, S., SAMUELS, M., MORGAN, B. A., TODA, T. & JONES, N. 1998. Regulation of the fission yeast transcription factor Pap1 by oxidative stress: requirement for the nuclear export factor Crm1 (Exportin) and the stress-activated MAP kinase Sty1/Spc1. *Genes & Development,* 12**,** 1453-1463.
TORRES, E., CID, A., FIDALGO, P., HERRERO, C. & ABALDE, J. 1997. Long-chain class III metallothioneins as a mechanism of cadmium tolerance in the marine diatom Phaeodactylum tricornutum Bohlin. *Aquatic Toxicology* 39**,** 231-246.
TORRES, E., CID, A., HERRERO, C. & ABALDE, J. 2000. Effect of Cadmium on growth, ATP content, carbon fixation and ultrastructure in the marine diatom *Phaeodactylum tricornutum* bohlin. *Water, Air and Soil Pollution,* 117**,** 1-14.
TORRES, E., MERA, R., HERRERO, C. & ABALDE, J. 2014. Isotherm studies for the determination of Cd (II) ions removal capacity in living biomass of a microalga with high tolerance to cadmium toxicity. *Environmental Science and Pollution Research,* 21**,** 12616-28.
TORRES, M. A., BARROS, M. P., CAMPOS, S. C., PINTO, E., RAJAMANI, S., SAYRE, R. T. & COLEPICOLO, P. 2008. Biochemical biomarkers in algae and marine pollution: a review. *Ecotoxicology and Environmental Safety,* 71**,** 1-15.
VIVARES, D., ARNOUX, P. & PIGNOL, D. 2005. A papain-like enzyme at work: native and acyl-enzyme intermediate structures in phytochelatin synthesis. *Proceedings of the National Academy of Sciences of the United States of America,* 102**,** 18848-53.
WORLDHEALTHORGANIZATION 2011. Cadmium in drinking-water: background document for development of WHO guidelines for drinking-water quality.

Supplementary Information/Appendix:

A.1. Diatom culture media:

Artificial algal culture medium (Aquil) – Composition

Substance	Final concentration (M)
Aquil salts	
NaCl	$4.20 * 10^{-1}$
Na_2SO_4	$2.88 * 10^{-2}$
KCl	$9.39 * 10^{-3}$
$NaHCO_3$	$2.38 * 10^{-3}$
KBr	$8.40 * 10^{-4}$
H_3BO_3	$4.85 * 10^{-4}$
NaF	$7.14 * 10^{-5}$
$MgCl_2.6H_2O$	$5.46 * 10^{-2}$
$CaCl_2.2H_2O$	$1.05 * 10^{-2}$
$SrCl_2.6H_2O$	$6.38 * 10^{-5}$
Nutrients	
NaH_2PO_4	$1.00 * 10^{-5}$
$NaNO_3$	$3.00 * 10^{-4}$
$Na_2SiO_3.5H_2O$	$1.00 * 10^{-4}$
Trace Metals	
Na_2EDTA	$5.00 * 10^{-6}$
$FeCl_3.6H_2O$	$4.51 * 10^{-7}$
$ZnSO_4.7H_2O$	$4.00 * 10^{-9}$
$MnCl_2.4H_2O$	$2.30 * 10^{-8}$
$CoCl_2.6H_2O$	$2.50 * 10^{-9}$
$CuSO_4.5H_2O$	$9.97 * 10^{-10}$
$Na_2MoO_4.2H_2O$	$1.00 * 10^{-7}$
Na_2SeO_3	$1.00 * 10^{-8}$

Vitamins

B12	$5.50 * 10^{-7}$ g/L
Biotin	$5.00 * 10^{-7}$ g/L
Thiamine HCl	$1.00 * 10^{-4}$ g/L

Artificial algal culture medium (Aquil) – Preparation procedure

The synthesis of Aquil medium is divided into three parts i) chelex preparation ii) medium preparation iii) sterilization

(i) The target concentrations of the trace metals are very low and therefore it is necessary to remove impurities from the chemical reagents used in the medium preparation. This is achieved by passing the major salt and nutrient solutions through ion exchange columns. Chelex 100 resin (Molecular biology grade, 200-400 mesh, sodium form) is considered suitable in the Aquil preparation because it selects compounds to trap based on the chelate formation rather than on the charge of the cation or physical characteristics.

After the adjustment of the pH, the slurry was transferred into a chromatography column of desired size. The strength and ionic form of Chelex 100 vary significantly with the pH. And hence, it is necessary to equilibrate each column to the pH and ionic strength of the solution being purified. The pH of the resin in this experiment was 8.6. Column chromatography is generally used as a purification technique as it helps in the extraction of desired compounds from a mixture. The liquid mixture when loaded on the top of the column flows down due to gravity or external pressure and the desired compounds are isolated from the mixture.

(ii) The procedure for medium preparation is diagrammatically represented as below:

- Hydrous and anhydrous salts in Synthetic Ocean Water (SOW):

24.53g NaCl

4.09g Na_2SO_4

0.7g KCl

0.2g $NaHCO_3$

0.1g KBr

0.03g H_3BO_3

0.003g NaF

1.54g $CaCl_2.2H_2O$ (dried)

0.017g $SrCl_2.6H_2O$ (dried)

Weighed

11.1g $MgCl_2.6H_2O$ (dried)

Weighed

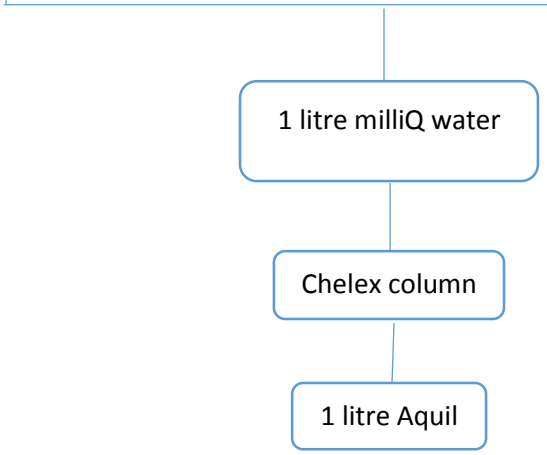

- Nutrients

1.20g NaH_2PO_4

Weighed

25.5g $NaNO_3$

Weighed

28.40g $Na_2SiO_3.5H_2O$

Weighed

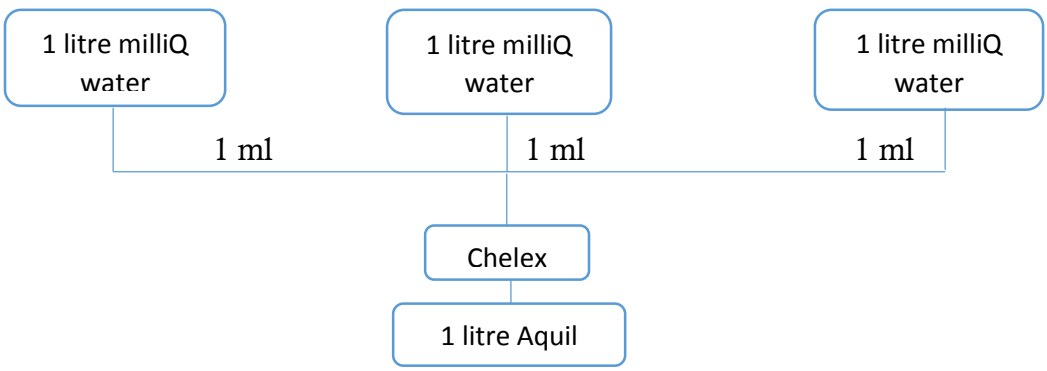

- Trace Metals

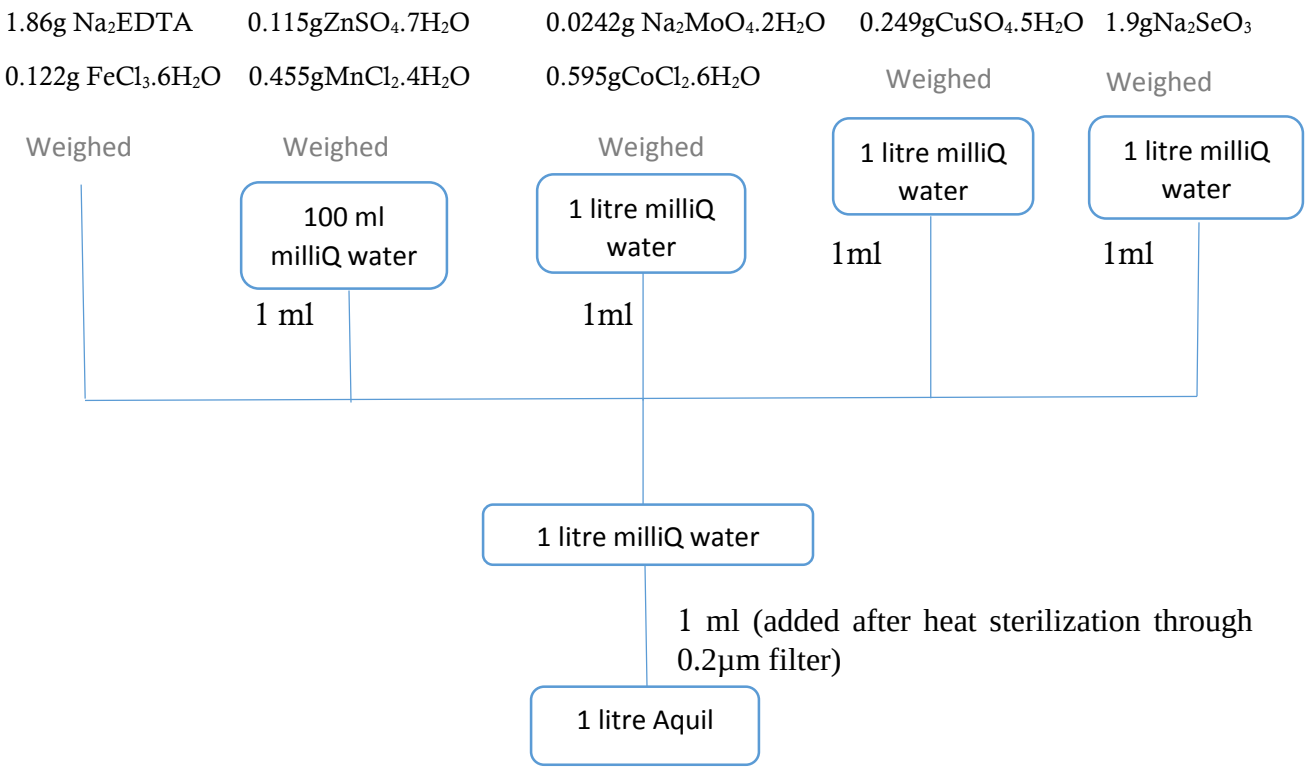

- Vitamins

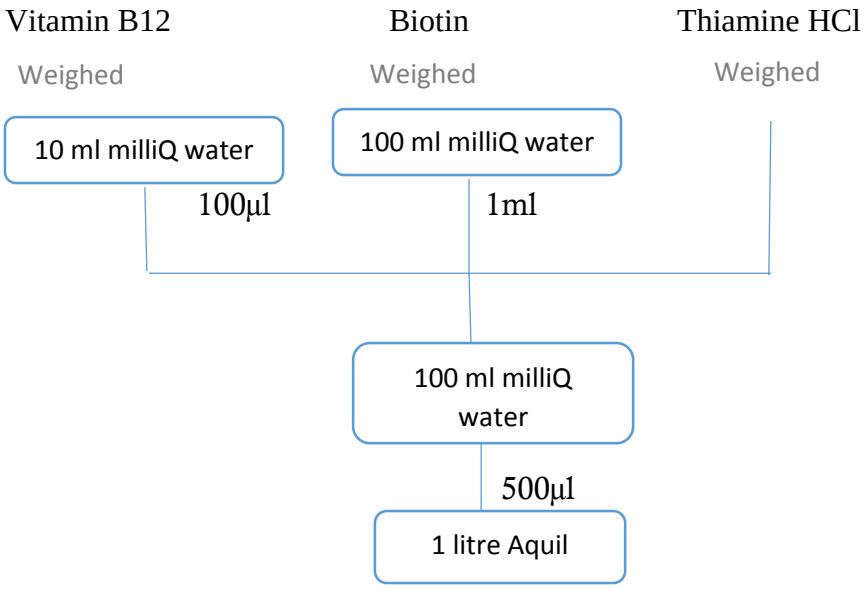

(iii) Since autoclaving might introduce some trace metal contamination through the steam that could result in precipitation of some of the carbonate species, it is not recommended.

Sterilization was performed using a 700-W microwave oven. This method takes just 10 minutes in intervals of 3,2,3,2 minutes between the heating cycles. The container of the Aquil medium has to be mixed well between the intervals.

An alternative method of sterilization is filter sterilization using a 0.25- or 0.45µm acid-washed Nucleopore filter using a sterile, metal clean filtering apparatus.

A.2. Acid Washing:

Acid washing the glasswares – Composition:

Distilled water	2150 ml
65% HNO_3	350 ml

Acid washing the glasswares – Preparation Procedure:

- Prepare the washing solution as mentioned above
- Pour the washing solution into the glass equipment which has to be treated until the brim. Also, soak the lids of the containers into a separate beaker that contains the solution.
- After overnight/whole day soaking, empty or collect the 'used' solution into a separate container.
- Wash the bottles 6X with distilled water and then 1X with milliQ water.
- Let the equipment air dry by turning them upside down on papers underneath.
- The equipment are ready to be used from the next day.

A.3. Preparation of Serial dilutions:

Molecular weight of CdCl2. 2H2O = 219

Molecular weight of Cd2+ = 112

Stock Solution:

To prepare 15.625 g/l of Cd2+ stock solution

Amount of CdCl2. 2H2O required = (15.625*219)/112

= 30 g/l

30 g of CdCl2 in 1 litre milliQ water

- ⇨ 3 g of CdCl2 in 100 ml of milliQ water.

Dilution series:

500 µl of 15.625 g/l solution in 50 ml Aquil medium = 156.25 mg/l (con_7)

10 ml of the solution of above concentration (con_7) in 40 ml of Aquil = 31.25 mg/l

1.6 ml of con_7 in 40 ml of Aquil = 6 mg/l

320 µl of con_7 in 40 ml of Aquil = 1.25 mg/l

64 µl of con_7 in 40 ml of Aquil = 0.25 mg/l

12.8 µl of con_7 in 40 ml of Aquil = 0.05 mg/l

2.56 µl of con_7 in 40 ml of Aquil = 0.01 mg/l

50 ml of Aquil = Control

A.4. Preparation of Master Mix solutions:

Components of Master Mix:

Volume per reaction (µl)

Autoclaved milliQ water	= 3
PCR primer (10X)	= 2
LightCycler 480 SYBR Green Master kit (2X)	= 10
Total volume	= 15

A.5. Primer details:

List of Primers for Target genes:

Seminavis robusta:

Gene	Primer Name	Sequence	Orientation	Melting pt	Size
SrCA1	qSrCA1F	GCATTCATGCTCTGGTCTATGA	Forward	53.0	141
	qSrCA1R	AGCAACAACTCTGCTTCCTTGA	Reverse	53.0	
SrCYCB1	qCYCB1bF	AAATGCCCGTATGATGATGCAC	Forward	53.0	113
	qCYCB1bR	GAAGATGGCACAAATCCTAGTC	Reverse	53.0	
SrHMA2	qSrHMA2F	GACGGTCTGTGCTAACAAATCC	Forward	54.8	158
	qSrHMA2R	CCAGCAACGTAACATCGGCAGT	Reverse	56.7	
SrVIT1	qSrVIT1F	GTTGGAACTCGGTTTCCTCGAA	Forward	54.8	147
	qSrVIT1R	TGCAGCAATGAAACCAACAGTC	Reverse	53.0	
SrZIP-T1	qSrZIP1F	CATTCCCACGGAATGGAGACTG	Forward	56.7	129
	qSrZIP1R	CGGCTTTGAGGTTGGAACTGCT	Reverse	56.7	
SrPCS1	qSrPCS1F	TCAGCCTGTTGCAAGTGTCGAA	Forward	54.8	66
	qSrPCS1R	AGATGGCTTCTTGCGGTGTCAT	Reverse	54.8	
SrNTF2-L	qSrNTF2F	AATGGAAGATCTCGCACCATCA	Forward	53.0	144
	qSrNTF2R	CACTTGGCAACCTTATCAGAGT	Reverse	53.0	
SrSOD1	qSrSOD1F	TACCTAAAGTACCAGAACCGTC	Forward	53.0	76
	qSrSOD1R	TCAGAAACCTTGTCCCAGTTGA	Reverse	53.0	
SrGsr_2	qSrGSR2F	AAAGTTGTGGGTCTCCACGTCA	Forward	54.8	73
	qSrGSR2R	ATCTTCAGCGCAATGCCGAAAC	Reverse	54.8	

Phaeodactylum tricornutum:

Gene	Primer Name	Sequence	Orientation	Melting pt	Size
PtCA1	qPtCA1F	GTCATACGACCTCGACATCACT	Forward	54.8	138
	qPtCA1R	ATCGACGCATCCAATGTACAAG	Reverse	53	
PtCYCB1	qPtCYCB1F	TGAGACAATGCGTTATGACCGA	Forward	53	89
	qPtCYCB1R	GGTTCCAGCGAAAATCTGTGTA	Reverse	53	
PtHMA2	qPtHMA2_F3	ACACGGCTTGCCAGAAGAATTG	Forward	54.8	81
	qPtHMA2_R3	CGGTATCCTTTCTGGAAAGCCA	Reverse	54.8	
PtVIT1	qPtVIT1F	CTGCCTTGGAGAATCTGGTCAT	Forward	54.8	124
	qPtVIT1R	TTGGCCCAACAATACCGCACAT	Reverse	54.8	
PtZIP-T1	qPtZIP-T1_F1	AAATTCGGTGCTTCTCTATTGG	Forward	51.1	88
	qPtZIP-T1_R1	ACATCACAATCCTCGATATCAG	Reverse	51.1	
PtPCS1	qPtPCS1_F1	CATCGTTGACCAAGTGCTAACT	Forward	53	108
	qPtPCS1_R1	TTCGCCATTCTGACAAACCGTA	Reverse	53	
PtNTF2-L	qPtNTF2F	TACCATGGGTATCGACAACACT	Forward	53	66
	qPtNTF2R	GCCATTTTCCTTGGTGTAAACG	Reverse	53	
PtCAT1	qPtCAT1_F1	GCACCGATTAGGGACAAACTAC	Forward	54.8	88
	qPtCAT1_R1	CGTCTCGCTGGTAATTGTGCTG	Reverse	56.7	
PtGsr_2	qPtGSR2F	AAGTTGCTCGTCTTGGTGGAAC	Forward	54.8	122
	qPtGSR2R	CCATACCAGAGAACCCATAGTG	Reverse	54.8	

List of Reference genes:

Seminavis robusta:

srH4A, srVPS35, srAGC1

Phaeodactylum tricornutum:

ptRPS5, ptDLST

A.6. Sample calculation of Growth rate (μ):

Growth rate (μ) calculation illustration:

Number of cells on beginning of time interval, N1 = 1880

Number of cells on end of time interval, N2 = 2190

N2/N1 = 1.1649

Length of time interval, Δt = 1

Proportional rate of change, r = ln (N2/N1) / Δt

r = 0.1526 is equal to μ when mortality is zero

Therefore Growth rate (μ) = 0.1526

A.7. Illustration of reading data from flow cytometry:

Absolute cell count from flow cytometry- illustration:

After loading the sample into the flow cytometer, a dot plot was made with forward scatter height (FSC-H) on x axis and side scatter height (SSC-H) on the y axis.

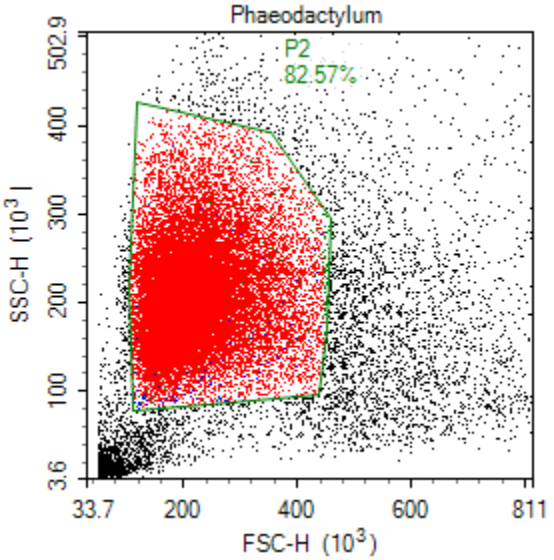

Cell debris, microorganisms and other noise were removed by gating the selected area that contained the sample of interest.

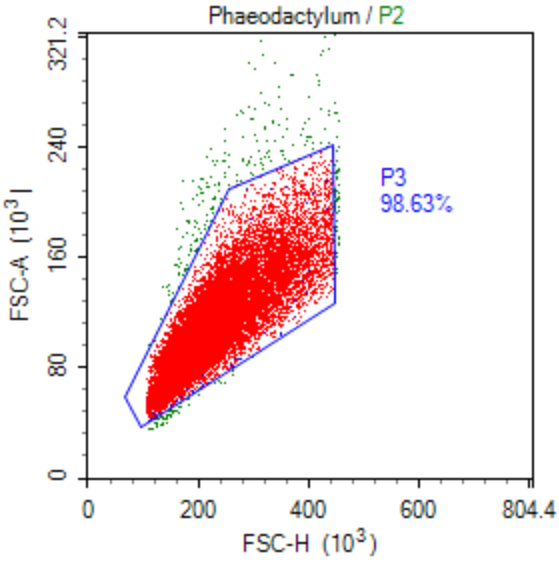

With the gated area, another dot plot was created with the forward scatter data between height (x axis) and area (y axis). Another gate was made to avoid the doublets. With the gated data, a histogram was made with the Chlorophyll on the x axis and the count on y axis.

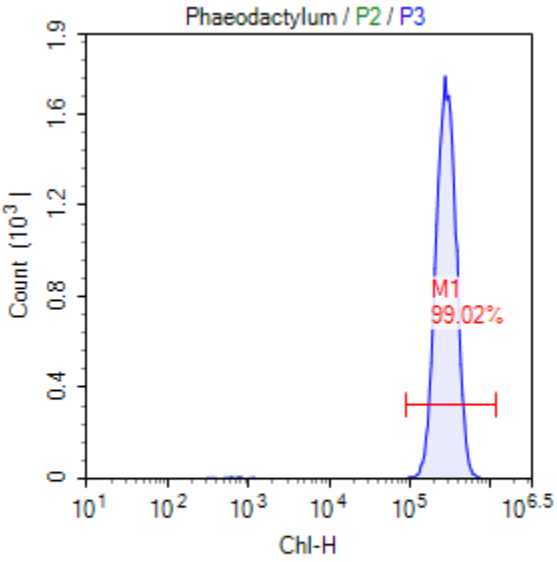

Gate	Count	Abs. Count	% P3	Mean X	CV X
P3	24,432	971	100.00 %	299,238	29.29 %
M1	24,193	961	99.02 %	302,108	27.52 %

In general a sharp peak ensures pure culture. The target width was gated and with the help of statistics, absolute count was obtained as shown in the figure above.

A.8. Illustration of Tm- calling analysis (Dissociation curve):

Tm-calling analysis using Light Cycler 96 software – Illustration:

Melting curves for the triplicates and the peaks obtained are represented in the picture. The gene analyzed was catalase in the control group of *Phaeodactylum tricornutum* after 48 hours of exposure.

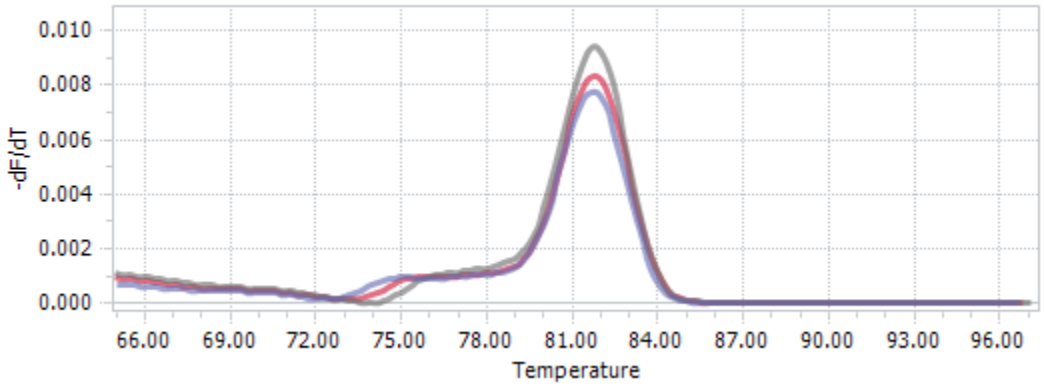

A.9. Cq values of qPCR analysis:

Quantification cycle (cq) values of all the genes analyzed by qPCR are shown below. It has to be noted that the triplicates DO NOT lie on adjacent wells.

Seminavis robusta:

Sample name	indiv_PCR_eff	Amplicon	threshold	mean_PCR_eff	Cq
48hrs_0 (1)	1.885	CA1	0.039	1.860	26.648
48hrs_0.01 (1)	1.860	CA1	0.039	1.860	24.917
48hrs_0.05 (1)	1.833	CA1	0.039	1.860	25.890
48hrs_1.25 (1)	1.848	CA1	0.039	1.860	26.797
72hrs_0 (1)	1.778	CA1	0.039	1.860	32.131
72hrs_0.01 (1)	1.845	CA1	0.039	1.860	29.965
72hrs_0.05 (1)	1.864	CA1	0.039	1.860	28.970
72hrs_1.25 (1)	1.842	CA1	0.039	1.860	30.572
48hrs_0 (2)	1.862	CA1	0.039	1.860	26.450
48hrs_0.01 (2)	1.868	CA1	0.039	1.860	25.193
48hrs_0.05 (2)	1.866	CA1	0.039	1.860	25.271
48hrs_1.25 (2)	1.867	CA1	0.039	1.860	26.659
72hrs_0 (2)	1.863	CA1	0.039	1.860	30.322
72hrs_0.01 (2)	1.855	CA1	0.039	1.860	31.632
72hrs_0.05 (2)	1.884	CA1	0.039	1.860	28.622

72hrs_1.25 (2)	1.835	CA1	0.039	1.860	31.134
48hrs_0 (3)	1.871	CA1	0.039	1.860	28.232
48hrs_0.01 (3)	1.856	CA1	0.039	1.860	24.958
48hrs_0.05 (3)	1.860	CA1	0.039	1.860	26.055
48hrs_1.25 (3)	1.868	CA1	0.039	1.860	26.099
72hrs_0 (3)	1.861	CA1	0.039	1.860	30.624
72hrs_0.05 (3)	1.865	CA1	0.039	1.860	30.270
72hrs_1.25 (3)	1.864	CA1	0.039	1.860	29.486
NEGATIVE	1.810	CA1	0.039	1.860	43.197
48hrs_0 (1)	1.833	CYCB1	0.053	1.833	29.064
48hrs_0.01 (1)	1.859	CYCB1	0.053	1.833	29.225
48hrs_0.05 (1)	1.851	CYCB1	0.053	1.833	29.629
48hrs_1.25 (1)	1.847	CYCB1	0.053	1.833	30.034
72hrs_0 (1)	1.858	CYCB1	0.053	1.833	30.354
72hrs_0.01 (1)	1.835	CYCB1	0.053	1.833	30.254
72hrs_0.05 (1)	1.816	CYCB1	0.053	1.833	30.602
72hrs_1.25 (1)	1.851	CYCB1	0.053	1.833	30.217
48hrs_0 (2)	1.874	CYCB1	0.053	1.833	29.564
48hrs_0.01 (2)	1.824	CYCB1	0.053	1.833	30.410
48hrs_0.05 (2)	1.847	CYCB1	0.053	1.833	30.181
48hrs_1.25 (2)	1.816	CYCB1	0.053	1.833	30.300
72hrs_0 (2)	1.794	CYCB1	0.053	1.833	30.753
72hrs_0.01 (2)	1.793	CYCB1	0.053	1.833	31.537
72hrs_0.05 (2)	1.835	CYCB1	0.053	1.833	30.019
72hrs_1.25 (2)	1.826	CYCB1	0.053	1.833	30.786
48hrs_0 (3)	1.842	CYCB1	0.053	1.833	31.584
48hrs_0.01 (3)	1.844	CYCB1	0.053	1.833	30.707
48hrs_0.05 (3)	1.838	CYCB1	0.053	1.833	30.516
48hrs_1.25 (3)	1.829	CYCB1	0.053	1.833	29.753
72hrs_0 (3)	1.787	CYCB1	0.053	1.833	31.886
72hrs_0.05 (3)	1.822	CYCB1	0.053	1.833	30.660
72hrs_1.25 (3)	1.831	CYCB1	0.053	1.833	31.111
NEGATIVE	1.000	CYCB1	0.053	1.833	0.000
48hrs_0 (1)	1.697	HMA2	0.006	1.861	30.113
48hrs_0.01 (1)	1.853	HMA2	0.006	1.861	24.289
48hrs_0.05 (1)	1.834	HMA2	0.006	1.861	20.010
48hrs_1.25 (1)	1.760	HMA2	0.006	1.861	21.098
72hrs_0 (1)	1.860	HMA2	0.006	1.861	22.179
72hrs_0.01 (1)	1.836	HMA2	0.006	1.861	20.751
72hrs_0.05 (1)	1.876	HMA2	0.006	1.861	21.532
72hrs_1.25 (1)	1.795	HMA2	0.006	1.861	20.851

48hrs_0 (2)	1.853	HMA2	0.006	1.861	21.705
48hrs_0.01 (2)	1.876	HMA2	0.006	1.861	21.187
48hrs_0.05 (2)	1.726	HMA2	0.006	1.861	20.194
48hrs_1.25 (2)	1.828	HMA2	0.006	1.861	20.519
72hrs_0 (2)	1.811	HMA2	0.006	1.861	19.900
72hrs_0.01 (2)	1.860	HMA2	0.006	1.861	20.376
72hrs_0.05 (2)	1.894	HMA2	0.006	1.861	20.623
72hrs_1.25 (2)	1.841	HMA2	0.006	1.861	20.670
48hrs_0 (3)	1.877	HMA2	0.006	1.861	20.964
48hrs_0.01 (3)	1.790	HMA2	0.006	1.861	19.182
48hrs_0.05 (3)	1.884	HMA2	0.006	1.861	20.322
48hrs_1.25 (3)	1.905	HMA2	0.006	1.861	19.720
72hrs_0 (3)	1.893	HMA2	0.006	1.861	20.095
72hrs_0.05 (3)	1.948	HMA2	0.006	1.861	20.352
72hrs_1.25 (3)	1.910	HMA2	0.006	1.861	20.930
NEGATIVE	1.960	HMA2	0.006	1.861	43.262
48hrs_0 (1)	1.702	VIT1	0.050	1.852	30.536
48hrs_0.01 (1)	1.617	VIT1	0.050	1.852	33.169
48hrs_0.05 (1)	1.749	VIT1	0.050	1.852	28.780
48hrs_1.25 (1)	1.759	VIT1	0.050	1.852	29.310
72hrs_0 (1)	1.779	VIT1	0.050	1.852	29.211
72hrs_0.01 (1)	1.803	VIT1	0.050	1.852	28.194
72hrs_0.05 (1)	1.753	VIT1	0.050	1.852	30.198
72hrs_1.25 (1)	1.827	VIT1	0.050	1.852	27.406
48hrs_0 (2)	1.755	VIT1	0.050	1.852	30.564
48hrs_0.01 (2)	1.771	VIT1	0.050	1.852	31.125
48hrs_0.05 (2)	1.830	VIT1	0.050	1.852	28.291
48hrs_1.25 (2)	1.814	VIT1	0.050	1.852	29.054
72hrs_0 (2)	1.858	VIT1	0.050	1.852	27.036
72hrs_0.01 (2)	1.842	VIT1	0.050	1.852	28.749
72hrs_0.05 (2)	1.881	VIT1	0.050	1.852	27.102
72hrs_1.25 (2)	1.893	VIT1	0.050	1.852	26.548
48hrs_0 (3)	1.867	VIT1	0.050	1.852	28.065
48hrs_0.01 (3)	1.879	VIT1	0.050	1.852	28.128
48hrs_0.05 (3)	1.883	VIT1	0.050	1.852	27.205
48hrs_1.25 (3)	1.892	VIT1	0.050	1.852	26.241
72hrs_0 (3)	1.884	VIT1	0.050	1.852	27.277
72hrs_0.05 (3)	1.902	VIT1	0.050	1.852	26.765
72hrs_1.25 (3)	1.855	VIT1	0.050	1.852	26.020
NEGATIVE	1.686	VIT1	0.050	1.852	45.104
48hrs_0 (1)	1.767	ZIPT1	0.035	1.838	27.939

48hrs_0.01 (1)	1.733	ZIPT1	0.035	1.838	29.609
48hrs_0.05 (1)	1.614	ZIPT1	0.035	1.838	31.712
48hrs_1.25 (1)	1.721	ZIPT1	0.035	1.838	28.745
72hrs_0 (1)	1.713	ZIPT1	0.035	1.838	29.850
72hrs_0.01 (1)	1.831	ZIPT1	0.035	1.838	26.391
72hrs_0.05 (1)	1.779	ZIPT1	0.035	1.838	29.509
72hrs_1.25 (1)	1.836	ZIPT1	0.035	1.838	26.196
48hrs_0 (2)	1.841	ZIPT1	0.035	1.838	26.340
48hrs_0.01 (2)	1.807	ZIPT1	0.035	1.838	28.833
48hrs_0.05 (2)	1.841	ZIPT1	0.035	1.838	26.184
48hrs_1.25 (2)	1.837	ZIPT1	0.035	1.838	26.159
72hrs_0 (2)	1.847	ZIPT1	0.035	1.838	26.429
72hrs_0.01 (2)	1.819	ZIPT1	0.035	1.838	26.977
72hrs_0.05 (2)	1.829	ZIPT1	0.035	1.838	26.490
72hrs_1.25 (2)	1.847	ZIPT1	0.035	1.838	26.805
48hrs_0 (3)	1.850	ZIPT1	0.035	1.838	27.133
48hrs_0.01 (3)	1.872	ZIPT1	0.035	1.838	26.826
48hrs_0.05 (3)	1.850	ZIPT1	0.035	1.838	26.715
48hrs_1.25 (3)	1.857	ZIPT1	0.035	1.838	25.645
72hrs_0 (3)	1.817	ZIPT1	0.035	1.838	27.697
72hrs_0.05 (3)	1.838	ZIPT1	0.035	1.838	27.693
72hrs_1.25 (3)	1.835	ZIPT1	0.035	1.838	27.653
NEGATIVE	1.689	ZIPT1	0.035	1.838	41.250
48hrs_0 (1)	1.000	NTF2L	0.053	1.757	0.000
48hrs_0.01 (1)	1.637	NTF2L	0.053	1.757	45.096
48hrs_0.05 (1)	1.659	NTF2L	0.053	1.757	39.043
48hrs_1.25 (1)	1.771	NTF2L	0.053	1.757	29.265
72hrs_0 (1)	1.000	NTF2L	0.053	1.757	0.000
72hrs_0.01 (1)	1.900	NTF2L	0.053	1.757	45.092
72hrs_0.05 (1)	1.713	NTF2L	0.053	1.757	42.977
72hrs_1.25 (1)	1.812	NTF2L	0.053	1.757	30.696
48hrs_0 (2)	1.733	NTF2L	0.053	1.757	37.761
48hrs_0.01 (2)	1.000	NTF2L	0.053	1.757	0.000
48hrs_0.05 (2)	1.757	NTF2L	0.053	1.757	35.218
48hrs_1.25 (2)	1.846	NTF2L	0.053	1.757	27.531
72hrs_0 (2)	1.000	NTF2L	0.053	1.757	0.000
72hrs_0.01 (2)	1.758	NTF2L	0.053	1.757	38.284
72hrs_0.05 (2)	1.759	NTF2L	0.053	1.757	39.596
72hrs_1.25 (2)	1.841	NTF2L	0.053	1.757	29.349
48hrs_0 (3)	1.809	NTF2L	0.053	1.757	42.351
48hrs_0.01 (3)	1.754	NTF2L	0.053	1.757	37.445

48hrs_0.05 (3)	1.828	NTF2L	0.053	1.757	34.380
48hrs_1.25 (3)	1.840	NTF2L	0.053	1.757	26.054
72hrs_0 (3)	1.812	NTF2L	0.053	1.757	45.948
72hrs_0.05 (3)	1.769	NTF2L	0.053	1.757	38.005
72hrs_1.25 (3)	1.855	NTF2L	0.053	1.757	28.477
NEGATIVE	1.000	NTF2L	0.053	1.757	0.000
48hrs_0 (1)	1.579	SOD1	0.035	1.843	30.960
48hrs_0.01 (1)	1.776	SOD1	0.035	1.843	24.180
48hrs_0.05 (1)	1.615	SOD1	0.035	1.843	28.246
48hrs_1.25 (1)	1.591	SOD1	0.035	1.843	29.916
72hrs_0 (1)	1.596	SOD1	0.035	1.843	35.563
72hrs_0.01 (1)	1.666	SOD1	0.035	1.843	34.661
72hrs_0.05 (1)	1.590	SOD1	0.035	1.843	34.101
72hrs_1.25 (1)	1.621	SOD1	0.035	1.843	33.956
48hrs_0 (2)	1.844	SOD1	0.035	1.843	23.992
48hrs_0.01 (2)	1.864	SOD1	0.035	1.843	23.810
48hrs_0.05 (2)	1.683	SOD1	0.035	1.843	27.002
48hrs_1.25 (2)	1.834	SOD1	0.035	1.843	24.639
72hrs_0 (2)	1.796	SOD1	0.035	1.843	31.656
72hrs_0.01 (2)	1.731	SOD1	0.035	1.843	34.054
72hrs_0.05 (2)	1.856	SOD1	0.035	1.843	28.985
72hrs_1.25 (2)	1.866	SOD1	0.035	1.843	29.203
48hrs_0 (3)	1.790	SOD1	0.035	1.843	28.700
48hrs_0.01 (3)	1.859	SOD1	0.035	1.843	24.046
48hrs_0.05 (3)	1.828	SOD1	0.035	1.843	25.588
48hrs_1.25 (3)	1.846	SOD1	0.035	1.843	24.713
72hrs_0 (3)	1.825	SOD1	0.035	1.843	30.530
72hrs_0.05 (3)	1.856	SOD1	0.035	1.843	28.982
72hrs_1.25 (3)	1.874	SOD1	0.035	1.843	28.796
NEGATIVE	1.865	SOD1	0.035	1.843	37.425
48hrs_0 (1)	1.921	GSR2	0.047	1.891	29.595
48hrs_0.01 (1)	1.932	GSR2	0.047	1.891	28.720
48hrs_0.05 (1)	1.912	GSR2	0.047	1.891	29.646
48hrs_1.25 (1)	1.882	GSR2	0.047	1.891	30.252
72hrs_0 (1)	1.761	GSR2	0.047	1.891	35.692
72hrs_0.01 (1)	1.862	GSR2	0.047	1.891	33.776
72hrs_0.05 (1)	1.874	GSR2	0.047	1.891	33.015
72hrs_1.25 (1)	1.845	GSR2	0.047	1.891	33.501
48hrs_0 (2)	1.926	GSR2	0.047	1.891	29.836
48hrs_0.01 (2)	1.924	GSR2	0.047	1.891	29.745
48hrs_0.05 (2)	1.909	GSR2	0.047	1.891	28.191

48hrs_1.25 (2)	1.904	GSR2	0.047	1.891	30.178
72hrs_0 (2)	1.907	GSR2	0.047	1.891	32.752
72hrs_0.01 (2)	1.876	GSR2	0.047	1.891	33.767
72hrs_0.05 (2)	1.883	GSR2	0.047	1.891	33.221
72hrs_1.25 (2)	1.866	GSR2	0.047	1.891	33.920
48hrs_0 (3)	1.878	GSR2	0.047	1.891	32.951
48hrs_0.01 (3)	1.899	GSR2	0.047	1.891	30.195
48hrs_0.05 (3)	1.910	GSR2	0.047	1.891	29.304
48hrs_1.25 (3)	1.912	GSR2	0.047	1.891	30.261
72hrs_0 (3)	1.870	GSR2	0.047	1.891	33.762
72hrs_0.05 (3)	1.878	GSR2	0.047	1.891	34.776
72hrs_1.25 (3)	1.841	GSR2	0.047	1.891	33.956
NEGATIVE	1.895	GSR2	0.047	1.891	46.689
48hrs_0 (1)	1.919	H4A	0.601	1.918	30.717
48hrs_0.01 (1)	1.965	H4A	0.601	1.918	29.557
48hrs_0.05 (1)	1.960	H4A	0.601	1.918	30.174
48hrs_1.25 (1)	1.964	H4A	0.601	1.918	30.319
72hrs_0 (1)	1.991	H4A	0.601	1.918	28.814
72hrs_0.01 (1)	1.857	H4A	0.601	1.918	28.431
72hrs_0.05 (1)	2.019	H4A	0.601	1.918	27.839
72hrs_1.25 (1)	2.009	H4A	0.601	1.918	29.713
48hrs_0 (2)	1.860	H4A	0.601	1.918	29.851
48hrs_0.01 (2)	1.936	H4A	0.601	1.918	29.834
48hrs_0.05 (2)	1.911	H4A	0.601	1.918	28.292
48hrs_1.25 (2)	1.922	H4A	0.601	1.918	32.132
72hrs_0 (2)	1.905	H4A	0.601	1.918	28.949
72hrs_0.01 (2)	1.896	H4A	0.601	1.918	28.249
72hrs_0.05 (2)	1.825	H4A	0.601	1.918	27.811
72hrs_1.25 (2)	1.880	H4A	0.601	1.918	28.948
48hrs_0 (3)	2.064	H4A	0.601	1.918	31.869
48hrs_0.01 (3)	1.972	H4A	0.601	1.918	27.752
48hrs_0.05 (3)	1.897	H4A	0.601	1.918	27.883
48hrs_1.25 (3)	1.885	H4A	0.601	1.918	29.374
72hrs_0 (3)	1.897	H4A	0.601	1.918	27.034
72hrs_0.05 (3)	1.941	H4A	0.601	1.918	26.824
72hrs_1.25 (3)	1.929	H4A	0.601	1.918	27.973
NEGATIVE	1.887	H4A	0.601	1.918	39.460
48hrs_0 (1)	1.928	VPS35	0.637	1.924	30.018
48hrs_0.01 (1)	1.866	VPS35	0.637	1.924	29.410
48hrs_0.05 (1)	1.848	VPS35	0.637	1.924	29.517
48hrs_1.25 (1)	1.865	VPS35	0.637	1.924	29.092

72hrs_0 (1)	1.954	VPS35	0.637	1.924	30.018
72hrs_0.01 (1)	1.847	VPS35	0.637	1.924	29.168
72hrs_0.05 (1)	1.871	VPS35	0.637	1.924	29.541
72hrs_1.25 (1)	1.915	VPS35	0.637	1.924	28.681
48hrs_0 (2)	1.814	VPS35	0.637	1.924	29.098
48hrs_0.01 (2)	1.925	VPS35	0.637	1.924	28.622
48hrs_0.05 (2)	1.899	VPS35	0.637	1.924	28.436
48hrs_1.25 (2)	1.937	VPS35	0.637	1.924	28.791
72hrs_0 (2)	1.892	VPS35	0.637	1.924	29.201
72hrs_0.01 (2)	2.012	VPS35	0.637	1.924	30.426
72hrs_0.05 (2)	1.889	VPS35	0.637	1.924	28.147
72hrs_1.25 (2)	1.909	VPS35	0.637	1.924	29.365
48hrs_0 (3)	1.937	VPS35	0.637	1.924	29.461
48hrs_0.01 (3)	1.886	VPS35	0.637	1.924	27.041
48hrs_0.05 (3)	1.943	VPS35	0.637	1.924	27.532
48hrs_1.25 (3)	1.979	VPS35	0.637	1.924	27.443
72hrs_0 (3)	1.922	VPS35	0.637	1.924	27.927
72hrs_0.05 (3)	1.958	VPS35	0.637	1.924	28.473
72hrs_1.25 (3)	1.958	VPS35	0.637	1.924	28.797
NEGATIVE	1.525	VPS35	0.637	1.924	44.304
48hrs_0 (1)	2.120	PCS1	0.501	2.109	30.734
48hrs_0.01 (1)	2.136	PCS1	0.501	2.109	29.617
48hrs_0.05 (1)	2.107	PCS1	0.501	2.109	29.731
48hrs_1.25 (1)	2.101	PCS1	0.501	2.109	30.415
72hrs_0 (1)	2.123	PCS1	0.501	2.109	31.553
72hrs_0.01 (1)	2.081	PCS1	0.501	2.109	31.004
72hrs_0.05 (1)	2.044	PCS1	0.501	2.109	31.169
72hrs_1.25 (1)	2.101	PCS1	0.501	2.109	30.313
48hrs_0 (2)	2.154	PCS1	0.501	2.109	29.535
48hrs_0.01 (2)	2.091	PCS1	0.501	2.109	30.360
48hrs_0.05 (2)	2.077	PCS1	0.501	2.109	30.540
48hrs_1.25 (2)	2.102	PCS1	0.501	2.109	30.621
72hrs_0 (2)	2.100	PCS1	0.501	2.109	31.367
72hrs_0.01 (2)	2.120	PCS1	0.501	2.109	31.650
72hrs_0.05 (2)	2.091	PCS1	0.501	2.109	30.379
72hrs_1.25 (2)	2.138	PCS1	0.501	2.109	30.591
48hrs_0 (3)	2.124	PCS1	0.501	2.109	30.708
48hrs_0.01 (3)	2.096	PCS1	0.501	2.109	28.356
48hrs_0.05 (3)	2.002	PCS1	0.501	2.109	28.787
48hrs_1.25 (3)	1.990	PCS1	0.501	2.109	29.465
72hrs_0 (3)	2.151	PCS1	0.501	2.109	29.903

72hrs_0.05 (3)	2.077	PCS1	0.501	2.109	30.222
72hrs_1.25 (3)	2.139	PCS1	0.501	2.109	30.854
NEGATIVE	1.872	PCS1	0.501	2.109	42.407

Phaeodactylum tricornutum:

Sample name	indiv_PCR_eff	Amplicon	threshold	mean_PCR_eff	Cq
48hrs_0 (1)	1.496	CA1	0.041	1.843	30.511
48hrs_0.01 (1)	1.542	CA1	0.041	1.843	26.246
48hrs_0.05 (1)	1.390	CA1	0.041	1.843	31.158
48hrs_1.25 (1)	1.761	CA1	0.041	1.843	19.860
72hrs_0 (1)	1.612	CA1	0.041	1.843	23.635
72hrs_0.05 (1)	1.395	CA1	0.041	1.843	30.121
72hrs_1.25 (1)	1.771	CA1	0.041	1.843	21.403
48hrs_0 (2)	1.668	CA1	0.041	1.843	22.760
48hrs_0.01 (2)	1.696	CA1	0.041	1.843	22.226
48hrs_0.05 (2)	1.804	CA1	0.041	1.843	20.180
48hrs_1.25 (2)	1.643	CA1	0.041	1.843	23.432
72hrs_0 (2)	1.853	CA1	0.041	1.843	17.956
72hrs_0.05 (2)	1.853	CA1	0.041	1.843	18.910
72hrs_1.25 (2)	1.862	CA1	0.041	1.843	19.945
48hrs_0 (3)	1.886	CA1	0.041	1.843	17.562
48hrs_0.01 (3)	1.863	CA1	0.041	1.843	18.446
48hrs_0.05 (3)	1.879	CA1	0.041	1.843	16.729
48hrs_1.25 (3)	1.842	CA1	0.041	1.843	15.594
72hrs_0 (3)	1.847	CA1	0.041	1.843	17.118
72hrs_0.05 (3)	1.836	CA1	0.041	1.843	18.704
72hrs_1.25 (3)	1.817	CA1	0.041	1.843	16.831
NEGATIVE	1.939	CA1	0.041	1.843	44.685
NEGATIVE	1.857	CA1	0.041	1.843	41.198
NEGATIVE	1.809	CA1	0.041	1.843	42.419
48hrs_0 (1)	1.869	VIT1	0.046	1.902	25.918
48hrs_0.01 (1)	1.804	VIT1	0.046	1.902	26.140
48hrs_0.05 (1)	1.749	VIT1	0.046	1.902	27.053
48hrs_1.25 (1)	1.859	VIT1	0.046	1.902	23.318
72hrs_0 (1)	1.854	VIT1	0.046	1.902	23.970
72hrs_0.05 (1)	1.887	VIT1	0.046	1.902	23.513
72hrs_1.25 (1)	1.892	VIT1	0.046	1.902	21.251
48hrs_0 (2)	1.828	VIT1	0.046	1.902	24.656
48hrs_0.01 (2)	1.888	VIT1	0.046	1.902	22.965

48hrs_0.05 (2)	1.919	VIT1	0.046	1.902	24.731
48hrs_1.25 (2)	1.917	VIT1	0.046	1.902	21.694
72hrs_0 (2)	1.908	VIT1	0.046	1.902	23.292
72hrs_0.05 (2)	1.908	VIT1	0.046	1.902	24.271
72hrs_1.25 (2)	1.904	VIT1	0.046	1.902	21.157
48hrs_0 (3)	1.904	VIT1	0.046	1.902	24.106
48hrs_0.01 (3)	1.934	VIT1	0.046	1.902	23.616
48hrs_0.05 (3)	1.891	VIT1	0.046	1.902	23.963
48hrs_1.25 (3)	1.899	VIT1	0.046	1.902	22.061
72hrs_0 (3)	1.898	VIT1	0.046	1.902	22.039
72hrs_0.05 (3)	1.910	VIT1	0.046	1.902	24.555
72hrs_1.25 (3)	1.875	VIT1	0.046	1.902	20.961
NEGATIVE	1.930	VIT1	0.046	1.902	39.549
NEGATIVE	1.914	VIT1	0.046	1.902	38.950
NEGATIVE	1.933	VIT1	0.046	1.902	39.947
48hrs_0 (1)	1.824	ZIPT1	0.040	1.872	27.136
48hrs_0.01 (1)	1.816	ZIPT1	0.040	1.872	23.911
48hrs_0.05 (1)	1.764	ZIPT1	0.040	1.872	26.337
48hrs_1.25 (1)	1.865	ZIPT1	0.040	1.872	21.759
72hrs_0 (1)	1.879	ZIPT1	0.040	1.872	20.639
72hrs_0.05 (1)	1.820	ZIPT1	0.040	1.872	20.932
72hrs_1.25 (1)	1.900	ZIPT1	0.040	1.872	20.705
48hrs_0 (2)	1.870	ZIPT1	0.040	1.872	23.165
48hrs_0.01 (2)	1.870	ZIPT1	0.040	1.872	24.756
48hrs_0.05 (2)	1.881	ZIPT1	0.040	1.872	23.315
48hrs_1.25 (2)	1.868	ZIPT1	0.040	1.872	20.903
72hrs_0 (2)	1.882	ZIPT1	0.040	1.872	20.474
72hrs_0.05 (2)	1.891	ZIPT1	0.040	1.872	22.230
72hrs_1.25 (2)	1.853	ZIPT1	0.040	1.872	22.864
48hrs_0 (3)	1.872	ZIPT1	0.040	1.872	25.739
48hrs_0.01 (3)	1.857	ZIPT1	0.040	1.872	26.048
48hrs_0.05 (3)	1.885	ZIPT1	0.040	1.872	22.844
48hrs_1.25 (3)	1.885	ZIPT1	0.040	1.872	20.687
72hrs_0 (3)	1.895	ZIPT1	0.040	1.872	21.797
72hrs_0.05 (3)	1.880	ZIPT1	0.040	1.872	21.031
72hrs_1.25 (3)	1.874	ZIPT1	0.040	1.872	20.167
NEGATIVE	1.856	ZIPT1	0.040	1.872	39.331
NEGATIVE	1.861	ZIPT1	0.040	1.872	40.342
NEGATIVE	1.790	ZIPT1	0.040	1.872	38.906
48hrs_0 (1)	1.759	PCS1	0.007	1.898	25.783
48hrs_0.01 (1)	1.716	PCS1	0.007	1.898	26.684

48hrs_0.05 (1)	1.819	PCS1	0.007	1.898	24.597
48hrs_1.25 (1)	1.856	PCS1	0.007	1.898	23.753
72hrs_0 (1)	1.876	PCS1	0.007	1.898	23.005
72hrs_0.05 (1)	1.822	PCS1	0.007	1.898	22.723
72hrs_1.25 (1)	1.689	PCS1	0.007	1.898	26.222
48hrs_0 (2)	1.769	PCS1	0.007	1.898	24.176
48hrs_0.01 (2)	1.774	PCS1	0.007	1.898	23.581
48hrs_0.05 (2)	1.934	PCS1	0.007	1.898	21.618
48hrs_1.25 (2)	1.904	PCS1	0.007	1.898	20.853
72hrs_0 (2)	1.890	PCS1	0.007	1.898	21.453
72hrs_0.05 (2)	1.919	PCS1	0.007	1.898	21.408
72hrs_1.25 (2)	1.906	PCS1	0.007	1.898	20.851
48hrs_0 (3)	1.907	PCS1	0.007	1.898	21.053
48hrs_0.01 (3)	1.899	PCS1	0.007	1.898	21.371
48hrs_0.05 (3)	1.876	PCS1	0.007	1.898	20.317
48hrs_1.25 (3)	1.913	PCS1	0.007	1.898	19.793
72hrs_0 (3)	1.843	PCS1	0.007	1.898	19.949
72hrs_0.05 (3)	1.918	PCS1	0.007	1.898	22.060
72hrs_1.25 (3)	1.883	PCS1	0.007	1.898	20.054
NEGATIVE	1.082	PCS1	0.007	1.898	38.163
NEGATIVE	1.054	PCS1	0.007	1.898	47.668
NEGATIVE	1.067	PCS1	0.007	1.898	42.213
48hrs_0 (1)	1.813	NTF2L	0.052	1.856	31.712
48hrs_0.01 (1)	1.814	NTF2L	0.052	1.856	25.831
48hrs_0.05 (1)	1.844	NTF2L	0.052	1.856	24.230
48hrs_1.25 (1)	1.871	NTF2L	0.052	1.856	21.654
72hrs_0 (1)	1.851	NTF2L	0.052	1.856	24.906
72hrs_0.05 (1)	1.876	NTF2L	0.052	1.856	21.498
72hrs_1.25 (1)	1.889	NTF2L	0.052	1.856	21.726
48hrs_0 (2)	1.822	NTF2L	0.052	1.856	29.314
48hrs_0.01 (2)	1.795	NTF2L	0.052	1.856	31.983
48hrs_0.05 (2)	1.824	NTF2L	0.052	1.856	29.031
48hrs_1.25 (2)	1.871	NTF2L	0.052	1.856	24.257
72hrs_0 (2)	1.847	NTF2L	0.052	1.856	25.945
72hrs_0.05 (2)	1.846	NTF2L	0.052	1.856	27.073
72hrs_1.25 (2)	1.885	NTF2L	0.052	1.856	23.359
48hrs_0 (3)	1.745	NTF2L	0.052	1.856	33.750
48hrs_0.01 (3)	1.713	NTF2L	0.052	1.856	33.496
48hrs_0.05 (3)	1.878	NTF2L	0.052	1.856	27.570
48hrs_1.25 (3)	1.884	NTF2L	0.052	1.856	24.644
72hrs_0 (3)	1.830	NTF2L	0.052	1.856	31.034

72hrs_0.05 (3)	1.882	NTF2L	0.052	1.856	26.247
72hrs_1.25 (3)	1.888	NTF2L	0.052	1.856	22.431
NEGATIVE	1.000	NTF2L	0.052	1.856	0.000
NEGATIVE	1.912	NTF2L	0.052	1.856	46.631
NEGATIVE	1.868	NTF2L	0.052	1.856	44.391
48hrs_0 (1)	1.887	GSR2	0.048	1.889	27.263
48hrs_0.01 (1)	1.844	GSR2	0.048	1.889	28.647
48hrs_0.05 (1)	1.833	GSR2	0.048	1.889	27.987
48hrs_1.25 (1)	1.867	GSR2	0.048	1.889	28.019
72hrs_0 (1)	1.828	GSR2	0.048	1.889	28.612
72hrs_0.05 (1)	1.738	GSR2	0.048	1.889	30.229
72hrs_1.25 (1)	1.875	GSR2	0.048	1.889	27.508
48hrs_0 (2)	1.886	GSR2	0.048	1.889	24.959
48hrs_0.01 (2)	1.903	GSR2	0.048	1.889	25.548
48hrs_0.05 (2)	1.911	GSR2	0.048	1.889	25.553
48hrs_1.25 (2)	1.903	GSR2	0.048	1.889	24.372
72hrs_0 (2)	1.913	GSR2	0.048	1.889	25.842
72hrs_0.05 (2)	1.903	GSR2	0.048	1.889	26.814
72hrs_1.25 (2)	1.911	GSR2	0.048	1.889	27.760
48hrs_0 (3)	1.912	GSR2	0.048	1.889	26.596
48hrs_0.01 (3)	1.886	GSR2	0.048	1.889	27.312
48hrs_0.05 (3)	1.881	GSR2	0.048	1.889	26.085
48hrs_1.25 (3)	1.874	GSR2	0.048	1.889	24.939
72hrs_0 (3)	1.877	GSR2	0.048	1.889	27.102
72hrs_0.05 (3)	1.876	GSR2	0.048	1.889	27.640
72hrs_1.25 (3)	1.885	GSR2	0.048	1.889	25.208
NEGATIVE	1.797	GSR2	0.048	1.889	44.627
NEGATIVE	1.702	GSR2	0.048	1.889	47.334
NEGATIVE	1.771	GSR2	0.048	1.889	46.873
48hrs_0 (1)	1.801	CYCB1	0.584	1.879	29.557
48hrs_0.01 (1)	1.761	CYCB1	0.584	1.879	29.464
48hrs_0.05 (1)	1.803	CYCB1	0.584	1.879	32.015
48hrs_1.25 (1)	1.880	CYCB1	0.584	1.879	31.704
72hrs_0 (1)	1.818	CYCB1	0.584	1.879	32.378
72hrs_0.05 (1)	1.811	CYCB1	0.584	1.879	34.328
72hrs_1.25 (1)	1.857	CYCB1	0.584	1.879	32.119
48hrs_0 (2)	1.881	CYCB1	0.584	1.879	30.707
48hrs_0.01 (2)	1.883	CYCB1	0.584	1.879	31.692
48hrs_0.05 (2)	1.927	CYCB1	0.584	1.879	31.287
48hrs_1.25 (2)	1.904	CYCB1	0.584	1.879	32.565
72hrs_0 (2)	1.960	CYCB1	0.584	1.879	31.154

72hrs_0.05 (2)	1.992	CYCB1	0.584	1.879	31.624
72hrs_1.25 (2)	1.955	CYCB1	0.584	1.879	31.177
48hrs_0 (3)	1.852	CYCB1	0.584	1.879	29.390
48hrs_0.01 (3)	2.025	CYCB1	0.584	1.879	31.585
48hrs_0.05 (3)	1.967	CYCB1	0.584	1.879	31.144
48hrs_1.25 (3)	1.847	CYCB1	0.584	1.879	29.392
72hrs_0 (3)	2.023	CYCB1	0.584	1.879	31.482
72hrs_0.05 (3)	1.965	CYCB1	0.584	1.879	32.604
72hrs_1.25 (3)	1.987	CYCB1	0.584	1.879	31.121
NEGATIVE	1.898	CYCB1	0.584	1.879	42.900
NEGATIVE	1.890	CYCB1	0.584	1.879	42.947
NEGATIVE	1.967	CYCB1	0.584	1.879	43.204
48hrs_0 (1)	1.956	HMA2	0.223	1.956	24.678
48hrs_0.01 (1)	1.925	HMA2	0.223	1.956	26.191
48hrs_0.05 (1)	1.937	HMA2	0.223	1.956	26.480
48hrs_1.25 (1)	1.920	HMA2	0.223	1.956	27.047
72hrs_0 (1)	1.932	HMA2	0.223	1.956	26.608
72hrs_0.05 (1)	1.947	HMA2	0.223	1.956	26.581
72hrs_1.25 (1)	1.927	HMA2	0.223	1.956	24.933
48hrs_0 (2)	1.947	HMA2	0.223	1.956	26.272
48hrs_0.01 (2)	1.936	HMA2	0.223	1.956	26.542
48hrs_0.05 (2)	1.965	HMA2	0.223	1.956	25.934
48hrs_1.25 (2)	1.984	HMA2	0.223	1.956	24.911
72hrs_0 (2)	1.954	HMA2	0.223	1.956	25.311
72hrs_0.05 (2)	1.961	HMA2	0.223	1.956	23.924
72hrs_1.25 (2)	1.977	HMA2	0.223	1.956	23.589
48hrs_0 (3)	1.968	HMA2	0.223	1.956	24.131
48hrs_0.01 (3)	1.972	HMA2	0.223	1.956	24.045
48hrs_0.05 (3)	1.955	HMA2	0.223	1.956	23.979
48hrs_1.25 (3)	1.960	HMA2	0.223	1.956	23.135
72hrs_0 (3)	1.970	HMA2	0.223	1.956	23.210
72hrs_0.05 (3)	1.982	HMA2	0.223	1.956	23.808
72hrs_1.25 (3)	1.981	HMA2	0.223	1.956	23.276
NEGATIVE	1.955	HMA2	0.223	1.956	23.474
NEGATIVE	1.978	HMA2	0.223	1.956	23.745
NEGATIVE	1.953	HMA2	0.223	1.956	23.932
48hrs_0 (1)	2.012	CAT1	0.540	1.923	27.144
48hrs_0.01 (1)	1.919	CAT1	0.540	1.923	27.736
48hrs_0.05 (1)	1.910	CAT1	0.540	1.923	27.077
48hrs_1.25 (1)	1.918	CAT1	0.540	1.923	28.354
72hrs_0 (1)	1.911	CAT1	0.540	1.923	26.395

72hrs_0.05 (1)	2.030	CAT1	0.540	1.923	28.308
72hrs_1.25 (1)	2.089	CAT1	0.540	1.923	26.721
48hrs_0 (2)	1.938	CAT1	0.540	1.923	27.856
48hrs_0.01 (2)	2.071	CAT1	0.540	1.923	27.598
48hrs_0.05 (2)	1.968	CAT1	0.540	1.923	29.949
48hrs_1.25 (2)	1.915	CAT1	0.540	1.923	29.048
72hrs_0 (2)	2.084	CAT1	0.540	1.923	26.822
72hrs_0.05 (2)	1.940	CAT1	0.540	1.923	26.530
72hrs_1.25 (2)	2.025	CAT1	0.540	1.923	27.874
48hrs_0 (3)	1.923	CAT1	0.540	1.923	28.257
48hrs_0.01 (3)	2.056	CAT1	0.540	1.923	30.894
48hrs_0.05 (3)	1.994	CAT1	0.540	1.923	30.330
48hrs_1.25 (3)	1.924	CAT1	0.540	1.923	28.159
72hrs_0 (3)	2.025	CAT1	0.540	1.923	29.090
72hrs_0.05 (3)	1.989	CAT1	0.540	1.923	30.513
72hrs_1.25 (3)	2.000	CAT1	0.540	1.923	28.152
NEGATIVE	1.893	CAT1	0.540	1.923	40.469
NEGATIVE	1.855	CAT1	0.540	1.923	41.408
NEGATIVE	1.841	CAT1	0.540	1.923	41.599
48hrs_0 (1)	1.898	RPS5	0.580	1.904	25.198
48hrs_0.01 (1)	1.904	RPS5	0.580	1.904	25.365
48hrs_0.05 (1)	1.889	RPS5	0.580	1.904	25.010
48hrs_1.25 (1)	1.883	RPS5	0.580	1.904	26.023
72hrs_0 (1)	1.906	RPS5	0.580	1.904	23.745
72hrs_0.05 (1)	1.972	RPS5	0.580	1.904	26.010
72hrs_1.25 (1)	1.898	RPS5	0.580	1.904	23.375
48hrs_0 (2)	1.884	RPS5	0.580	1.904	25.886
48hrs_0.01 (2)	1.910	RPS5	0.580	1.904	25.418
48hrs_0.05 (2)	1.905	RPS5	0.580	1.904	28.535
48hrs_1.25 (2)	1.904	RPS5	0.580	1.904	27.423
72hrs_0 (2)	1.923	RPS5	0.580	1.904	24.730
72hrs_0.05 (2)	1.927	RPS5	0.580	1.904	24.756
72hrs_1.25 (2)	1.895	RPS5	0.580	1.904	24.248
48hrs_0 (3)	1.922	RPS5	0.580	1.904	26.665
48hrs_0.01 (3)	1.949	RPS5	0.580	1.904	30.077
48hrs_0.05 (3)	1.918	RPS5	0.580	1.904	28.704
48hrs_1.25 (3)	1.896	RPS5	0.580	1.904	27.492
72hrs_0 (3)	1.903	RPS5	0.580	1.904	27.630
72hrs_0.05 (3)	1.876	RPS5	0.580	1.904	27.991
72hrs_1.25 (3)	1.922	RPS5	0.580	1.904	26.228
NEGATIVE	1.349	RPS5	0.580	1.904	45.265

NEGATIVE	1.882	RPS5	0.580	1.904	38.731
NEGATIVE	1.104	RPS5	0.580	1.904	47.690
48hrs_0 (1)	1.791	DLST	0.633	1.790	25.358
48hrs_0.01 (1)	1.796	DLST	0.633	1.790	25.394
48hrs_0.05 (1)	1.795	DLST	0.633	1.790	25.386
48hrs_1.25 (1)	1.769	DLST	0.633	1.790	26.836
72hrs_0 (1)	1.811	DLST	0.633	1.790	24.618
72hrs_0.05 (1)	1.776	DLST	0.633	1.790	26.949
72hrs_1.25 (1)	1.784	DLST	0.633	1.790	24.019
48hrs_0 (2)	1.801	DLST	0.633	1.790	26.631
48hrs_0.01 (2)	1.811	DLST	0.633	1.790	26.714
48hrs_0.05 (2)	1.793	DLST	0.633	1.790	29.313
48hrs_1.25 (2)	1.781	DLST	0.633	1.790	28.759
72hrs_0 (2)	1.794	DLST	0.633	1.790	25.278
72hrs_0.05 (2)	1.796	DLST	0.633	1.790	25.338
72hrs_1.25 (2)	1.781	DLST	0.633	1.790	25.040
48hrs_0 (3)	1.793	DLST	0.633	1.790	27.291
48hrs_0.01 (3)	1.855	DLST	0.633	1.790	31.429
48hrs_0.05 (3)	1.848	DLST	0.633	1.790	30.636
48hrs_1.25 (3)	1.765	DLST	0.633	1.790	28.817
72hrs_0 (3)	1.775	DLST	0.633	1.790	27.992
72hrs_0.05 (3)	1.842	DLST	0.633	1.790	29.834
72hrs_1.25 (3)	1.799	DLST	0.633	1.790	27.483
NEGATIVE	1.731	DLST	0.633	1.790	41.343
NEGATIVE	1.730	DLST	0.633	1.790	41.376
NEGATIVE	1.750	DLST	0.633	1.790	41.756

A.10. Flow cytometry data:

Results are shown for the various exposure groups (control, 0.01, 0.05, 0.25, 1.25, 6.25, 31.25, 156.25 mg/l Cd^{2+}) respectively in the same order.

Seminavis robusta:

Flask 1:

Day 0:

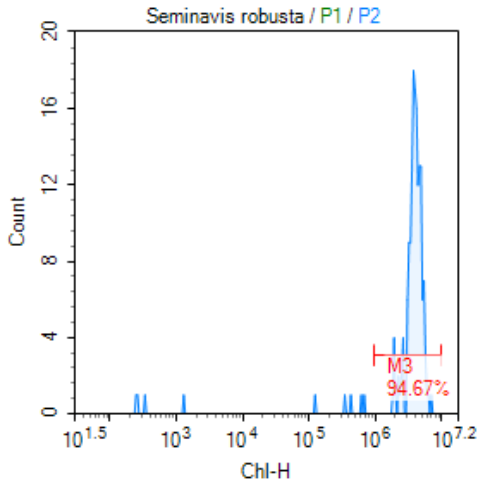

Gate	Count	Abs. Count	% P2	Mean X	CV X
P2	169	1.69	100.00 %	3,889,326	32.25 %
M3	160	1.6	94.67 %	4,094,074	22.73 %

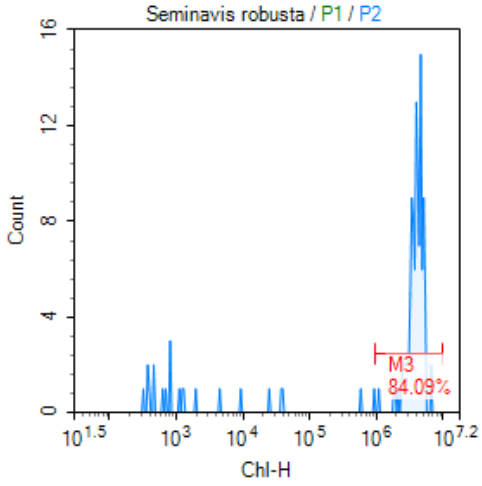

Gate	Count	Abs. Count	% P2	Mean X	CV X
P2	132	1.32	100.00 %	3,448,730	50.72 %
M3	111	1.11	84.09 %	4,094,649	24.36 %

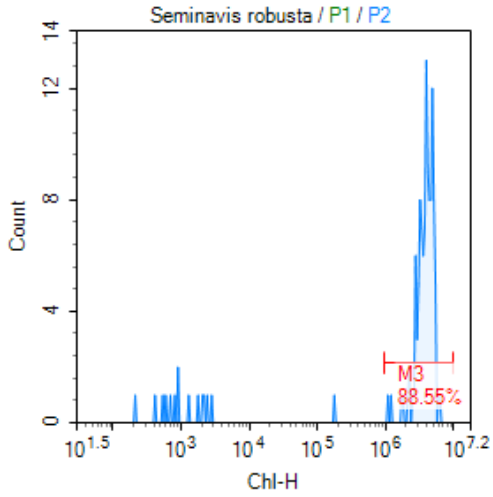

Gate	Count	Abs. Count	% P2	Mean X	CV X
P2	131	1.31	100.00 %	3,551,331	44.57 %
M3	116	1.16	88.55 %	4,008,846	24.79 %

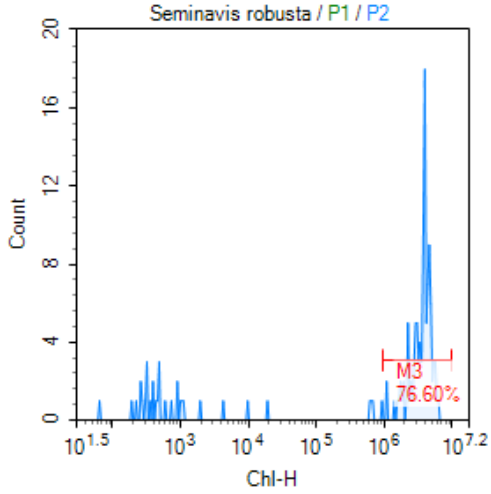

Gate	Count	Abs. Count	% P2	Mean X	CV X
P2	141	1.41	100.00 %	2,912,823	63.69 %
M3	108	1.08	76.60 %	3,774,983	29.96 %

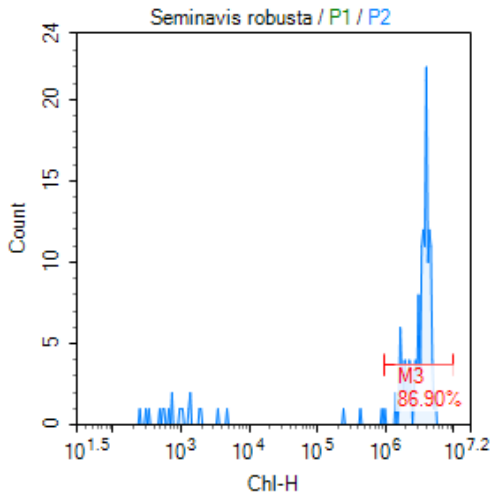

Gate	Count	Abs. Count	% P2	Mean X	CV X
P2	168	1.68	100.00 %	3,082,824	48.70 %
M3	146	1.46	86.90 %	3,536,529	28.38 %

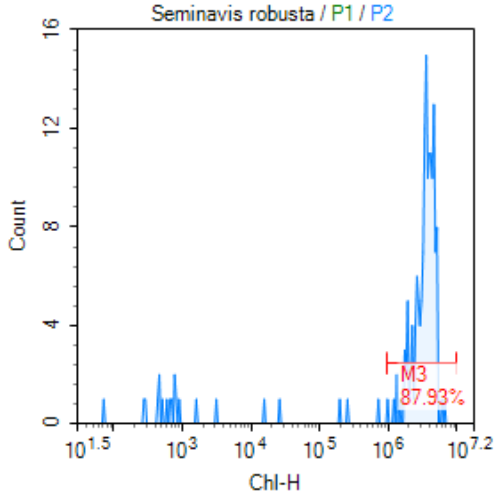

Gate	Count	Abs. Count	% P2	Mean X	CV X
P2	174	1.74	100.00 %	3,210,697	47.84 %
M3	153	1.53	87.93 %	3,643,170	29.07 %

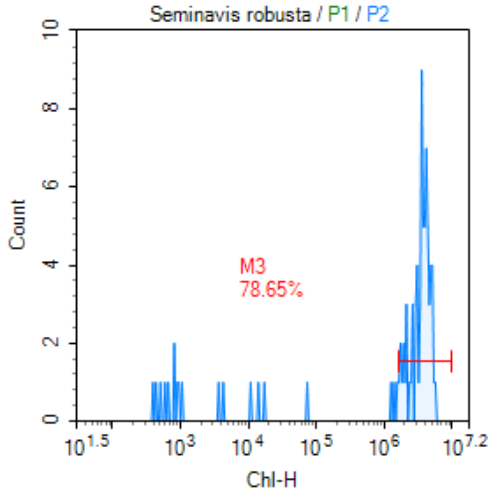

Gate	Count	Abs. Count	% P2	Mean X	CV X
P2	89	0.89	100.00 %	2,959,557	57.83 %
M3	70	0.7	78.65 %	3,697,971	27.92 %

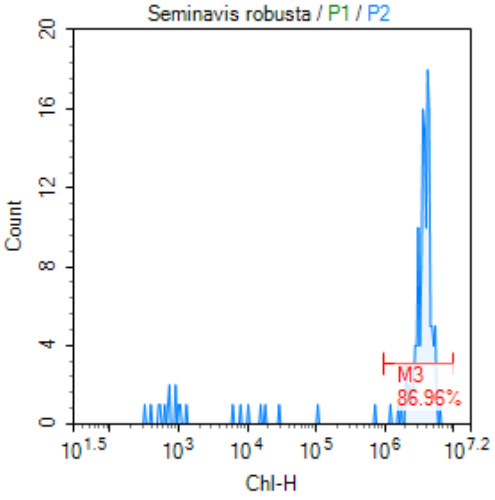

Gate	Count	Abs. Count	% P2	Mean X	CV X
P2	161	1.61	100.00 %	3,364,580	45.62 %
M3	140	1.4	86.96 %	3,862,522	23.07 %

Day 1:

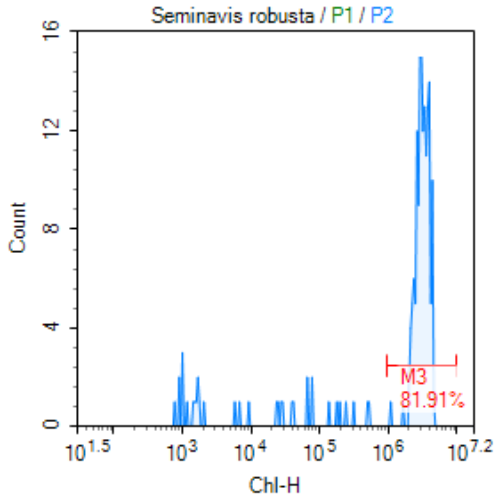

Gate	Count	Abs. Count	% P2	Mean X	CV X
P2	188	1.88	100.00 %	2,706,246	51.18 %
M3	154	1.54	81.91 %	3,286,349	20.80 %

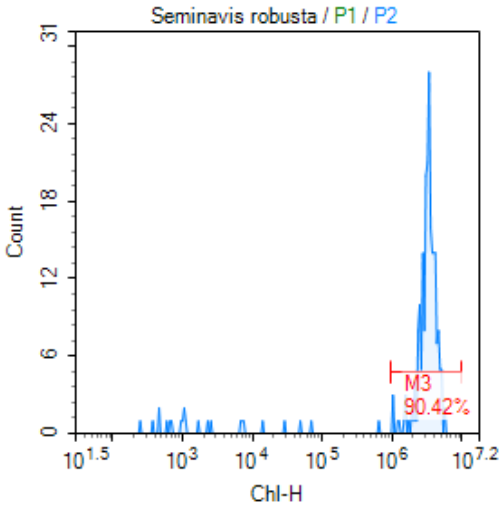

Gate	Count	Abs. Count	% P2	Mean X	CV X
P2	240	2.4	100.00 %	3,089,406	41.90 %
M3	217	2.17	90.42 %	3,412,789	25.48 %

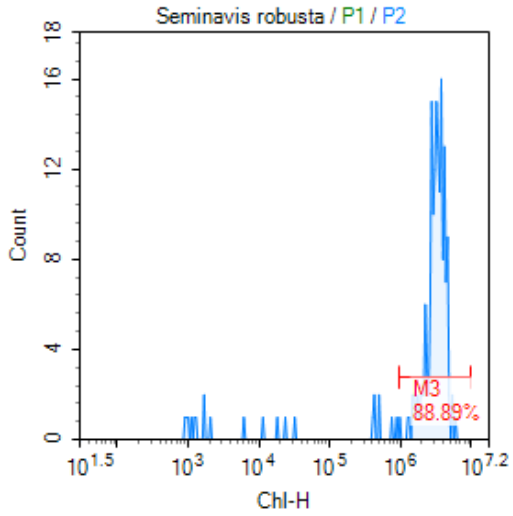

Gate	Count	Abs. Count	% P2	Mean X	CV X
P2	189	1.89	100.00 %	3,015,913	43.46 %
M3	168	1.68	88.89 %	3,368,458	26.53 %

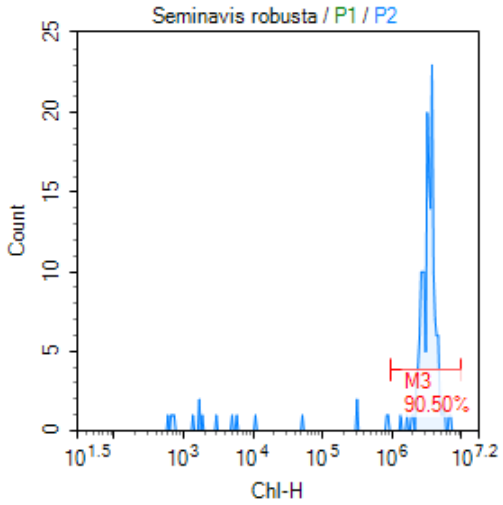

Gate	Count	Abs. Count	% P2	Mean X	CV X
P2	179	1.79	100.00 %	3,205,806	39.95 %
M3	162	1.62	90.50 %	3,526,601	23.96 %

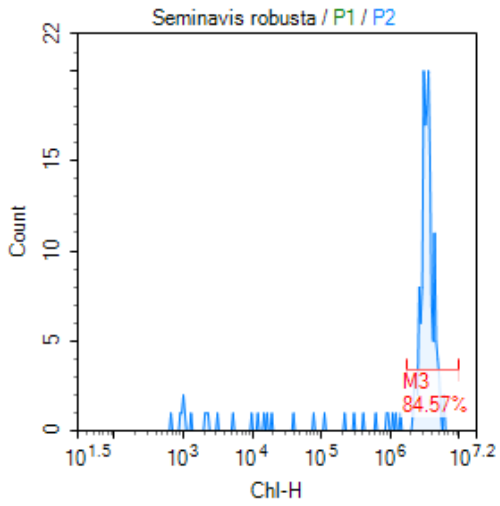

Gate	Count	Abs. Count	% P2	Mean X	CV X
P2	188	1.88	100.00 %	3,076,920	45.25 %
M3	159	1.59	84.57 %	3,590,657	20.45 %

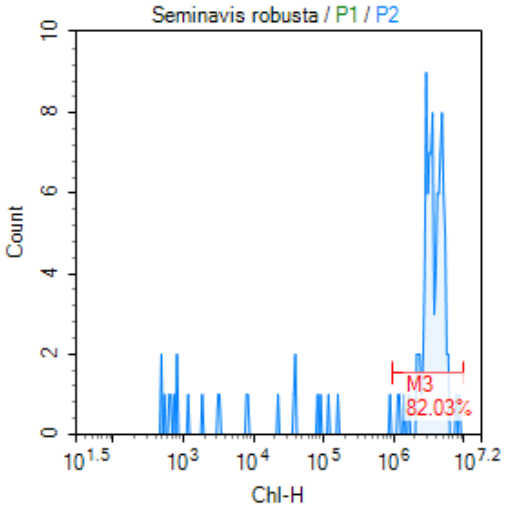

Gate	Count	% P2	Mean X	CV X
P2	128	100.00 %	3,243,045	57.94 %
M3	105	82.03 %	3,938,639	31.96 %

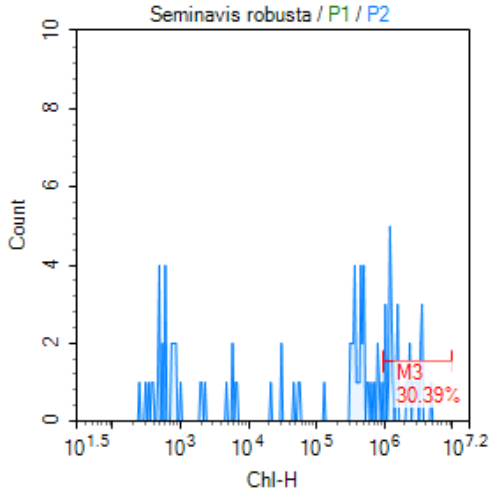

Gate	Count	Abs. Count	% P2	Mean X	CV X
P2	102	1.02	100.00 %	804,522	133.50 %
M3	31	0.31	30.39 %	2,128,927	49.46 %

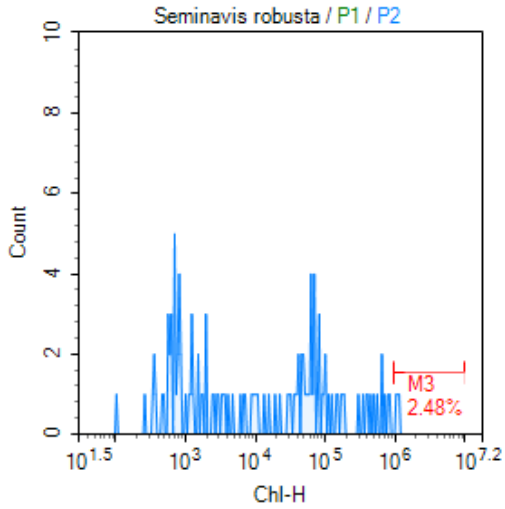

Gate	Count	Abs. Count	% P2	Mean X	CV X
P2	121	1.21	100.00 %	111,221	212.85 %
M3	3	0.03	2.48 %	1,115,064	6.55 %

Day 2:

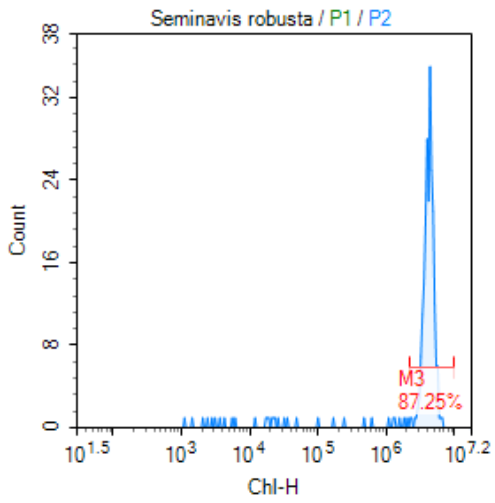

Gate	Count	Abs. Count	% P2	Mean X	CV X
P2	251	2.51	100.00 %	3,837,293	39.23 %
M3	219	2.19	87.25 %	4,346,542	16.28 %

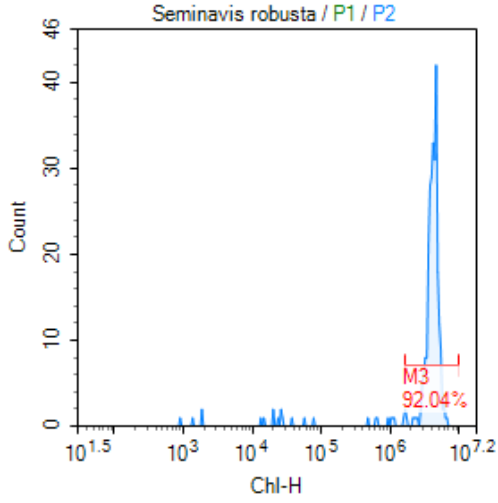

Gate	Count	Abs. Count	% P2	Mean X	CV X
P2	289	2.89	100.00 %	3,945,188	32.70 %
M3	266	2.66	92.04 %	4,256,080	17.72 %

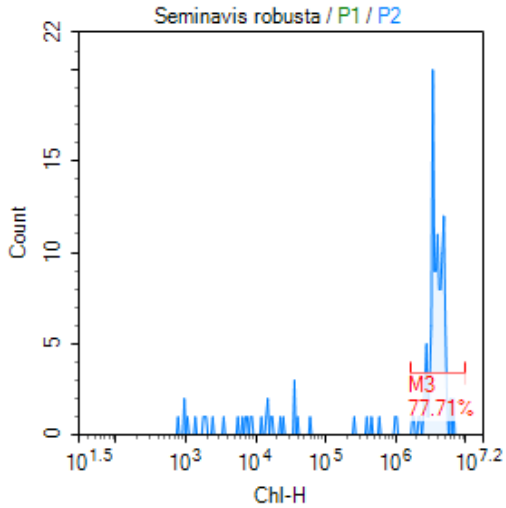

Gate	Count	Abs. Count	% P2	Mean X	CV X
P2	157	1.57	100.00 %	3,153,997	57.68 %
M3	122	1.22	77.71 %	4,024,445	22.51 %

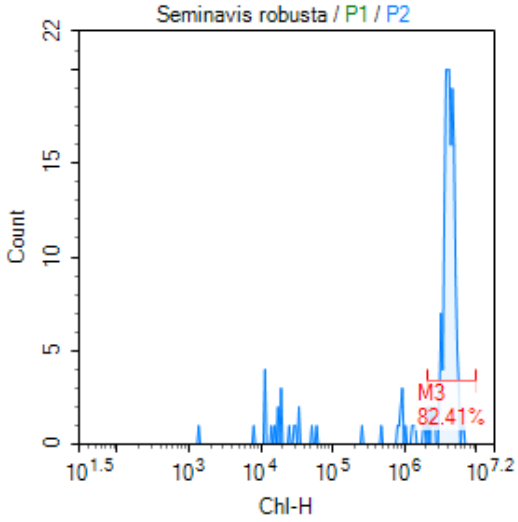

Gate	Count	Abs. Count	% P2	Mean X	CV X
P2	199	1.99	100.00 %	3,602,257	45.03 %
M3	164	1.64	82.41 %	4,270,022	17.66 %

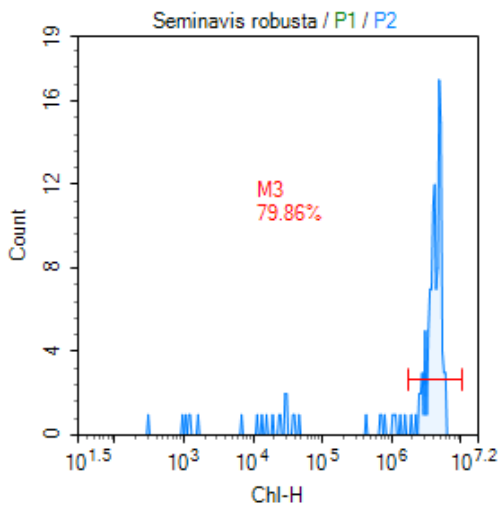

Gate	Count	Abs. Count	% P2	Mean X	CV X
P2	144	1.44	100.00 %	3,549,664	51.46 %
M3	115	1.15	79.86 %	4,362,890	20.63 %

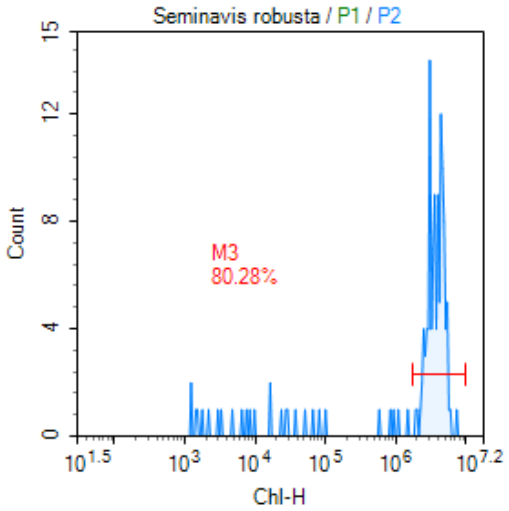

Gate	Count	Abs. Count	% P2	Mean X	CV X
P2	142	1.42	100.00 %	3,193,141	54.26 %
M3	114	1.14	80.28 %	3,928,509	24.67 %

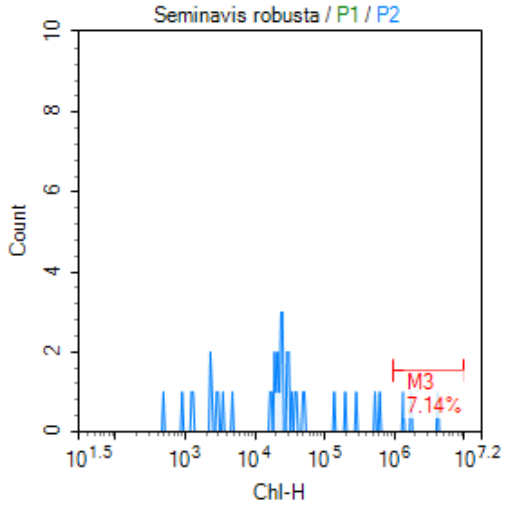

Gate	Count	Abs. Count	% P2	Mean X	CV X
P2	42	0.42	100.00 %	236,803	309.68 %
M3	3	0.03	7.14 %	2,483,158	63.92 %

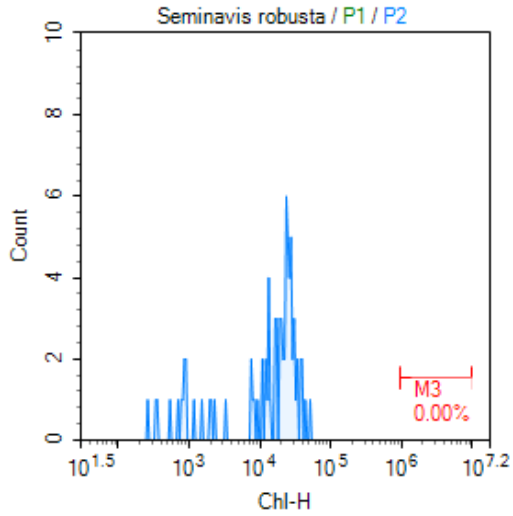

Gate	Count	Abs. Count	% P2	Mean X	CV X
P2	82	0.82	100.00 %	18,834	65.84 %
M3	0	0	0.00 %	0	0.00 %

Day 3:

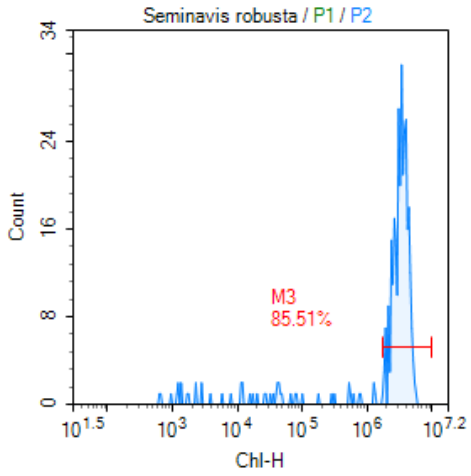

Gate	Count	Abs. Count	% P2	Mean X	CV X
P2	352	3.52	100.00 %	2,987,216	46.26 %
M3	301	3.01	85.51 %	3,461,380	23.40 %

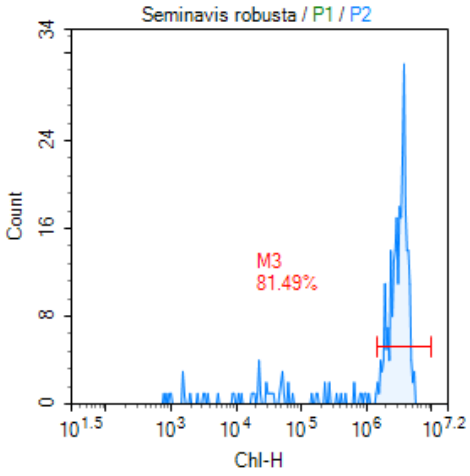

Gate	Count	Abs. Count	% P2	Mean X	CV X
P2	335	3.35	100.00 %	2,746,805	53.38 %
M3	273	2.73	81.49 %	3,329,005	26.51 %

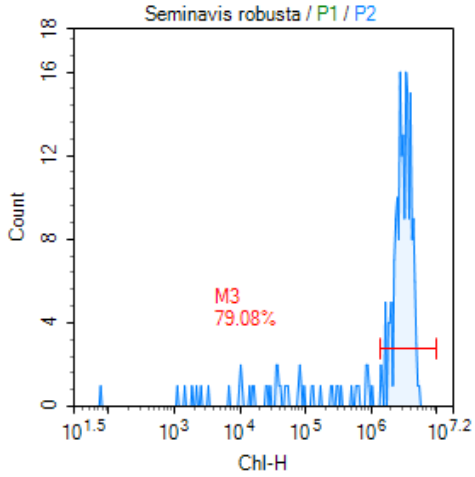

Gate	Count	Abs. Count	% P2	Mean X	CV X
P2	239	2.39	100.00 %	2,593,557	55.69 %
M3	189	1.89	79.08 %	3,221,926	26.29 %

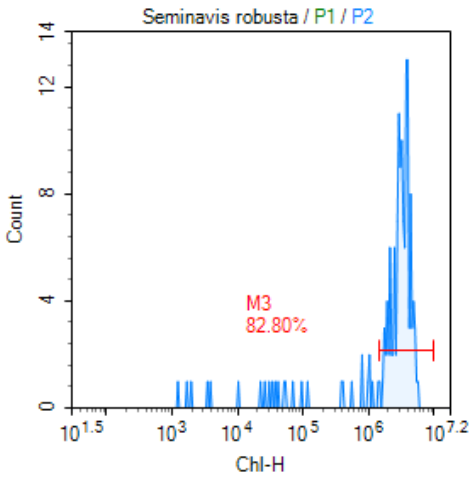

Gate	Count	Abs. Count	% P2	Mean X	CV X
P2	157	1.57	100.00 %	2,860,191	50.23 %
M3	130	1.3	82.80 %	3,382,191	27.37 %

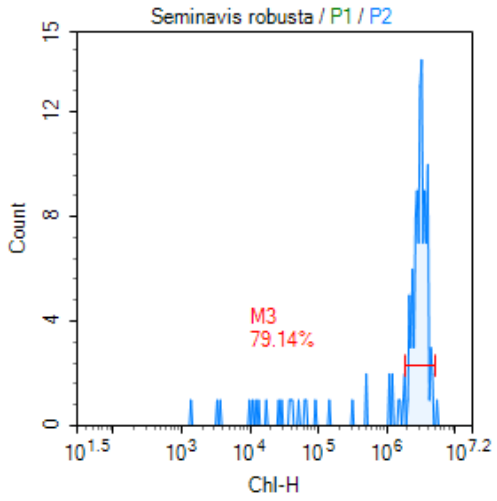

Gate	Count	Abs. Count	% P2	Mean X	CV X
P2	139	1.39	100.00 %	2,652,312	49.13 %
M3	110	1.1	79.14 %	3,197,869	19.88 %

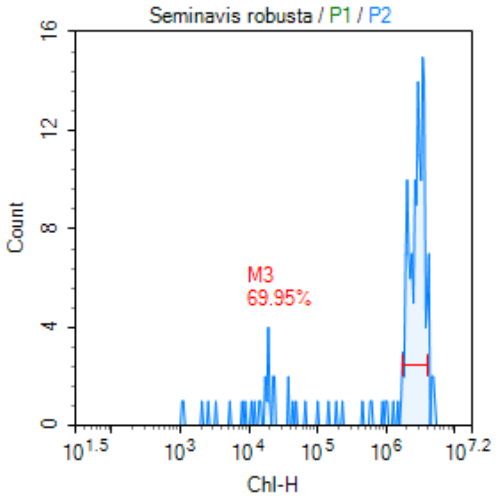

Gate	Count	Abs. Count	% P2	Mean X	CV X
P2	193	1.93	100.00 %	2,419,958	55.48 %
M3	135	1.35	69.95 %	2,858,853	20.85 %

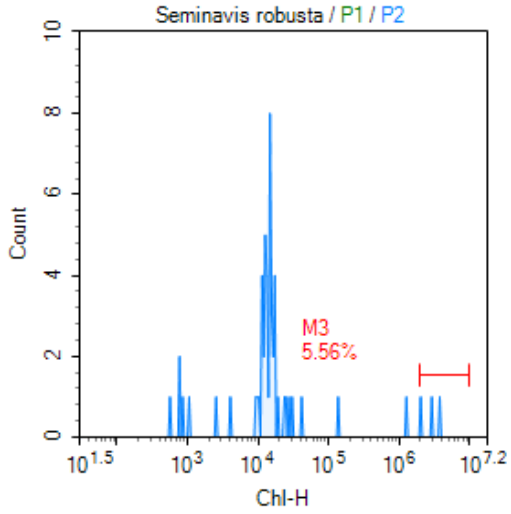

Gate	Count	Abs. Count	% P2	Mean X	CV X
P2	54	0.54	100.00 %	203,164	351.34 %
M3	3	0.03	5.56 %	2,952,882	28.39 %

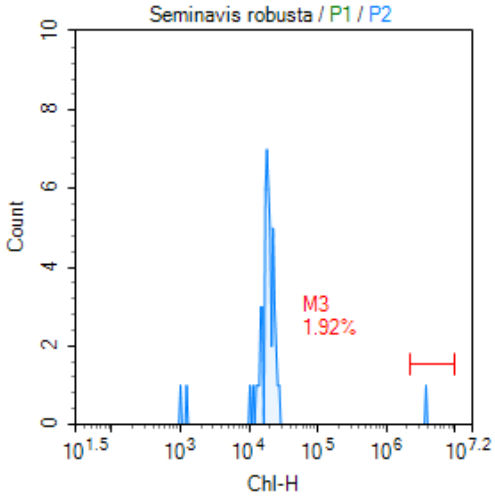

Gate	Count	Abs. Count	% P2	Mean X	CV X
P2	52	0.52	100.00 %	91,383	573.72 %
M3	1	0.01	1.92 %	3,799,166	0.00 %

Flask 2:

Day 0:

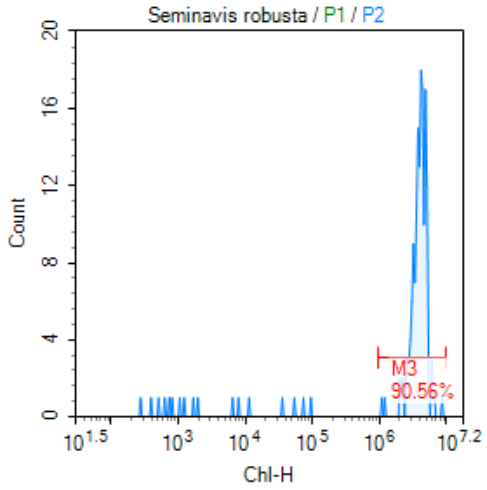

Gate	Count	Abs. Count	% P2	Mean X	CV X
P2	180	1.8	100.00 %	3,744,909	41.11 %
M3	163	1.63	90.56 %	4,133,629	24.30 %

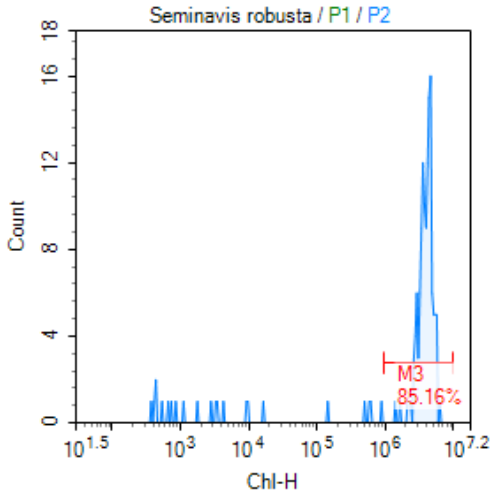

Gate	Count	Abs. Count	% P2	Mean X	CV X
P2	155	1.55	100.00 %	3,495,194	46.94 %
M3	132	1.32	85.16 %	4,082,536	22.04 %

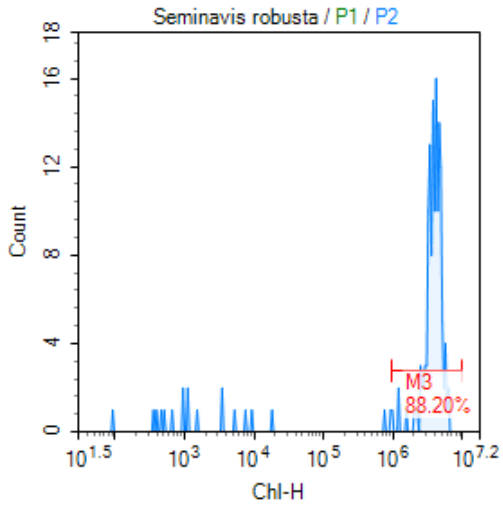

Gate	Count	Abs. Count	% P2	Mean X	CV X
P2	161	1.61	100.00 %	3,567,532	43.95 %
M3	142	1.42	88.20 %	4,032,466	23.98 %

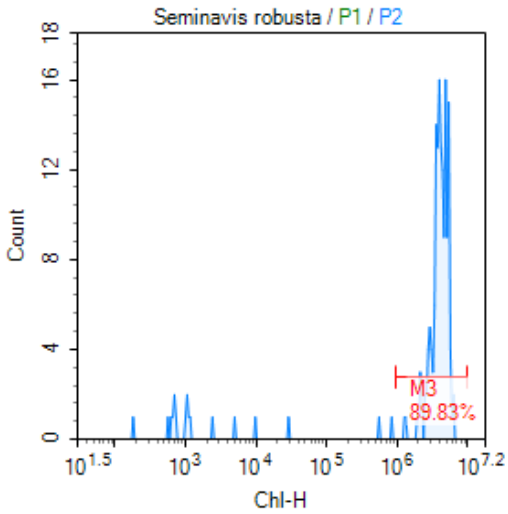

Gate	Count	Abs. Count	% P2	Mean X	CV X
P2	177	1.77	100.00 %	3,775,245	41.66 %
M3	159	1.59	89.83 %	4,193,318	24.08 %

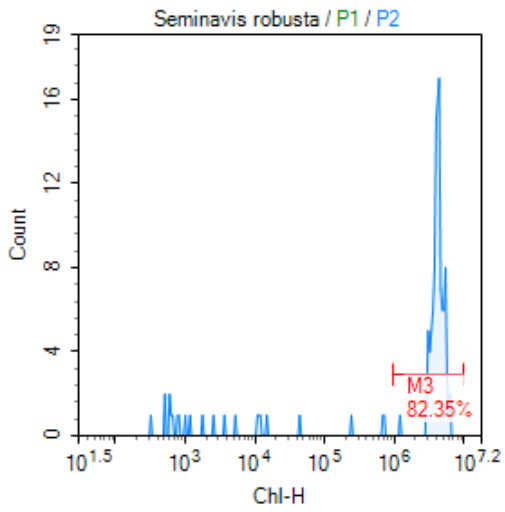

Gate	Count	Abs. Count	% P2	Mean X	CV X
P2	136	1.36	100.00 %	3,591,692	49.96 %
M3	112	1.12	82.35 %	4,345,154	18.71 %

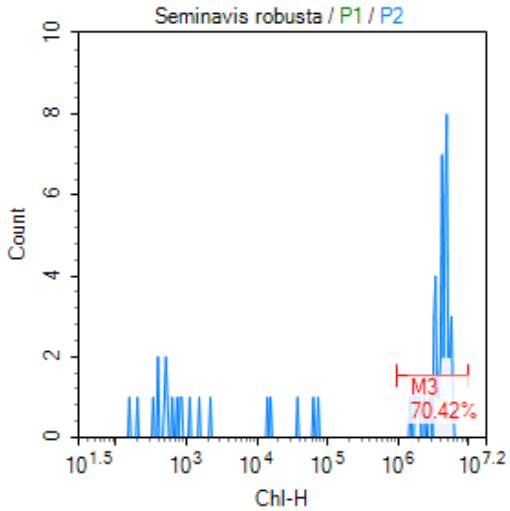

Gate	Count	Abs. Count	% P2	Mean X	CV X
P2	71	0.71	100.00 %	2,936,685	72.56 %
M3	50	0.5	70.42 %	4,165,643	27.12 %

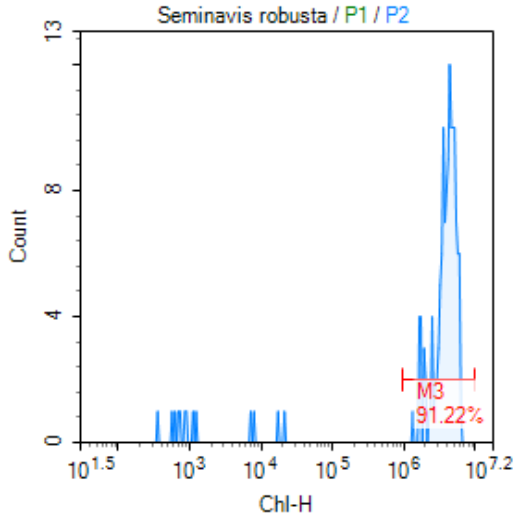

Gate	Count	Abs. Count	% P2	Mean X	CV X
P2	148	1.48	100.00 %	3,757,230	43.64 %
M3	135	1.35	91.22 %	4,118,576	29.25 %

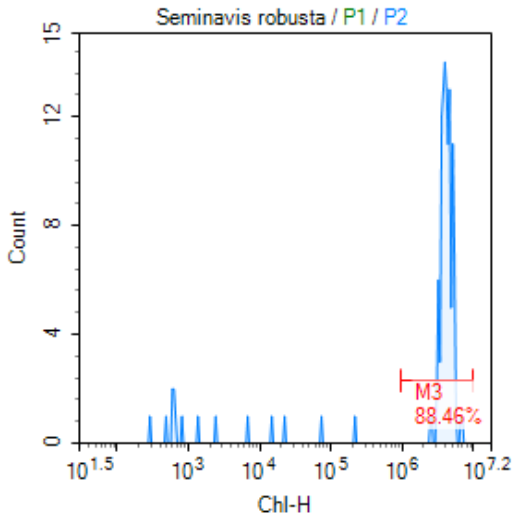

Gate	Count	Abs. Count	% P2	Mean X	CV X
P2	130	1.3	100.00 %	3,835,058	40.58 %
M3	115	1.15	88.46 %	4,332,139	17.57 %

Day 1:

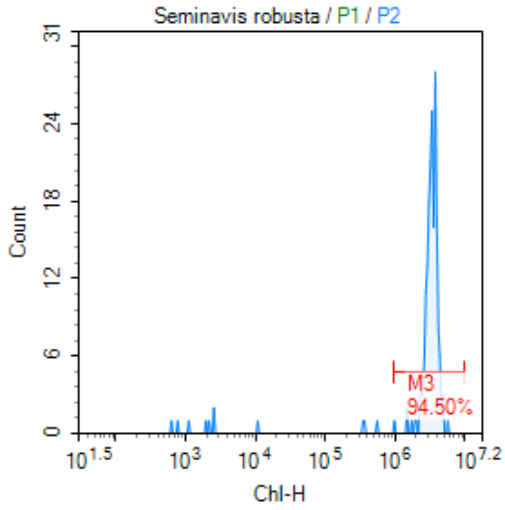

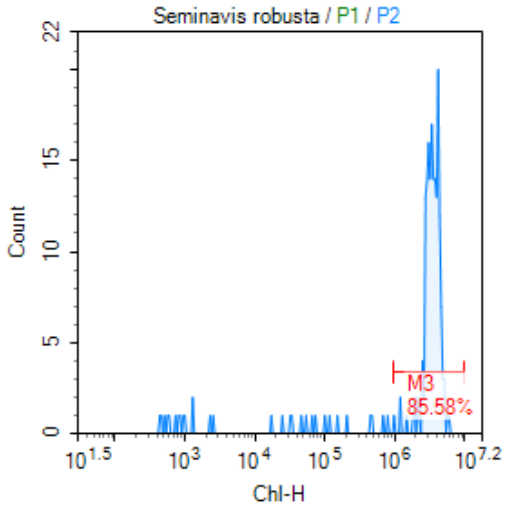

Gate	Count	Abs. Count	% P2	Mean X	CV X
P2	200	2	100.00 %	3,262,286	30.52 %
M3	189	1.89	94.50 %	3,445,143	19.16 %

Gate	Count	Abs. Count	% P2	Mean X	CV X
P2	208	2.08	100.00 %	3,088,184	46.58 %
M3	178	1.78	85.58 %	3,589,538	22.64 %

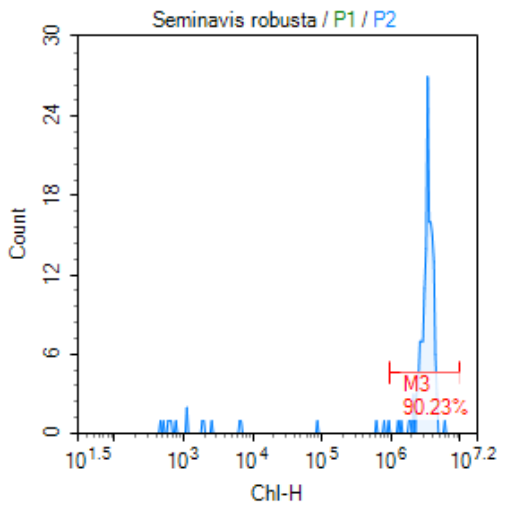

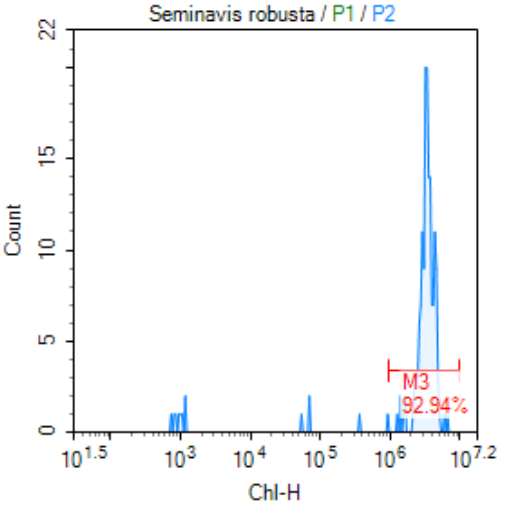

Gate	Count	Abs. Count	% P2	Mean X	CV X
P2	174	1.74	100.00 %	3,157,802	37.51 %
M3	157	1.57	90.23 %	3,483,841	19.27 %

Gate	Count	Abs. Count	% P2	Mean X	CV X
P2	170	1.7	100.00 %	3,259,420	37.07 %
M3	158	1.58	92.94 %	3,503,304	24.26 %

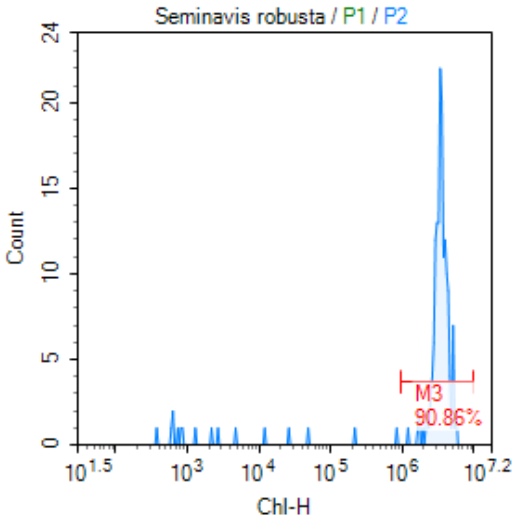

Gate	Count	Abs. Count	% P2	Mean X	CV X
P2	175	1.75	100.00 %	3,284,052	38.57 %
M3	159	1.59	90.86 %	3,607,117	21.72 %

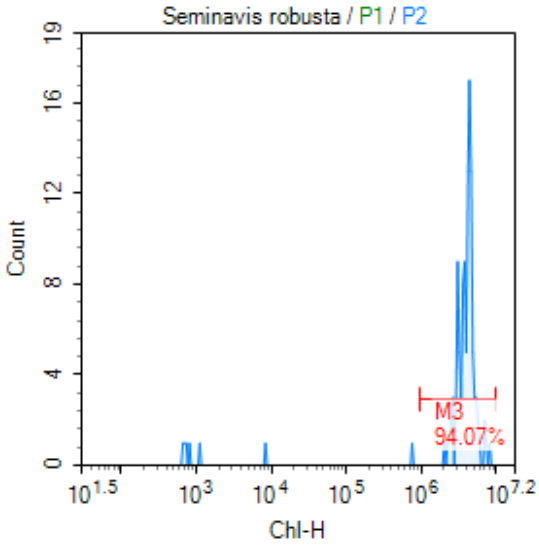

Gate	Count	Abs. Count	% P2	Mean X	CV X
P2	118	1.18	100.00 %	3,953,226	35.20 %
M3	111	1.11	94.07 %	4,195,418	24.51 %

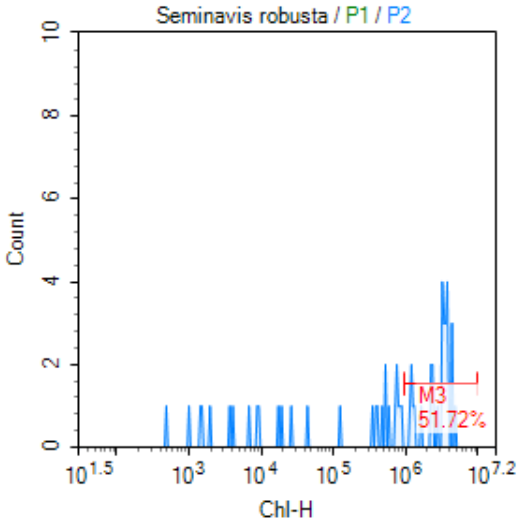

Gate	Count	Abs. Count	% P2	Mean X	CV X
P2	58	0.58	100.00 %	1,742,457	93.34 %
M3	30	0.3	51.72 %	3,088,036	35.69 %

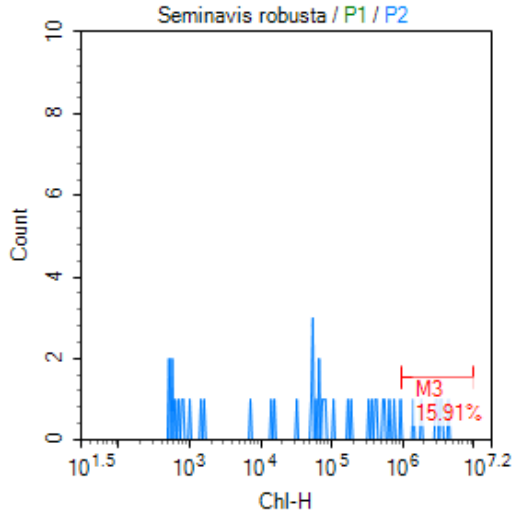

Gate	Count	Abs. Count	% P2	Mean X	CV X
P2	44	0.44	100.00 %	617,902	184.18 %
M3	7	0.07	15.91 %	2,987,799	35.37 %

Day 2:

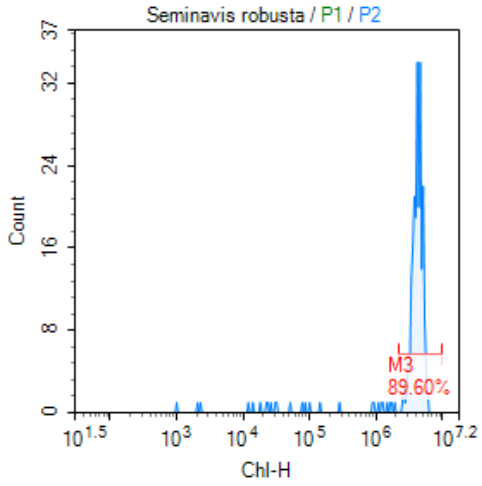

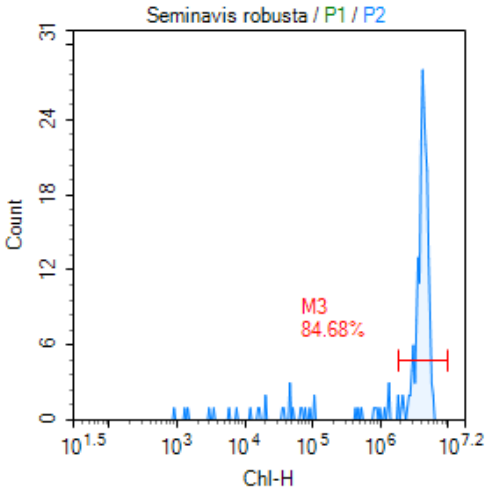

Gate	Count	Abs. Count	% P2	Mean X	CV X
P2	250	2.5	100.00 %	3,951,172	34.54 %
M3	224	2.24	89.60 %	4,349,739	16.14 %

Gate	Count	Abs. Count	% P2	Mean X	CV X
P2	235	2.35	100.00 %	3,667,970	43.65 %
M3	199	1.99	84.68 %	4,268,259	18.48 %

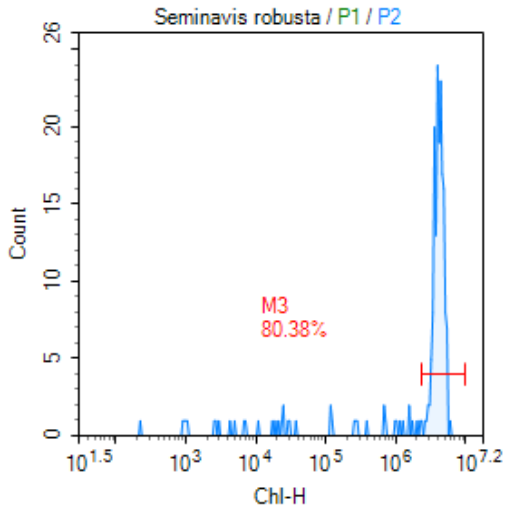

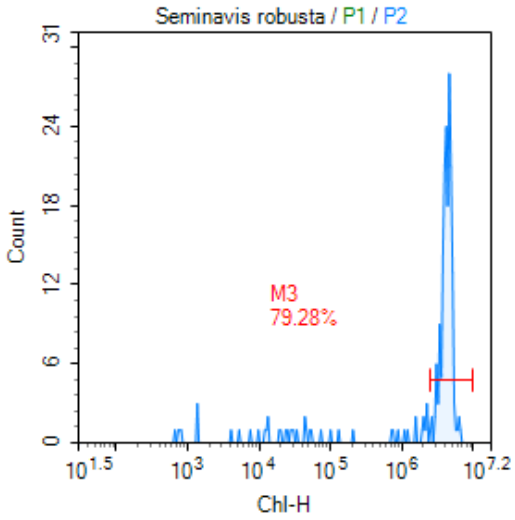

Gate	Count	Abs. Count	% P2	Mean X	CV X
P2	209	2.09	100.00 %	3,506,671	47.10 %
M3	168	1.68	80.38 %	4,256,441	15.10 %

Gate	Count	Abs. Count	% P2	Mean X	CV X
P2	222	2.22	100.00 %	3,586,597	48.19 %
M3	176	1.76	79.28 %	4,387,022	15.98 %

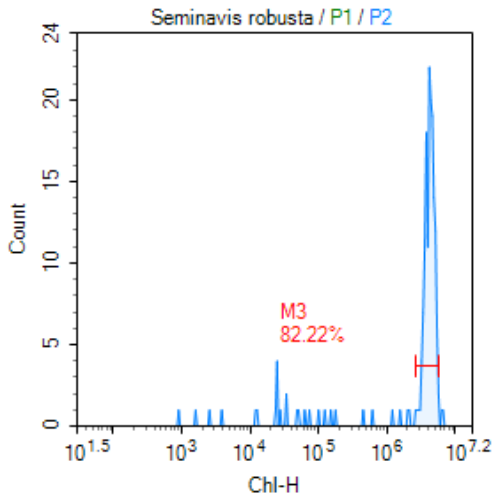

Gate	Count	Abs. Count	% P2	Mean X	CV X
P2	180	1.8	100.00 %	3,758,900	43.27 %
M3	148	1.48	82.22 %	4,339,685	14.34 %

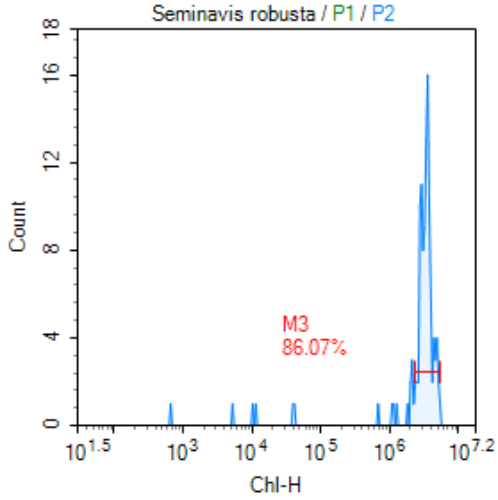

Gate	Count	Abs. Count	% P2	Mean X	CV X
P2	122	1.22	100.00 %	3,221,471	34.21 %
M3	105	1.05	86.07 %	3,528,929	18.48 %

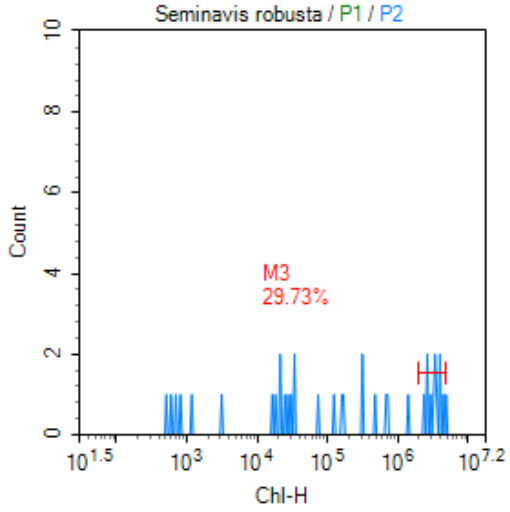

Gate	Count	Abs. Count	% P2	Mean X	CV X
P2	37	0.37	100.00 %	1,260,626	130.29 %
M3	11	0.11	29.73 %	3,359,856	18.53 %

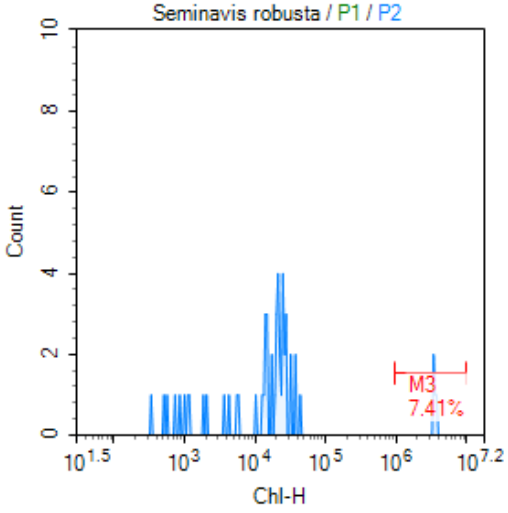

Gate	Count	Abs. Count	% P2	Mean X	CV X
P2	54	0.54	100.00 %	284,173	335.54 %
M3	4	0.04	7.41 %	3,619,783	5.39 %

Day 3:

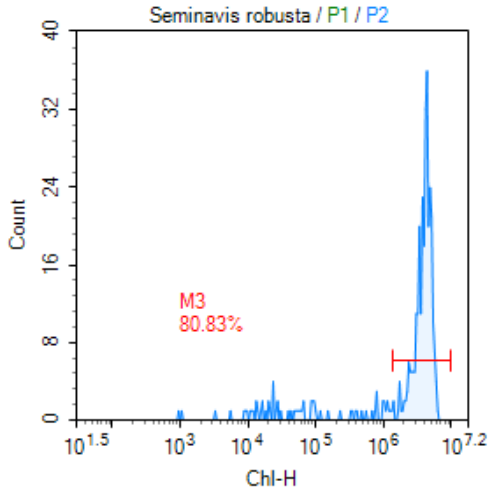

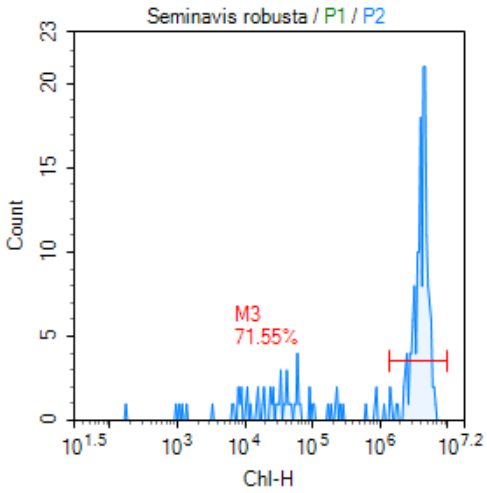

Gate	Count	Abs. Count	% P2	Mean X	CV X
P2	360	3.6	100.00 %	3,360,963	51.92 %
M3	291	2.91	80.83 %	4,088,260	23.95 %

Gate	Count	Abs. Count	% P2	Mean X	CV X
P2	232	2.32	100.00 %	3,018,194	67.16 %
M3	166	1.66	71.55 %	4,170,700	24.36 %

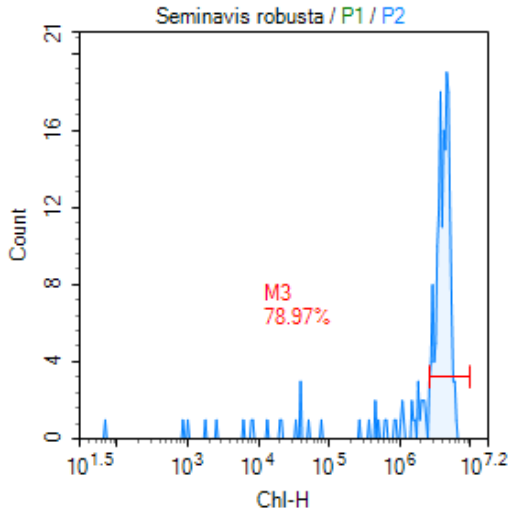

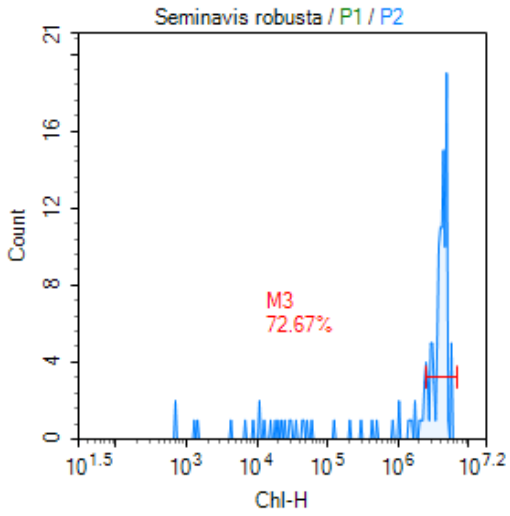

Gate	Count	Abs. Count	% P2	Mean X	CV X
P2	214	2.14	100.00 %	3,565,954	45.33 %
M3	169	1.69	78.97 %	4,281,573	19.06 %

Gate	Count	Abs. Count	% P2	Mean X	CV X
P2	150	2.47	100.00 %	3,219,686	55.07 %
M3	109	1.79	72.67 %	4,184,917	18.71 %

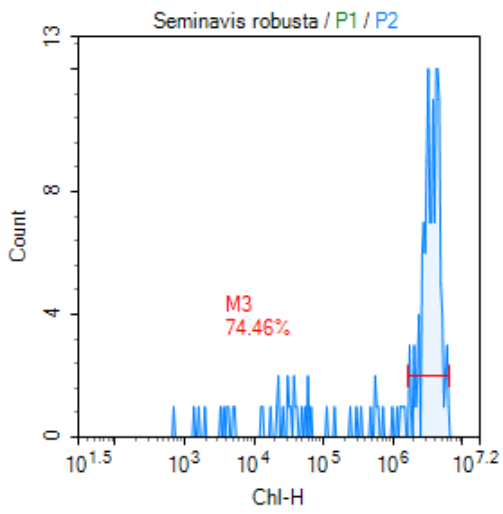

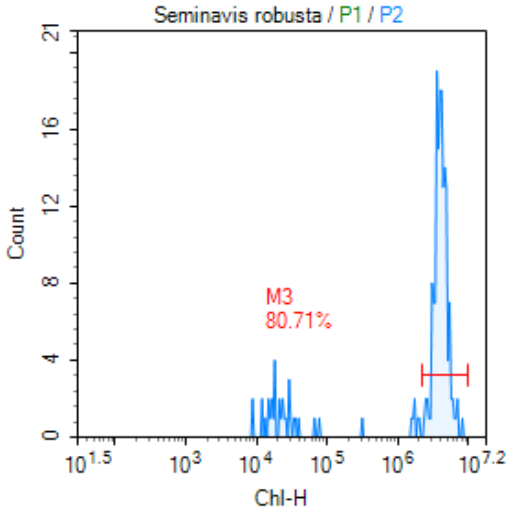

Gate	Count	Abs. Count	% P2	Mean X	CV X
P2	184	1.84	100.00 %	2,873,166	61.14 %
M3	137	1.37	74.46 %	3,761,951	26.18 %

Gate	Count	Abs. Count	% P2	Mean X	CV X
P2	197	1.97	100.00 %	3,490,674	51.05 %
M3	159	1.59	80.71 %	4,249,343	21.48 %

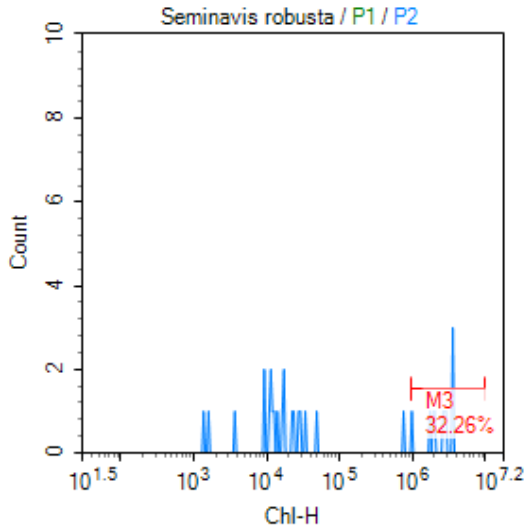

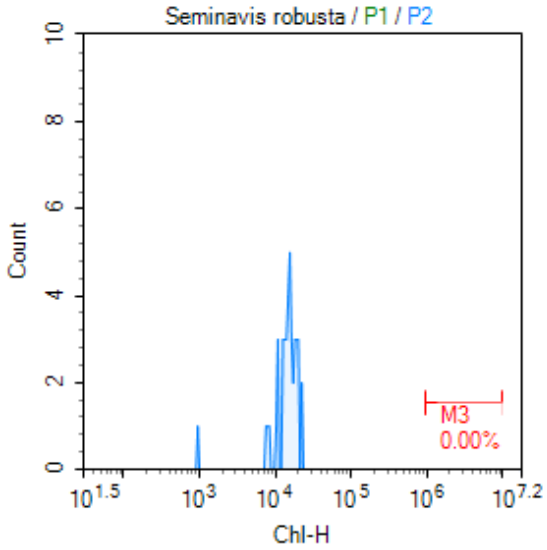

Gate	Count	Abs. Count	% P2	Mean X	CV X
P2	31	0.31	100.00 %	881,809	150.76 %
M3	10	0.1	32.26 %	2,623,114	35.32 %

Gate	Count	Abs. Count	% P2	Mean X	CV X
P2	42	0.42	100.00 %	15,303	28.32 %
M3	0	0	0.00 %	0	0.00 %

Flask 1 :

Day 0 (data for 0.05 mg/l Cd^{2+} is missing)

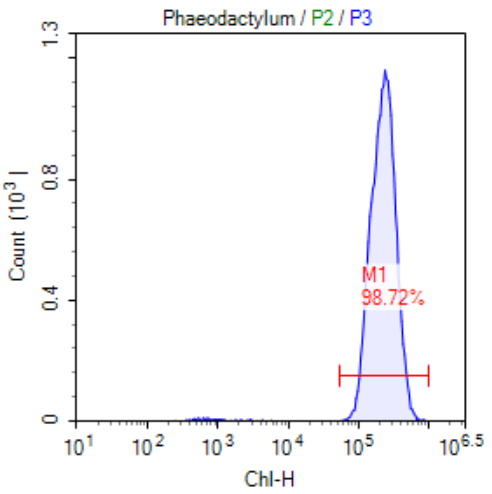

Gate	Count	Abs. Count	% P3	Mean X	CV X
P3	22,823	645	100.00 %	244,584	40.78 %
M1	22,531	637	98.72 %	247,620	38.84 %

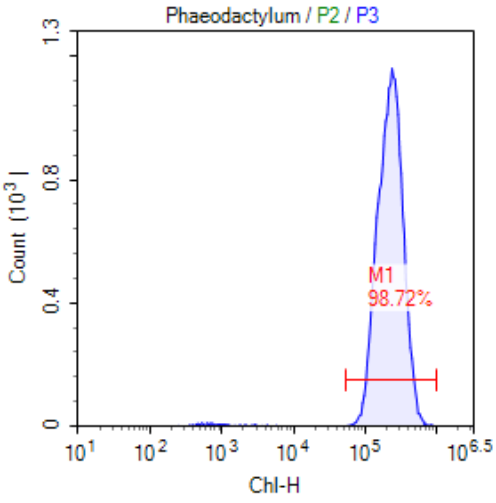

Gate	Count	Abs. Count	% P3	Mean X	CV X
P3	22,823	645	100.00 %	244,584	40.78 %
M1	22,531	637	98.72 %	247,620	38.84 %

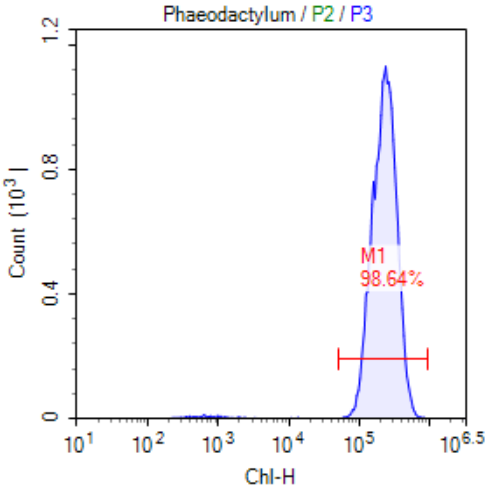

Gate	Count	Abs. Count	% P3	Mean X	CV X
P3	21,766	659	100.00 %	247,337	40.02 %
M1	21,471	650	98.64 %	250,701	38.05 %

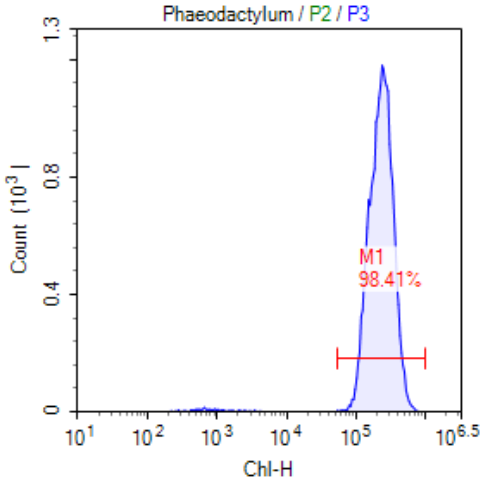

Gate	Count	Abs. Count	% P3	Mean X	CV X
P3	22,652	677	100.00 %	248,880	40.21 %
M1	22,292	666	98.41 %	252,786	37.74 %

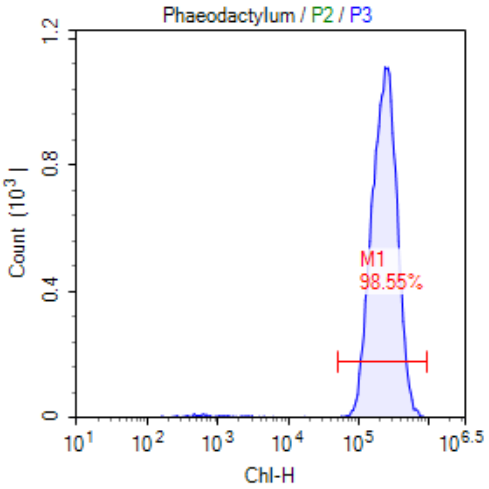

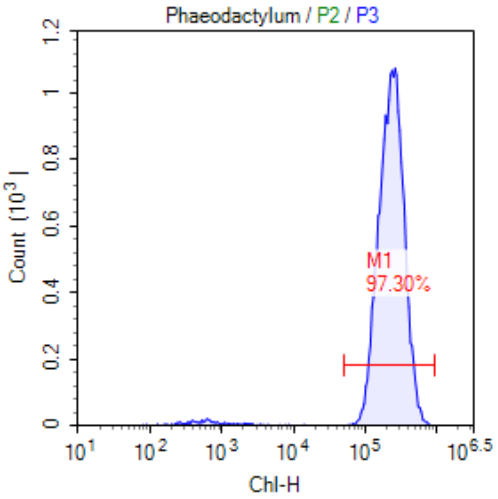

Gate	Count	Abs. Count	% P3	Mean X	CV X
P3	22,318	730	100.00 %	253,221	41.19 %
M1	21,995	719	98.55 %	256,903	39.12 %

Gate	Count	Abs. Count	% P3	Mean X	CV X
P3	21,474	655	100.00 %	250,072	42.48 %
M1	20,895	637	97.30 %	256,903	38.57 %

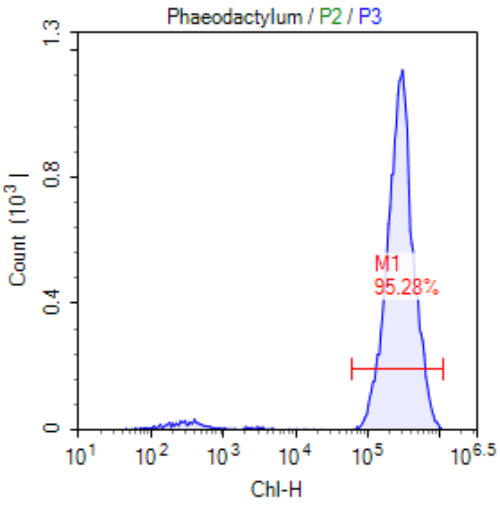

Gate	Count	Abs. Count	% P3	Mean X	CV X
P3	22,692	531	100.00 %	304,146	50.13 %
M1	21,622	506	95.28 %	319,062	43.88 %

Day 1:

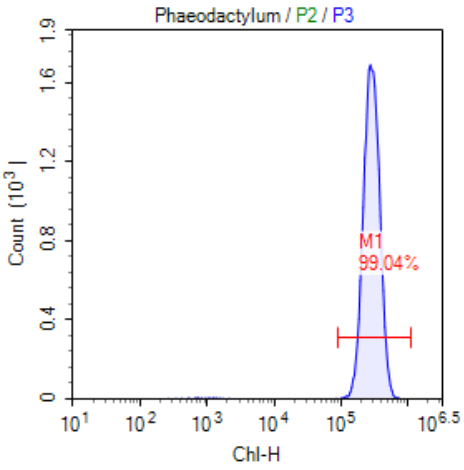

Gate	Count	Abs. Count	% P3	Mean X	CV X
P3	23,342	1,035	100.00 %	303,271	28.41 %
M1	23,118	1,025	99.04 %	306,129	26.62 %

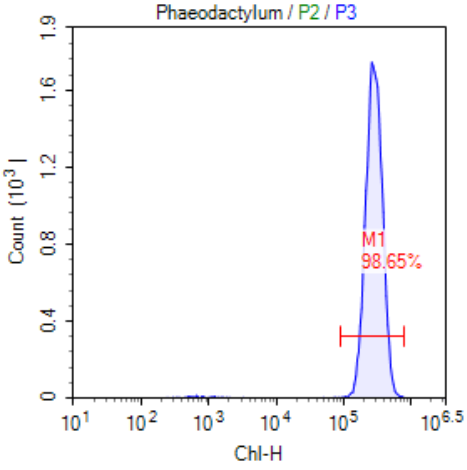

Gate	Count	Abs. Count	% P3	Mean X	CV X
P3	24,480	1,031	100.00 %	299,695	29.84 %
M1	24,150	1,017	98.65 %	303,511	27.35 %

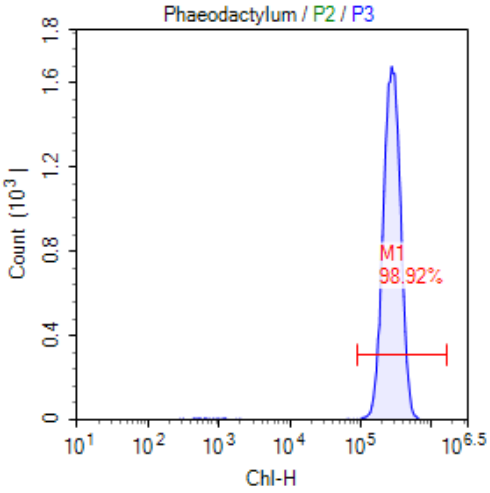

Gate	Count	Abs. Count	% P3	Mean X	CV X
P3	22,940	1,027	100.00 %	293,171	28.22 %
M1	22,692	1,016	98.92 %	296,271	26.20 %

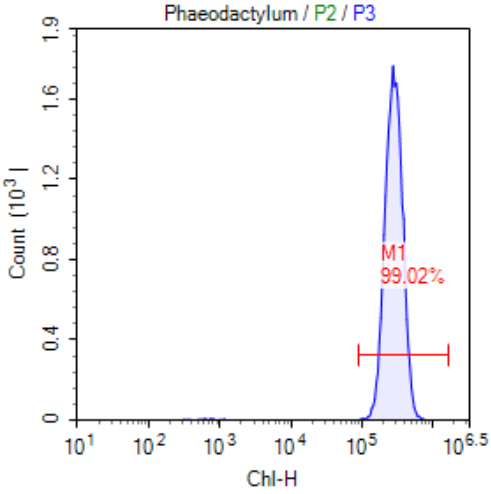

Gate	Count	Abs. Count	% P3	Mean X	CV X
P3	24,432	971	100.00 %	299,238	29.29 %
M1	24,193	961	99.02 %	302,108	27.52 %

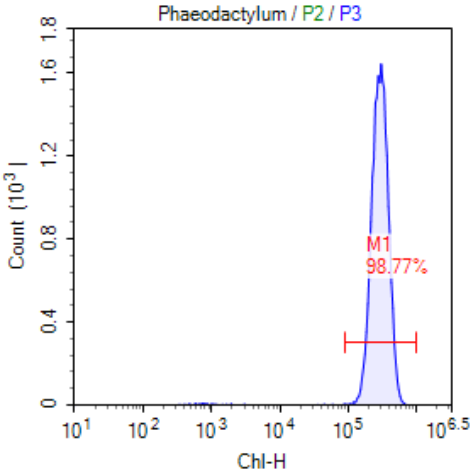

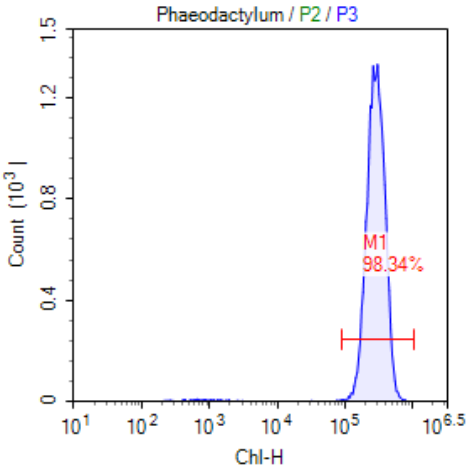

Gate	Count	Abs. Count	% P3	Mean X	CV X
P3	22,725	863	100.00 %	308,536	28.92 %
M1	22,445	852	98.77 %	312,252	26.67 %

Gate	Count	Abs. Count	% P3	Mean X	CV X
P3	20,327	751	100.00 %	303,260	32.25 %
M1	19,989	738	98.34 %	308,247	29.42 %

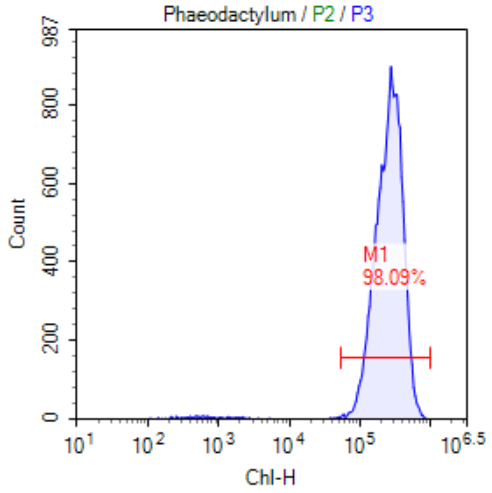

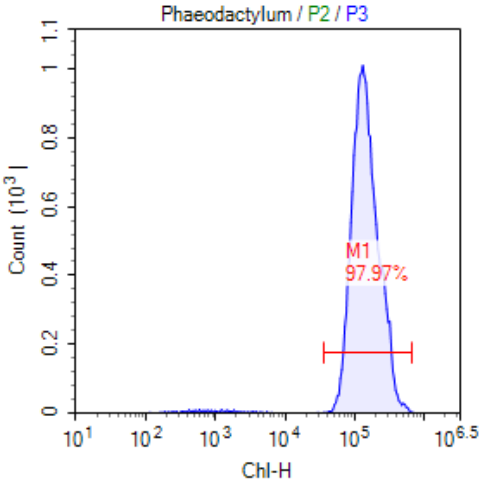

Gate	Count	Abs. Count	% P3	Mean X	CV X
P3	18,352	568	100.00 %	281,595	43.17 %
M1	18,001	557	98.09 %	286,996	40.54 %

Gate	Count	Abs. Count	% P3	Mean X	CV X
P3	20,966	367	100.00 %	161,524	50.38 %
M1	20,540	360	97.97 %	164,550	47.51 %

Day 2:

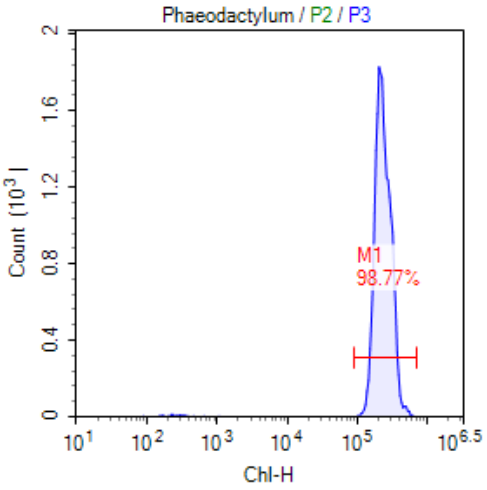

Gate	Count	Abs. Count	% P3	Mean X	CV X
P3	22,699	2,377	100.00 %	247,773	29.07 %
M1	22,420	2,348	98.77 %	250,808	26.75 %

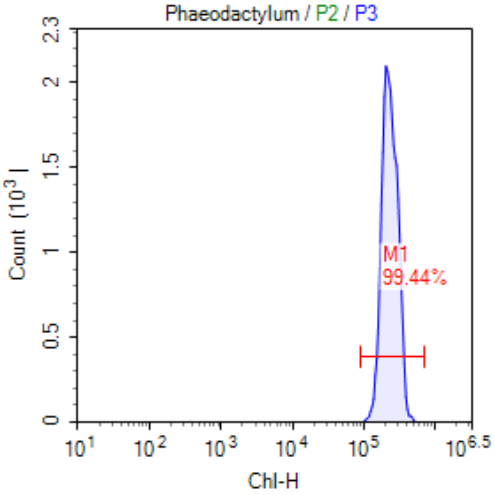

Gate	Count	Abs. Count	% P3	Mean X	CV X
P3	26,557	2,778	100.00 %	245,127	25.40 %
M1	26,409	2,762	99.44 %	246,465	24.26 %

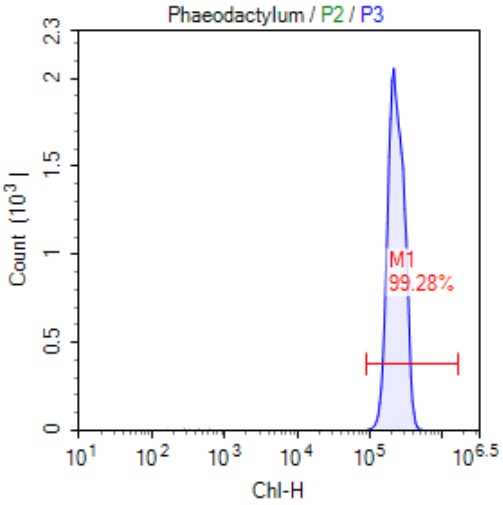

Gate	Count	Abs. Count	% P3	Mean X	CV X
P3	25,971	2,642	100.00 %	245,422	25.69 %
M1	25,783	2,623	99.28 %	247,181	24.18 %

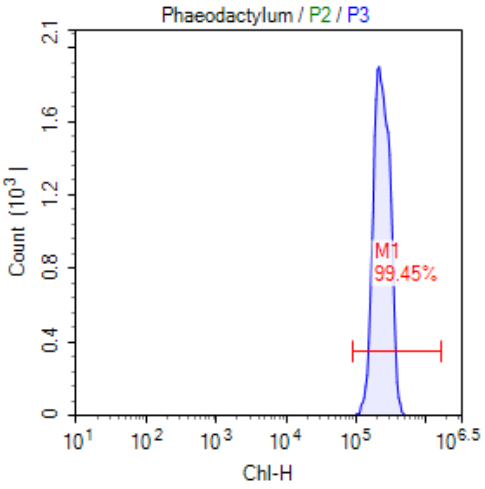

Gate	Count	Abs. Count	% P3	Mean X	CV X
P3	25,701	2,343	100.00 %	248,246	25.57 %
M1	25,560	2,330	99.45 %	249,572	24.47 %

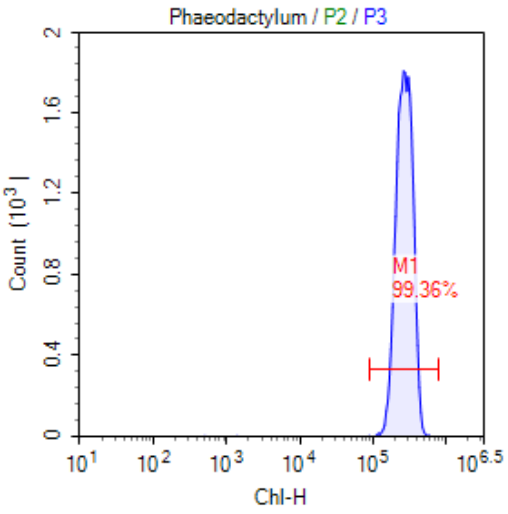

Gate	Count	Abs. Count	% P3	Mean X	CV X
P3	24,464	2,049	100.00 %	283,628	25.00 %
M1	24,307	2,036	99.36 %	285,402	23.68 %

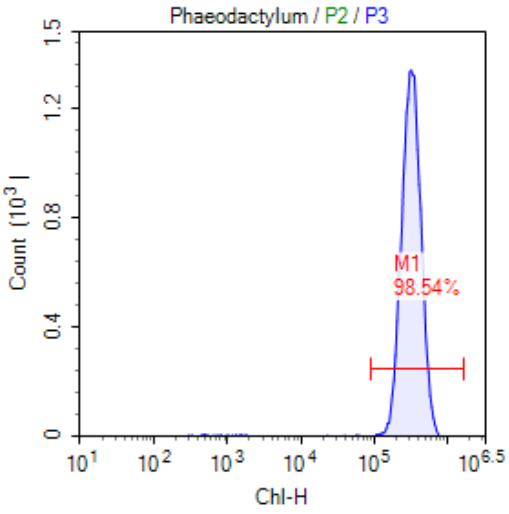

Gate	Count	Abs. Count	% P3	Mean X	CV X
P3	19,918	1,146	100.00 %	338,493	31.26 %
M1	19,627	1,129	98.54 %	343,341	28.76 %

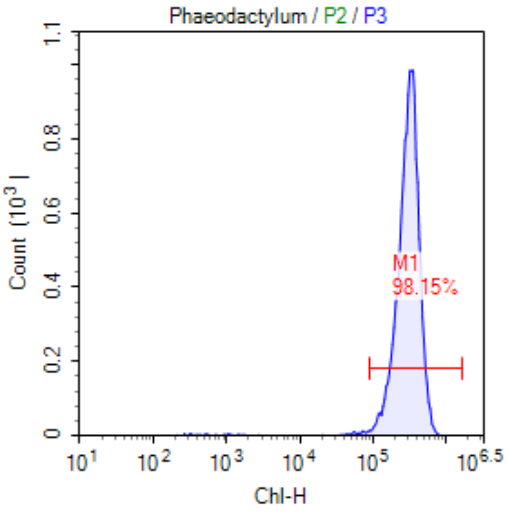

Gate	Count	Abs. Count	% P3	Mean X	CV X
P3	14,994	493	100.00 %	322,671	34.35 %
M1	14,716	484	98.15 %	328,189	31.75 %

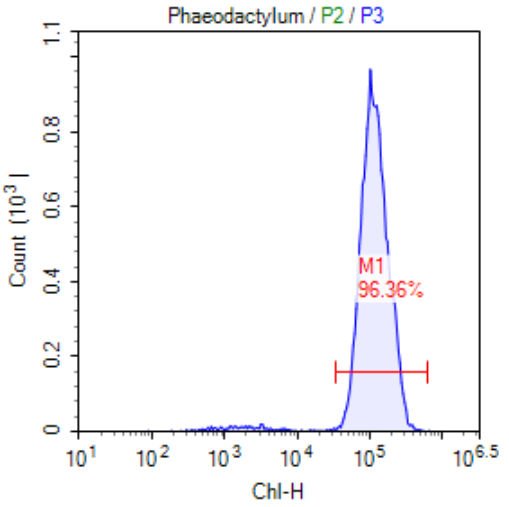

Gate	Count	Abs. Count	% P3	Mean X	CV X
P3	19,471	232	100.00 %	128,615	49.31 %
M1	18,763	224	96.36 %	133,117	44.42 %

Day 3:

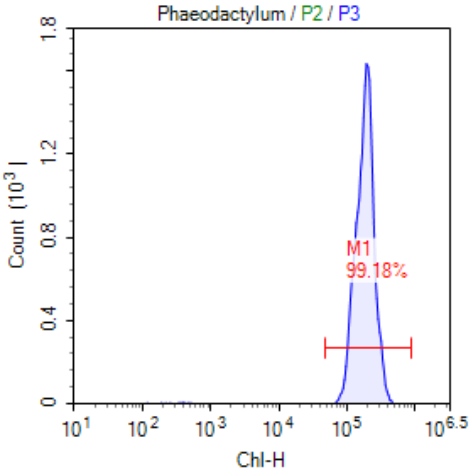

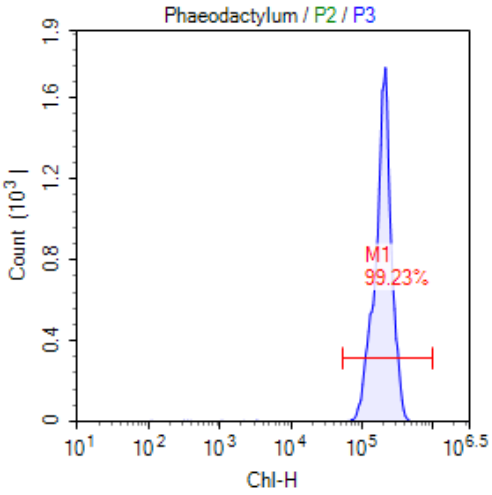

Gate	Count	Abs. Count	% P3	Mean X	CV X
P3	22,839	2,656	100.00 %	196,576	31.98 %
M1	22,651	2,634	99.18 %	198,199	30.55 %

Gate	Count	Abs. Count	% P3	Mean X	CV X
P3	21,080	2,379	100.00 %	209,075	29.85 %
M1	20,917	2,361	99.23 %	210,677	28.46 %

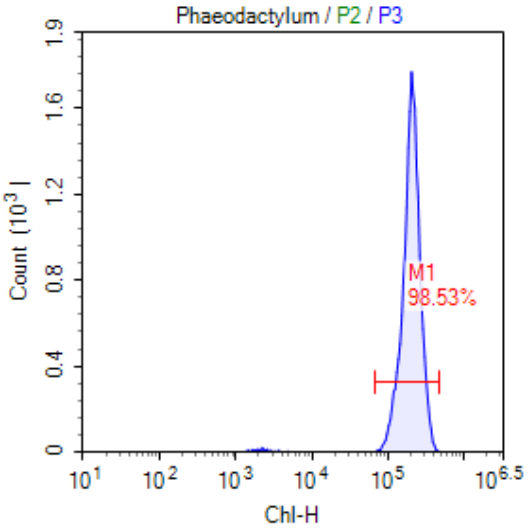

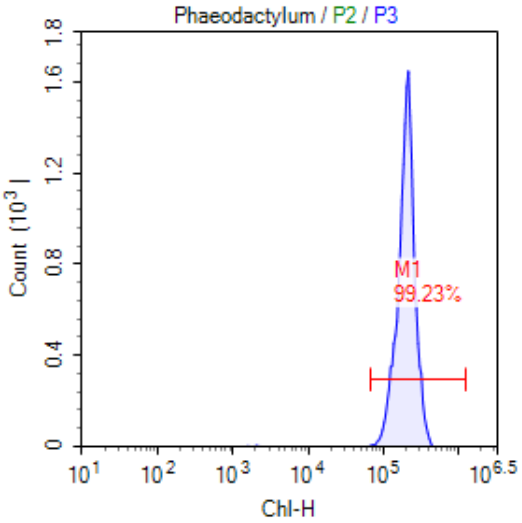

Gate	Count	Abs. Count	% P3	Mean X	CV X
P3	20,535	2,529	100.00 %	212,485	29.27 %
M1	20,234	2,492	98.53 %	215,505	26.50 %

Gate	Count	Abs. Count	% P3	Mean X	CV X
P3	18,516	2,264	100.00 %	212,304	28.37 %
M1	18,374	2,246	99.23 %	213,883	26.97 %

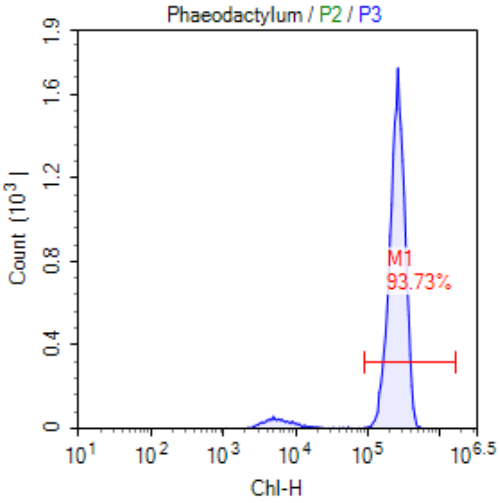

Gate	Count	Abs. Count	% P3	Mean X	CV X
P3	20,598	1,793	100.00 %	254,424	35.12 %
M1	19,307	1,680	93.73 %	270,807	24.01 %

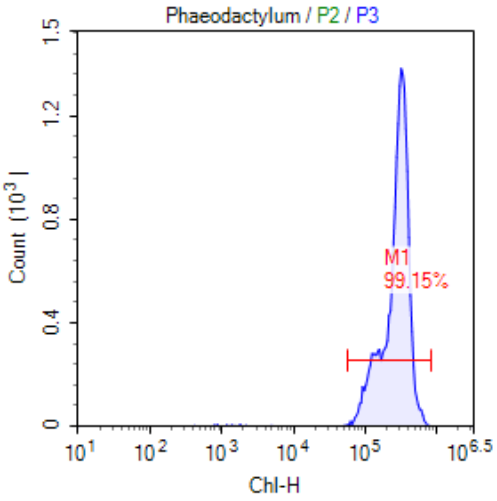

Gate	Count	Abs. Count	% P3	Mean X	CV X
P3	19,897	1,213	100.00 %	295,186	38.08 %
M1	19,727	1,203	99.15 %	297,607	36.83 %

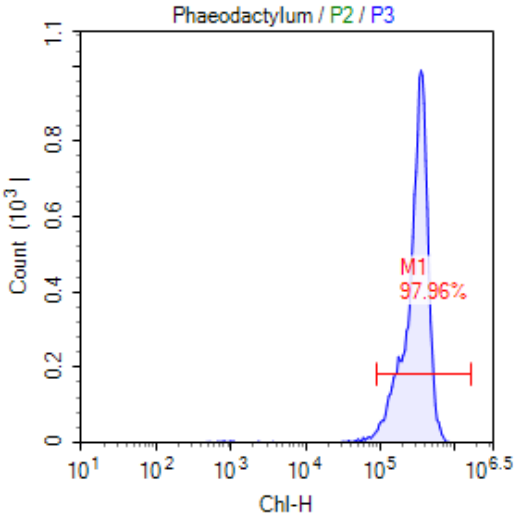

Gate	Count	Abs. Count	% P3	Mean X	CV X
P3	13,701	587	100.00 %	325,577	35.98 %
M1	13,422	575	97.96 %	331,432	33.46 %

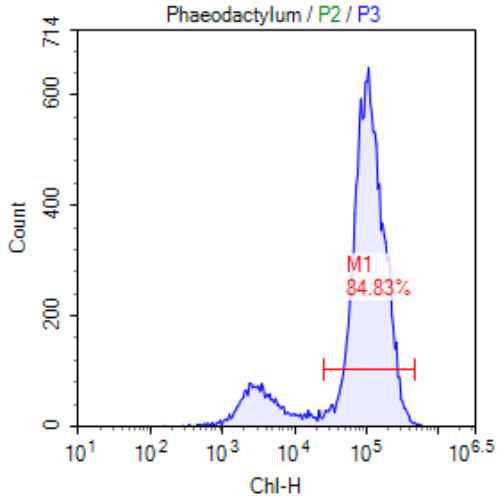

Gate	Count	Abs. Count	% P3	Mean X	CV X
P3	16,925	237	100.00 %	109,407	67.92 %
M1	14,358	201	84.83 %	127,075	49.57 %

Flask 2:

Day 0:

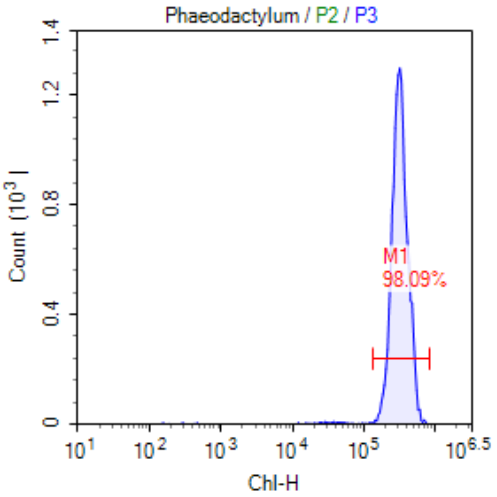

Gate	Count	Abs. Count	% P3	Mean X	CV X
P3	15,662	157	100.00 %	336,024	28.67 %
M1	15,363	154	98.09 %	341,874	25.58 %

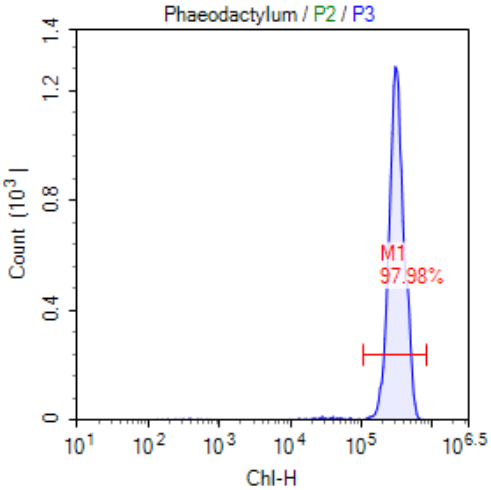

Gate	Count	Abs. Count	% P3	Mean X	CV X
P3	15,109	151	100.00 %	331,693	28.40 %
M1	14,804	148	97.98 %	338,009	24.87 %

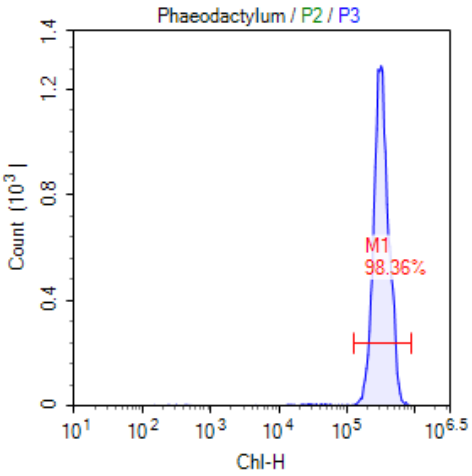

Gate	Count	Abs. Count	% P3	Mean X	CV X
P3	15,760	158	100.00 %	339,535	28.72 %
M1	15,501	155	98.36 %	344,719	25.97 %

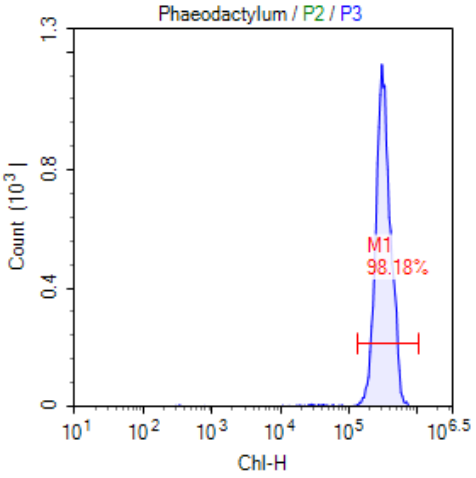

Gate	Count	Abs. Count	% P3	Mean X	CV X
P3	13,597	136	100.00 %	337,419	28.74 %
M1	13,349	133	98.18 %	343,176	25.64 %

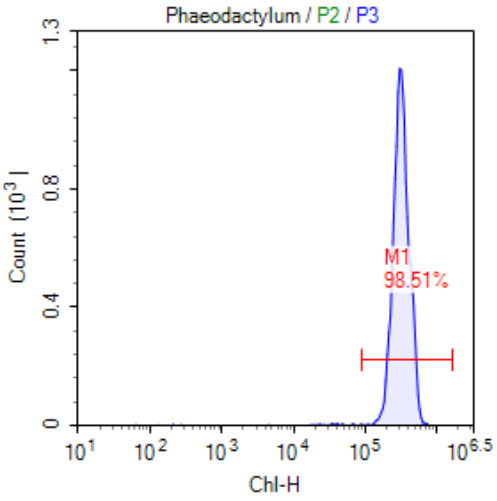

Gate	Count	Abs. Count	% P3	Mean X	CV X
P3	14,575	172	100.00 %	335,367	28.32 %
M1	14,358	170	98.51 %	340,095	25.71 %

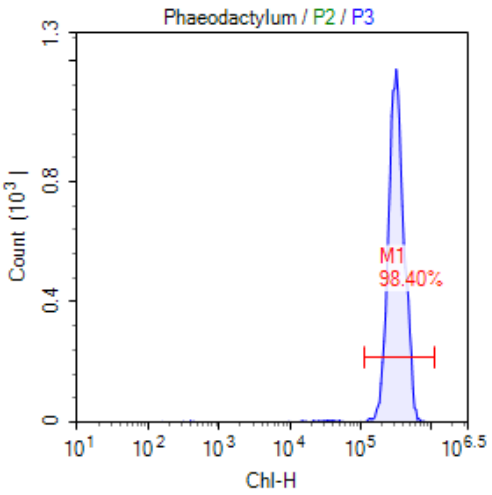

Gate	Count	Abs. Count	% P3	Mean X	CV X
P3	14,287	143	100.00 %	337,992	28.33 %
M1	14,059	141	98.40 %	343,078	25.55 %

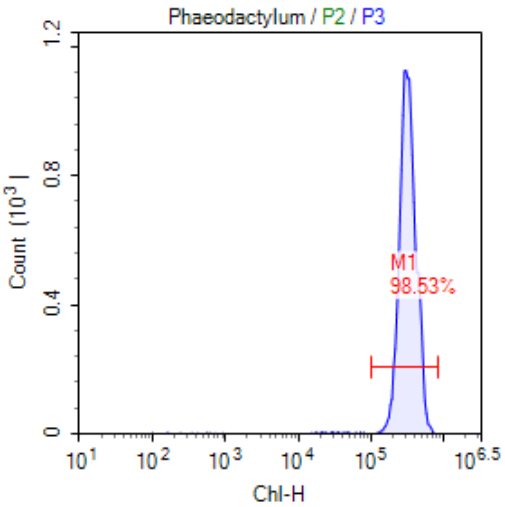

Gate	Count	Abs. Count	% P3	Mean X	CV X
P3	14,191	179	100.00 %	339,086	28.33 %
M1	13,983	177	98.53 %	343,610	25.72 %

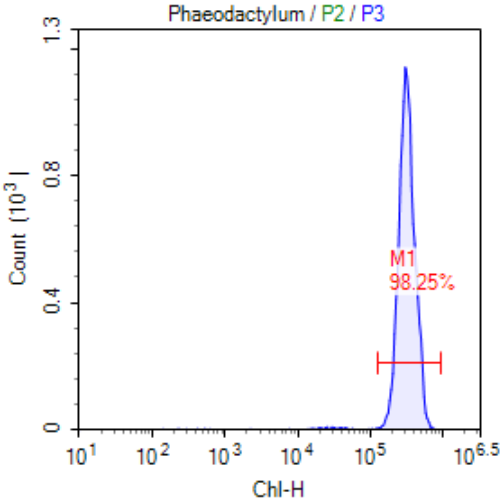

Gate	Count	Abs. Count	% P3	Mean X	CV X
P3	13,689	145	100.00 %	335,333	28.68 %
M1	13,449	143	98.25 %	340,821	25.71 %

Day 1:

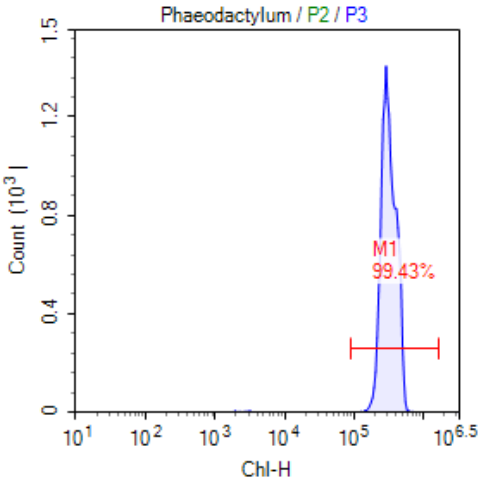

Gate	Count	Abs. Count	% P3	Mean X	CV X
P3	16,112	580	100.00 %	336,488	25.21 %
M1	16,020	576	99.43 %	338,403	23.99 %

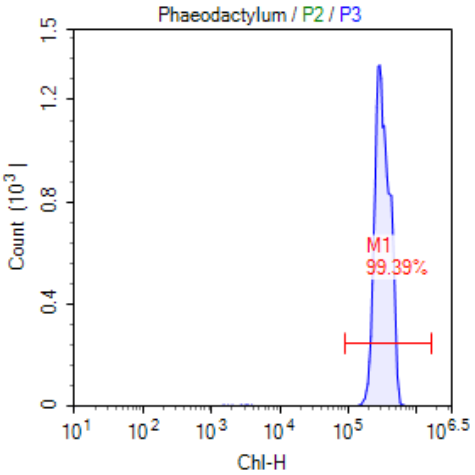

Gate	Count	Abs. Count	% P3	Mean X	CV X
P3	16,234	499	100.00 %	338,488	25.12 %
M1	16,135	496	99.39 %	340,544	23.82 %

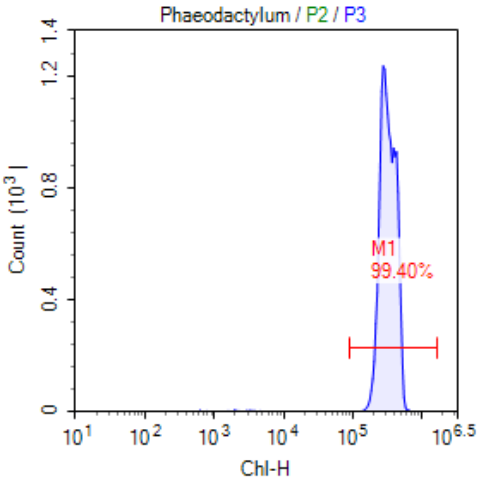

Gate	Count	Abs. Count	% P3	Mean X	CV X
P3	16,216	471	100.00 %	342,910	25.61 %
M1	16,119	469	99.40 %	344,948	24.37 %

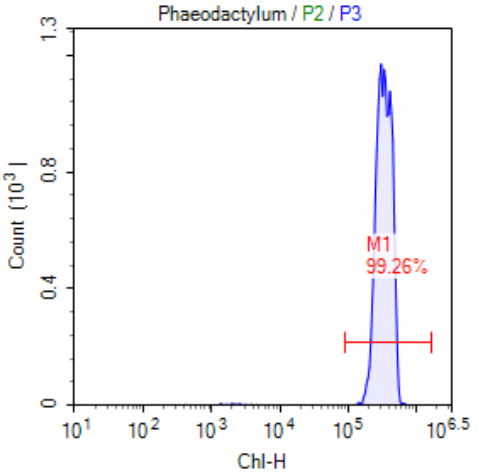

Gate	Count	Abs. Count	% P3	Mean X	CV X
P3	16,080	376	100.00 %	352,736	25.16 %
M1	15,961	374	99.26 %	355,328	23.59 %

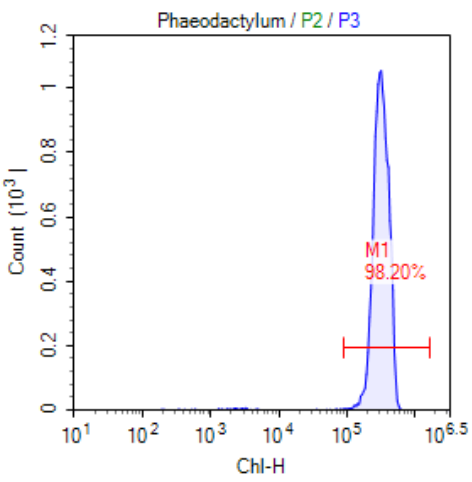

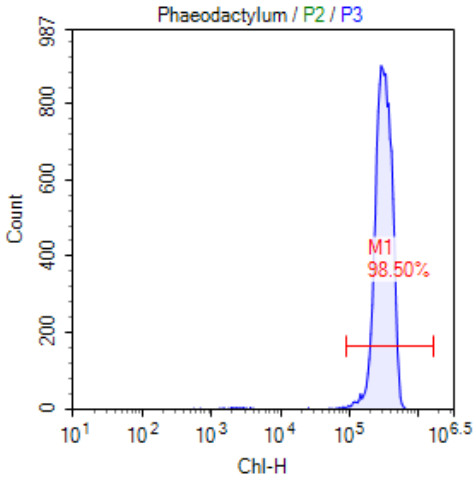

Gate	Count	Abs. Count	% P3	Mean X	CV X
P3	13,706	344	100.00 %	331,250	27.62 %
M1	13,459	338	98.20 %	337,105	24.12 %

Gate	Count	Abs. Count	% P3	Mean X	CV X
P3	12,523	243	100.00 %	327,205	28.11 %
M1	12,335	240	98.50 %	331,893	25.41 %

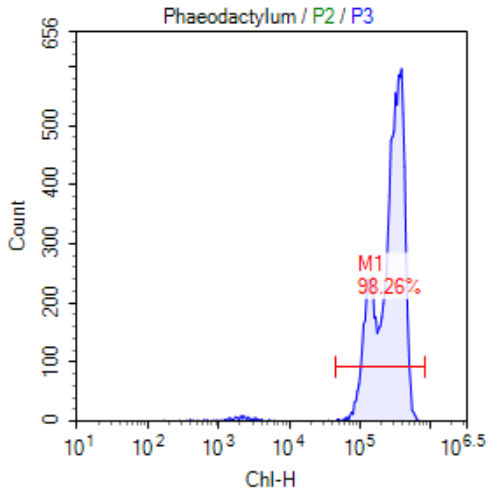

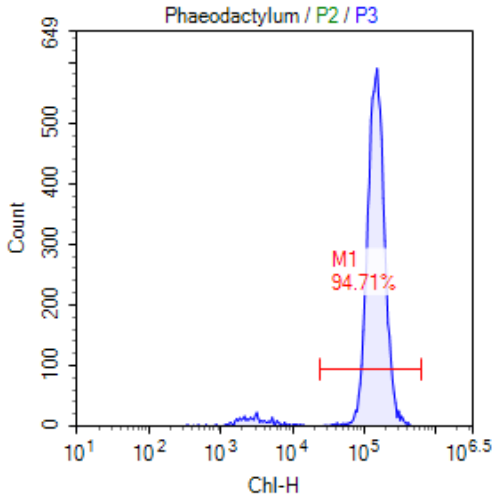

Gate	Count	Abs. Count	% P3	Mean X	CV X
P3	10,396	138	100.00 %	287,963	41.41 %
M1	10,215	136	98.26 %	293,004	38.93 %

Gate	Count	Abs. Count	% P3	Mean X	CV X
P3	8,110	81.1	100.00 %	149,832	37.97 %
M1	7,681	76.8	94.71 %	157,977	29.43 %

Day 2:

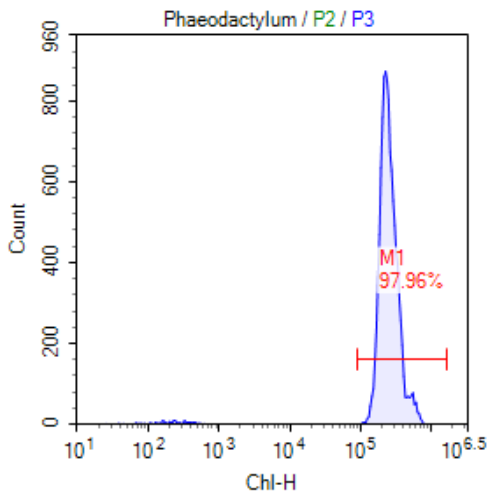

Gate	Count	Abs. Count	% P3	Mean X	CV X
P3	11,147	1,062	100.00 %	268,362	36.89 %
M1	10,920	1,040	97.96 %	273,927	33.62 %

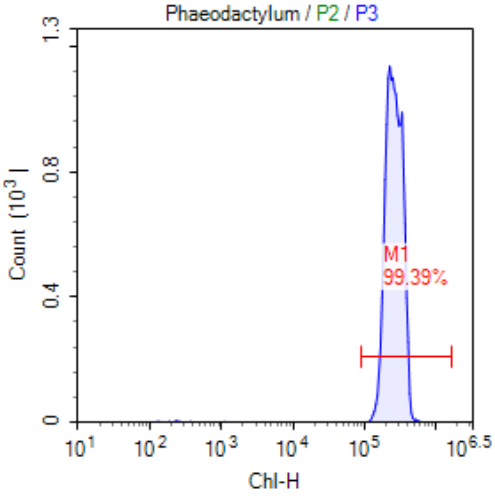

Gate	Count	Abs. Count	% P3	Mean X	CV X
P3	16,092	1,603	100.00 %	274,475	25.76 %
M1	15,994	1,593	99.39 %	276,144	24.48 %

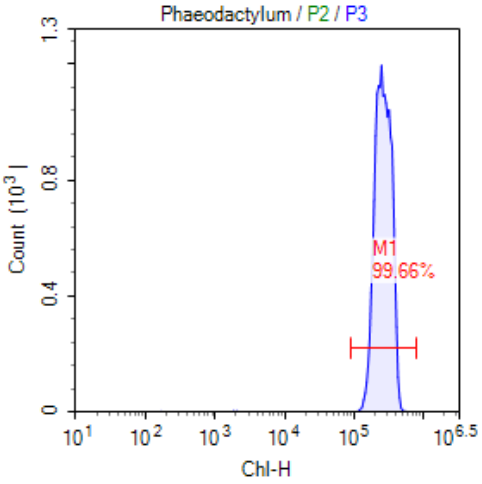

Gate	Count	Abs. Count	% P3	Mean X	CV X
P3	16,814	1,499	100.00 %	278,110	25.12 %
M1	16,756	1,493	99.66 %	279,050	24.41 %

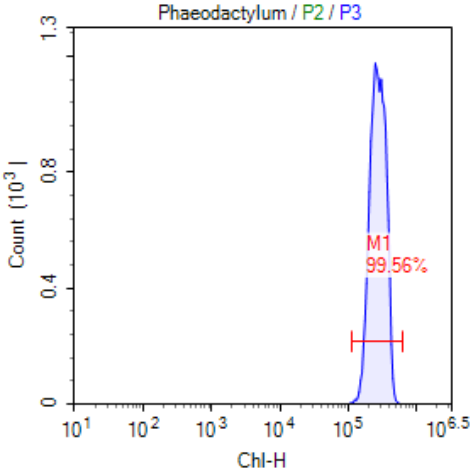

Gate	Count	Abs. Count	% P3	Mean X	CV X
P3	16,468	1,438	100.00 %	288,504	25.01 %
M1	16,396	1,432	99.56 %	289,640	24.17 %

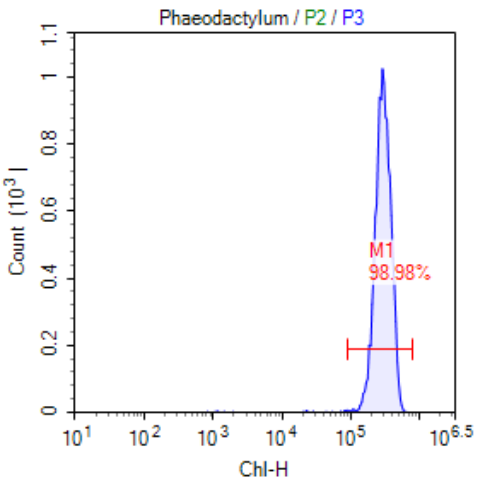

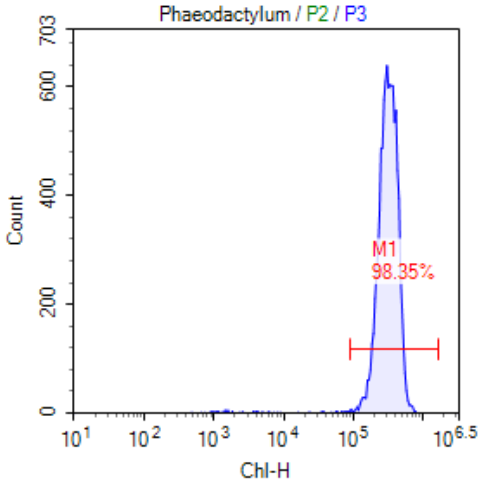

Gate	Count	Abs. Count	% P3	Mean X	CV X
P3	12,791	995	100.00 %	309,600	26.92 %
M1	12,660	984	98.98 %	312,561	25.10 %

Gate	Count	Abs. Count	% P3	Mean X	CV X
P3	9,865	477	100.00 %	333,454	31.64 %
M1	9,702	469	98.35 %	338,734	28.95 %

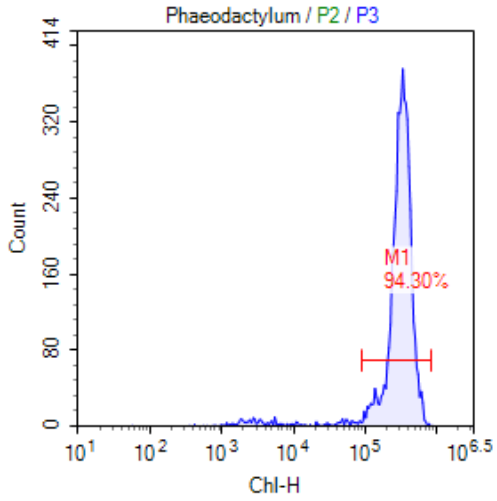

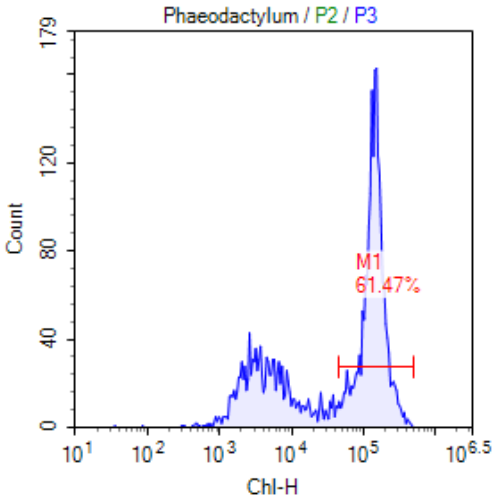

Gate	Count	Abs. Count	% P3	Mean X	CV X
P3	5,278	116	100.00 %	323,996	38.90 %
M1	4,977	109	94.30 %	342,196	30.43 %

Gate	Count	Abs. Count	% P3	Mean X	CV X
P3	3,343	33.4	100.00 %	96,954	87.42 %
M1	2,055	20.6	61.47 %	152,627	39.23 %

Day 3:

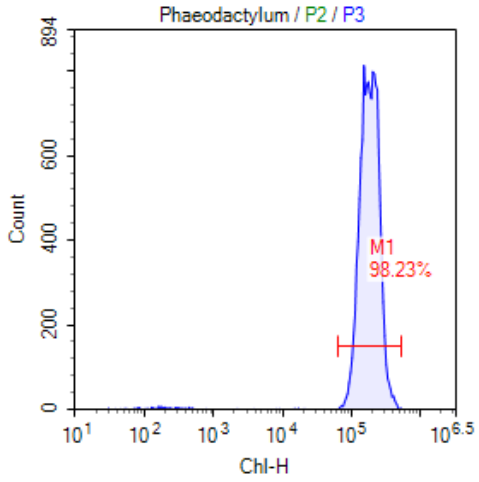

Gate	Count	Abs. Count	% P3	Mean X	CV X
P3	13,459	2,239	100.00 %	194,212	33.41 %
M1	13,221	2,200	98.23 %	197,489	30.28 %

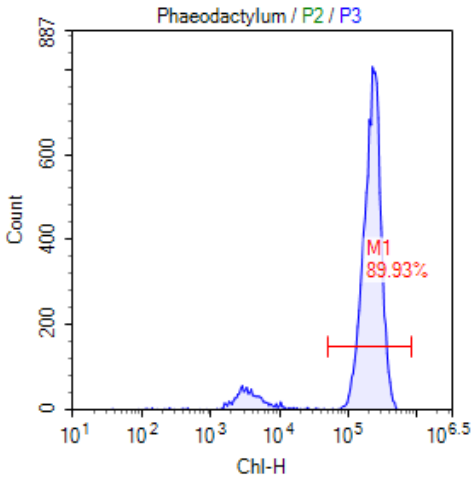

Gate	Count	Abs. Count	% P3	Mean X	CV X
P3	12,031	1,671	100.00 %	214,527	44.09 %
M1	10,820	1,503	89.93 %	237,963	28.15 %

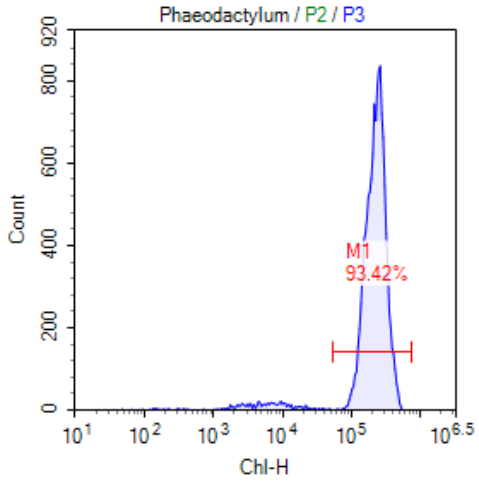

Gate	Count	Abs. Count	% P3	Mean X	CV X
P3	13,349	1,859	100.00 %	227,561	41.33 %
M1	12,471	1,737	93.42 %	243,011	31.43 %

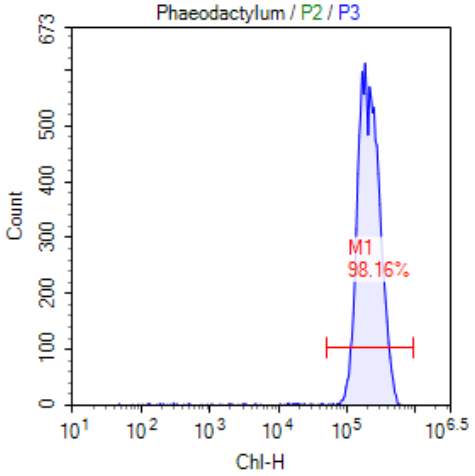

Gate	Count	Abs. Count	% P3	Mean X	CV X
P3	10,898	1,507	100.00 %	227,801	37.82 %
M1	10,697	1,480	98.16 %	231,932	35.12 %

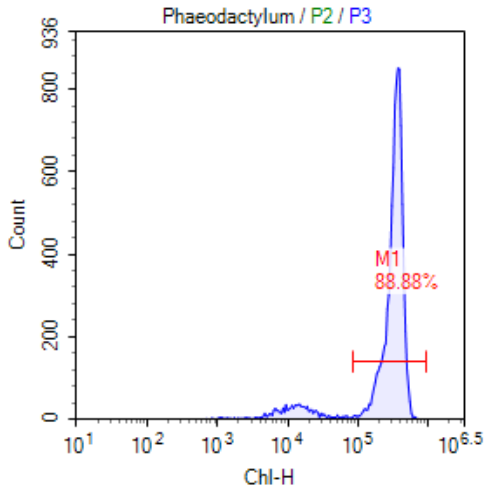

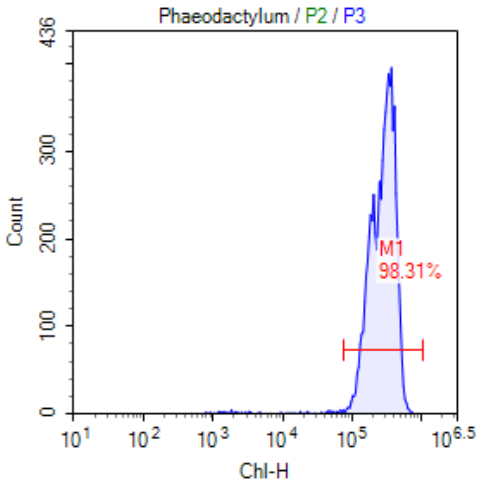

Gate	Count	Abs. Count	% P3	Mean X	CV X
P3	10,003	809	100.00 %	313,434	42.84 %
M1	8,891	719	88.88 %	350,482	25.37 %

Gate	Count	Abs. Count	% P3	Mean X	CV X
P3	7,103	356	100.00 %	299,342	37.96 %
M1	6,983	350	98.31 %	304,119	35.68 %

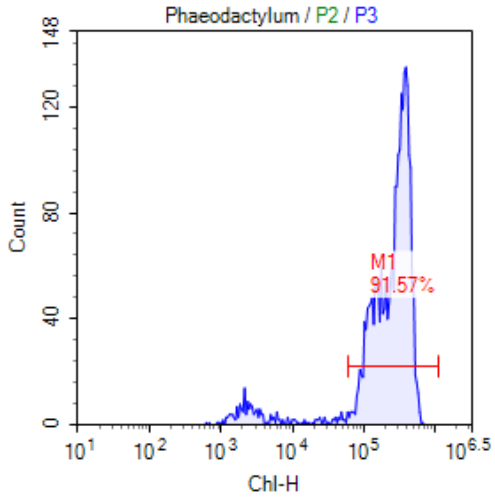

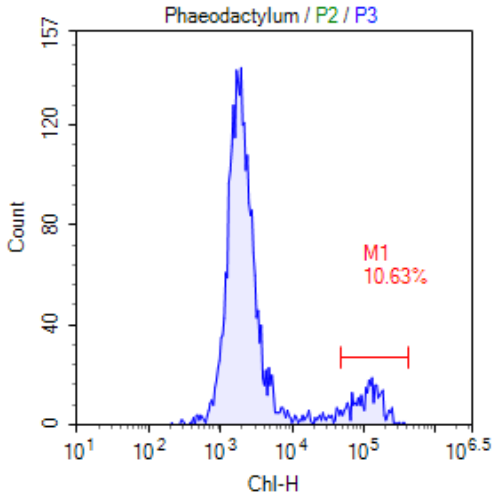

Gate	Count	Abs. Count	% P3	Mean X	CV X
P3	2,668	54.4	100.00 %	271,163	53.59 %
M1	2,443	49.8	91.57 %	295,138	43.15 %

Gate	Count	Abs. Count	% P3	Mean X	CV X
P3	3,114	31.7	100.00 %	16,577	263.80 %
M1	331	3.37	10.63 %	130,394	43.98 %